Copy 220

RM A51I07

NACA

RESEARCH MEMORANDUM

THE STATIC LONGITUDINAL CHARACTERISTICS AT MACH NUMBERS UP TO 0.95 OF A TRIANGULAR-WING CANARD MODEL HAVING A TRIANGULAR CONTROL

By Jack D. Stephenson and Ralph Selan

Ames Aeronautical Laboratory
Moffett Field, Calif.

NATIONAL ADVISORY COMMITTEE FOR AERONAUTICS

WASHINGTON

December 3, 1951

NATIONAL ADVISORY COMMITTEE FOR AERONAUTICS

RESEARCH MEMORANDUM

THE STATIC LONGITUDINAL CHARACTERISTICS AT MACH NUMBERS UP TO 0.95 OF A TRIANGULAR-WING CANARD MODEL HAVING A TRIANGULAR CONTROL

By Jack D. Stephenson and Ralph Selan

SUMMARY

The longitudinal stability and control of a canard model employing a triangular wing of aspect ratio 2 and a control surface of identical plan form have been investigated at Mach numbers up to 0.95. The sections of the wing in streamwise planes were the NACA 0008-63 and the sections of the canard surface were the NACA 0005-63. The model was tested both with the horizontal canard surface at several fixed angles of incidence and with it free to pivot about a lateral axis at 30 percent of its mean aerodynamic chord. The angle of attack of the free-floating surface was varied by means of a trailing-edge flap.

The fixed control surface was effective in producing pitching moments at angles of incidence up to 10°. Increasing the incidence of the control to 20°, however, did not produce any further increase in pitching moment at Mach numbers of 0.80 or above for the higher model angles of attack. The trailing-edge flap was effective in changing the incidence of the free-floating horizontal surface for all deflections for which tests were conducted and the free-floating surface was effective in producing pitching moment throughout the complete range of Mach numbers and angles of attack.

The data have been applied to the calculation of some of the static longitudinal characteristics of two hypothetical canard airplanes. The calculations indicate stick-fixed stability for the canard airplanes with either a fixed or a free-floating control surface at low Mach numbers, but the characteristics at the higher Mach numbers correspond to neutral stability or instability.

Within the angle-of-attack and Mach number ranges investigated, calculations show that the hypothetical canard airplane with the control surface free to trim itself at angles determined by the deflection of a

trailing-edge tab (simulated in the wind-tunnel tests by a split flap) would have a variation of normal acceleration with tab angle that corresponded to static longitudinal stability. A similar airplane with a horizontal canard surface, the incidence of which could be varied by means of an irreversible control system, would have a stable variation of normal acceleration with control-surface incidence for incidence angles under 10°, but this variation would become increasingly unstable as the incidence exceeded 10°. The calculations showed that adding the free-floating canard surface to the wing-body combination in order to obtain longitudinal balance caused no significant drag increase; whereas, to balance a corresponding tailless triangular-wing airplane at low speed by means of elevons, the drag coefficient would be increased by 0.02.

INTRODUCTION

Results of studies of the aerodynamic characteristics of several airplane configurations employing a low-aspect-ratio triangular wing have indicated that the arrangement of the airplane as a canard might offer advantages over other arrangements, such as a configuration with the tail behind the wing or the tailless airplane with longitudinal-control surfaces on the wing. In reference 1, it is shown that a horizontal tail behind a triangular wing may cause erratic stability changes and instability unless it is close to or below the wing chord plane extended. Such an arrangement of the tail imposes severe limitations on the landing angle of attack. The analysis presented in reference 2 for a tailless airplane having a triangular wing with trailing-edge elevons indicated excessively high power-off sinking speeds in the landing attitude, large and erratic control hinge moments at high subsonic speeds, and a loss in the wing efficiency accompanying the negative flap deflection required for longitudinal balance.

The canard arrangement appears to offer a means of alleviating some of these difficulties. With the horizontal stabilizer ahead of the wing, compared to the tail-aft location, it would be possible to avoid the deleterious effects of the wing wake and downwash upon the stability provided by the tail and to eliminate the restriction to the landing attitude due to a low tail behind the wing. Compared to the tailless airplane, the canard affords a greater range of speeds for efficient operation of the wing, and the control-surface hinge moments should be more tractable than those associated with a large trailing-edge control. In addition, the horizontal canard surface could be so devised as to afford the pilot some control over the static margin of the complete airplane. A canard surface which pivots so as to float freely in pitch should have little or no effect upon the static stability of the airplane. On the other hand, the addition of a canard surface at a fixed angle of

incidence would decrease the static margin by an amount depending upon the longitudinal location of the control, the area of the canard surface, the lift-curve slope of the canard surface, and the interference effects.

Tests of a model with a triangular wing having an aspect ratio of 2 (reference 3), showed that, as the speed was increased from low subsonic speeds to supersonic speeds, the static margin increased by about 12 percent of the wing mean aerodynamic chord as a result of a rearward movement of the aerodynamic center of the wing. This large increase in stability would produce objectionable reductions in the maneuverability at high speed. A means of overcoming this deficiency would be to permit the canard surface to pivot freely at low speeds and to lock irreversibly at supersonic speeds. At subsonic speeds, longitudinal control could be provided by a pilot-controlled servo tab on the canard surface, which would affect its floating angle. At supersonic speeds, the canard surface could be irreversibly linked to the pilot's controls. In order to evaluate the subsonic characteristics of a longitudinal control of the type described, wind-tunnel tests have been made of a canard configuration consisting of a triangular wing having an aspect ratio of 2.0 and a canard surface having the same plan form. The canard surface was located so that, with the surface at a fixed angle, the aerodynamic center would be about 12 percent of the wing mean aerodynamic chord ahead of the aerodynamic center of the model with the canard surface free. The tests were conducted of the model with an irreversible control and with the control surface free to trim about its pivot axis. The model was tested in the Ames 12-foot pressure wind tunnel at Mach numbers from 0.25 to 0.95.

NOTATION

b wing span, feet

c local wing chord, feet

$\bar{c}$ wing mean aerodynamic chord $\left(\dfrac{\int_0^{b/2} c^2 dy}{\int_0^{b/2} c\, dy}\right)$, feet

C_D drag coefficient $\left(\dfrac{\text{drag}}{qS}\right)$

C_L lift coefficient $\left(\dfrac{\text{lift}}{qS}\right)$

C_m pitching-moment coefficient $\left(\dfrac{\text{pitching moment}}{qS\bar{c}}\right)$

[redacted]

$C_{m_{\bar{c}/4}}$ pitching-moment coefficient referred to the quarter point of the wing mean aerodynamic chord

i_T angle of incidence of the horizontal control surface with respect to the longitudinal axis of the body, degrees

l length of the body including the portion removed to accommodate the sting, inches

M Mach number

n normal acceleration factor $\left(\frac{\text{normal acceleration}}{\text{acceleration due to gravity}}\right)$

q free-stream dynamic pressure, pounds per square foot

R Reynolds number based on mean aerodynamic chord of the wing

r radius of body, inches

r_o maximum radius of body, inches

S total wing area including the area formed by extending the leading and trailing edges to the plane of symmetry, square feet

V true airspeed, miles per hour

x longitudinal distance from nose of the body excluding the canard boom, inches

y distance perpendicular to plane of symmetry

α angle of attack of the model referred to the free-stream direction, degrees

α_T angle of attack of the control surface referred to the free-stream direction, degrees

δ deflection of the split flap simulating a tab on the horizontal control surface, degrees

δ_f deflection of the elevon of a tailless airplane, degrees

MODEL AND APPARATUS

The model consisted of a triangular wing, a triangular canard stabilizer and control, and a fuselage. A photograph of the model mounted on a sting support in the test section of the 12-foot pressure wind tunnel is presented in figure 1.

The fuselage was a slender body of revolution with a boom extending forward from the nose cone to support the canard surface. The body of revolution had a fineness ratio of 12.5, based upon the total length l (fig. 2) and was shaped according to the formula presented in figure 2.

Except for the addition of the canard surface and its supporting boom, the model was the same as that described in reference 3. A three-view sketch and certain model dimensions are given in figure 2. Other important geometric characteristics of the model are as follows:

Wing

Aspect ratio	2
Taper ratio	0
Airfoil section (streamwise)	NACA 0008-63
Total area, S, square feet	4.014
Mean aerodynamic chord, $\bar{c}$, feet	1.889
Dihedral, degrees	0
Camber	None
Twist, degrees	0
Incidence, degrees	0
Distance, wing-chord plane to body axis, feet	0

Body

Fineness ratio (based upon length, l, fig. 2)	12.5
Cross-section shape	Circular
Maximum cross-sectional area, square feet	0.204
Ratio of maximum cross-sectional area to wing area	0.0508

Horizontal control surface

Aspect ratio	2
Taper ratio	0
Airfoil section (streamwise)	NACA 0005-63
Total area, square feet	0.232
Mean aerodynamic chord, feet	0.454
Distance from pivot axis to the quarter-chord point of the wing mean aerodynamic chord, feet	3.917
Split-flap chord, feet	0.070

The wing was constructed by covering a steel spar with a tin-bismuth alloy. The body spar was also steel but was covered with aluminum. The canard surface, which was steel, was mounted on the nose extension boom on anti-friction bearings so as to pivot about an axis at 30 percent of its mean aerodynamic chord. This pivot axis was 2.07 $\bar{c}$ ahead of the quarter point of the wing mean aerodynamic chord. The ratio of the canard-surface area (including the area formed by extending the leading and trailing edges to the plane of symmetry) to the wing area was 0.0578.

The model was designed so that it could be tested either with the control surface fixed or with it free to rotate in pitch about the pivot axis. With the control surface free, the angle of attack of the control surface was varied by the deflection of a constant-chord, trailing-edge, split flap, simulated in the tests by the addition of wooden wedges to the after portion of the control on the upper surface and located so that the hinge line would be 0.070 feet ahead of the trailing edge. The split flap was rectangular in plan form, as shown in figure 2, and had an exposed area of 16.5 percent of the total control-surface area.

When the control surface was free to trim, the floating angle was measured by means of a selsyn indicator. Provision was made for statically balancing the floating surface and nose piece (which was fixed to the movable control surface) by inserting lead balancing weights. When the surface was free in pitch, a clearance gap of approximately 0.06 inch extended from the trailing edge forward to the movable nose fairing. In addition, there was a gap of approximately 0.05 inch between the fixed portion of the supporting boom and the movable nose piece. There was also air leakage near the control-surface trailing edge resulting from widening the space between the fixed boom and the surface as the incidence increased beyond 10°.

A three-component strain-gage balance mounted on the sting support and enclosed within the body of the model was used to measure the aerodynamic forces and moments on the model.

TESTS

Lift, drag, and pitching-moment data were obtained for the model with the canard surface at four angles of incidence, 0°, 5°, 10°, and 20°, and with this surface free to trim itself to the angle of zero moment about the pivot axis. With the control surface free, split flaps (simulated by wedges) at angles of 0°, -3°, -9°, -14°, and -18° were tested on the control surface. The tests included measurement of the characteristics of the model with the wing on and with the wing removed. The characteristics of the complete model are presented, and the

results of the wing-off tests are included as part of an analysis of the separate contributions of the wing and the canard surface to the pitching moments. Tests of the model were made throughout the Mach number range from 0.25 to 0.95 at a Reynolds number of 3 million. Tests were also made at a constant Mach number of 0.25 and Reynolds numbers of 8,000,000 and 15,000,000.

CORRECTIONS TO DATA

The data have been corrected for the jet-boundary effects of the tunnel walls resulting from lift on the model. Reference 4 was used to calculate these corrections, which were added to the angle of attack and to the drag coefficient, as follows:

$$\Delta\alpha = 0.265\ C_L, \text{ degrees}$$

$$\Delta C_D = 0.0046\ C_L^2$$

The tunnel-wall effects upon the model pitching-moment coefficients were estimated and found to be negligible.

Constriction effects due to the tunnel walls were computed by the method of reference 5. The following table presents the constriction corrections applied to the Mach number and to the dynamic pressure for the complete canard model:

Corrected Mach number	Uncorrected Mach number	$\frac{\text{Corrected } q}{\text{Uncorrected } q}$
0.25	0.250	1.0015
.40	.400	1.0018
.60	.599	1.0023
.80	.797	1.0045
.85	.846	1.0059
.90	.892	1.0091
.95	.934	1.0170

Drag data were corrected to correspond to a base pressure equal to the static pressure of the free stream.

[redacted]

RESULTS AND DISCUSSION

The data presented herein show the lift, drag, and pitching-moment characteristics of a model of a canard airplane which employs two methods of longitudinal control. One method is to maintain the incidence of the horizontal control surface at an angle independent of the aerodynamic hinge moments (an irreversible control), providing for an angle-of-incidence actuator controlled by the pilot. The other type of control is by means of a horizontal surface free to trim itself to a position of zero hinge moment as the airplane angle of attack varies. The angle of attack at which the control-surface trims in this case is varied by the pilot through deflection of a flap on the horizontal control surface.

Static Longitudinal Characteristics

Irreversible control.- Lift, drag, and pitching-moment characteristics are presented in figures 3 through 8 for the model with the horizontal control surface at fixed angles of incidence. The pitching-moment coefficients are referred to an axis at 20 percent of the wing mean aerodynamic chord. This axis was selected to illustrate the characteristics for a center-of-gravity location corresponding to a static margin of 0.05 at the lift coefficient for balance with a control-surface incidence angle of 5°, and at a Mach number of 0.25. This static margin was chosen on the basis of estimated low-speed control and trim requirements.

Figure 3 shows the longitudinal characteristics for a Mach number of 0.25 and a Reynolds number of 8 million. Similar data at Mach numbers of 0.8, 0.85, 0.90, and 0.95 and a Reynolds number of 3 million are presented in figures 4 through 7. Figure 8 shows a comparison of the characteristics at a Mach number of 0.25 for three Reynolds numbers, 3 million, 8 million, and 15 million, for two angles of incidence of the horizontal control surface.

Owing to the high angles of attack required to stall the wing, and to the excessive pitching moments on the strain-gage balance at these high angles of attack, the characteristics of the model at angles of attack approaching the stall were not investigated in detail. Tests at low dynamic pressure and low Mach number (fig. 8(a)) indicated that the wing was not stalled at an angle of attack of 22°. At an angle of incidence of the horizontal control surface of 20°, the control surface attained angles of attack of 34° at Mach numbers of 0.25 and 0.80. Even at this angle, the surface had not reached its maximum lift coefficient at a Mach number of 0.25. As the Mach number was increased to 0.80, however, the canard surface lost its effectiveness at the higher angles of attack. (See fig. 4.) With 20° incidence, the control surface

indicated no increase of lift with increase of model angle of attack above 6° at Mach numbers of 0.8 or above.

Free-floating control surface.- The lift, drag, and pitching-moment characteristics of the model with the canard surface free to rotate in pitch about its pivot axis are presented in figures 9 through 15. The pitching-moment coefficients are referred to an axis at 32 percent of the wing mean aerodynamic chord, which corresponds to a center-of-gravity position for which the static margin at low speed would be approximately equal to that selected for the model with the control surface fixed. When the control surface was free, its angle of attack was varied by means of a constant-chord split flap, simulated in the tests by the addition of rectangular wooden wedges to the upper surface adjacent to the trailing edge. The flap angles were 0°, -3°, -9°, -14°, and -18°.

Figure 9 shows the longitudinal characteristics at a Reynolds number of 8 million and a Mach number of 0.25; figures 10 through 15 present the characteristics at a Reynolds number of 3 million and Mach numbers of 0.4, 0.6, 0.8, 0.85, 0.9, and 0.95. Small deflections of the split flaps effectively varied the pitching moment under all the test conditions, but for the larger deflections there was a partial loss in effectiveness with increasing Mach number.

Control-Surface Effectiveness

Irreversible control.- Figure 16 shows, at several Mach numbers, the variations with control-surface incidence of the lift coefficient for longitudinal balance for the model with a fixed control surface and a center of gravity at 0.20 $\bar{c}$. As the Mach number increased in the range from 0.8 to 0.95, the incidence required for balance at any given lift coefficient increased. This increase in incidence was due primarily to an increase in the static stability rather than to a change in control-surface effectiveness. At an incidence of approximately 10°, a maximum lift coefficient for balance was reached and a further increase in incidence resulted in a lower lift coefficient for balance. This maximum lift coefficient decreased with increasing Mach number.

The variations of pitching-moment coefficient with control-surface incidence at constant values of model angle of attack are presented in figure 17 for a Mach number of 0.25 at a Reynolds number of 8 million, and in figure 18 for Mach numbers from 0.8 to 0.95 at a Reynolds number of 3 million. The moment coefficients in these figures are based upon a reference axis at the quarter point of the wing mean aerodynamic chord selected to provide a common reference for comparing moment characteristics of the two model configurations, that is, with the control surface fixed and with the surface free. These data show that the change

of pitching-moment coefficient with control incidence became increasingly nonlinear both with increasing Mach number and with increasing model angle of attack. For small variations of incidence from zero, the rate of change of pitching moment with incidence was substantially greater at the higher angles of attack. The major part of the changes with lift coefficient of the slope of the pitching-moment curves (figs. 3 through 7) at small angles of control incidence is associated with this change with model angle of attack of the control-surface effectiveness parameter dC_m/di_T.

In order to determine whether the control-surface characteristics were influenced by the presence of the wing, the model was tested without the wing. The incremental pitching-moment coefficients due to a variation in the control-surface incidence are shown in figures 19 and 20 for the model with the wing on and with the wing off. These data show that the increase in the effectiveness of the control surface at the higher model angles of attack also occurred when the wing was off. At the lower values of control-surface incidence with the wing off, the variation of incremental pitching-moment coefficient with control-surface incidence did not differ significantly from that of the complete model. At the higher angles of incidence of the control surface, the model without the wing had generally higher incremental pitching-moment coefficients than the complete model. The majority of the nonlinearities in the curves of pitching-moment coefficient as functions of lift coefficient for the complete model (figs. 3 through 7) apparently originated in the various effects of angle of attack and angle of incidence on the center of pressure of the canard surface and fuselage combination. Longitudinal movement of this center of pressure appears to result from the effects of changes in the flow on the fuselage and boom due to lift on the control surface, from effects of the fuselage upon the flow at the control surface, or from a combination of these two effects.

Free control surface and flap.- The effects of deflection of the trailing-edge flap upon the lift coefficient for longitudinal balance are presented in figure 21 for the model with the canard surface free. The balanced lift coefficient is shown at various Mach numbers as a function of flap deflection for an airplane center-of-gravity location of 0.32 $\bar{c}$. The variations of lift coefficient with flap angle indicated static longitudinal stability at all the test Mach numbers throughout the ranges of lift coefficients of the test, but, for a given lift coefficient, the flap deflection required for longitudinal balance increased considerably with an increase in Mach number. Part of this increase can be attributed to the increase in model static stability with increasing Mach number, and part is due to a loss of flap effectiveness with increasing Mach number.

Figures 22 and 23 show the variation with split-flap deflection of the canard control-surface angle of attack. Figure 22 presents a

comparison of data for several model angles of attack at a Mach number of 0.25. Comparisons at Mach numbers from 0.4 to 0.95 are presented in figure 23 for model angles of attack of 0°, 4°, 8°, and 12°. The split flap became less effective at large deflections as the Mach number increased above 0.60. The pitching-moment coefficients (referred to the quarter-chord point) as functions of angle of attack of the control surface are presented in figures 24 and 25 for several Mach numbers and model angles of attack. Within the control-surface-angle ranges covered in the tests, the variation of pitching-moment coefficient with control-surface angle of attack was relatively insensitive to changes in the Mach number.

As in the case of the model with the control surface fixed, the model with the control free indicated nonlinear variations of pitching-moment coefficient with lift coefficient for the larger deflections of the split flap. The nonlinearities were less severe than for the model with the control surface fixed, however, and decreased somewhat with increasing Mach number. The origin of some of these nonlinearities is indicated by data obtained in tests with the wing off.

For the complete model at a Mach number of 0.25, the data of figure 24 indicated that, at the higher control-surface angles of attack, the rate of change of pitching-moment coefficient with control-surface angle of attack increased as the model angle of attack was increased. Figure 26 presents the same type of data, pitching-moment coefficient as a function of α_T, for the model with the wing off. Compared with the data for the complete model, the variation of pitching-moment coefficient with control angle of attack was nearly linear for the canard-fuselage combination, and does not show as large a change in slope at high model angles of attack. This indicates that part of the nonlinearity in the moment data and part of the movement of the aerodynamic center of the complete model resulted from flow changes in the region of the wing due to the presence of the canard control surface. There was a slight increase in $dC_m/d\alpha_T$ with the wing off at the higher control-surface angles, apparently due to the effect of control-surface lift upon the flow near the fuselage.

The effect of model angle of attack upon the angle of attack at which the control surface trimmed is shown for various angles of the split flap in figure 27 for a Mach number of 0.25 and for the flap undeflected at various higher Mach numbers in figure 28. In general, increasing the model angle of attack resulted in a decrease in the floating angle, indicating a general upflow in the region of the canard surface. This upflow was apparently not induced by the wing, since the variations in floating angle with angle of attack were about the same with the wing on and with the wing off.

The preceding discussion of the nonlinearities in the pitching-moment data for the model with the control surface free was based principally upon data obtained at a Mach number of 0.25. Data for higher Mach numbers show essentially the same characteristics, although the nonlinearities generally diminished with increasing Mach number. (See figs. 9 through 15.)

Stability and Effectiveness Derivatives

The lift-curve slopes and aerodynamic-center locations at zero lift are presented as functions of Mach number in figure 29, for the model with the control surface fixed, with the control surface free, and, from reference 3, for the model without a control surface. The canard surface had only a small effect upon the lift-curve slope. The aerodynamic center of the wing-body combination was little affected by the addition of the free-floating canard surface. The aerodynamic center of the model with the fixed canard control surface was about 10 percent of the mean aerodynamic chord ahead of the aerodynamic center of the model without the canard surface. The rapid rearward movement of the aerodynamic centers for the three configurations as the Mach number increased above 0.9 was due primarily to the moment characteristics of the wing.

The effectiveness of the irreversible control surface indicated by the rate of change of pitching-moment coefficient with angle of incidence (measured at zero incidence) for several model angles of attack is presented as a function of Mach number in figure 30. The curves at Mach numbers between 0.25 and 0.8 are interpolated.

Figure 31 shows, for several model angles of attack, the variation with Mach number of the effectiveness of the split flap, measured as the slope parameter $d\alpha_T/d\delta$ near zero flap deflection. This parameter is the rate of change of control-surface angle of attack with flap deflection when the control surface trims itself at zero moment about an axis at 30 percent of its mean aerodynamic chord. Figure 31 also presents as a function of Mach number the effectiveness of the free control surface, measured as the slope parameter $dC_m/d\alpha_T$ near zero control-surface angle of attack.

Evaluation of the Split Flap Effectiveness

Because the split flap was somewhat less effective than had been expected, results of other tests of constant-chord trailing-edge flaps on surfaces of triangular plan form have been compared with the canard test results. This comparison was intended to indicate whether the poor effectiveness was due to the low Reynolds number of the canard surface,

whether the effects of the split flap differed significantly from the effects of a plain flap, and whether other factors in the canard tests, such as air leakage at the inner ends of the flap, decreased the effectiveness. In figure 32 the variations of angle of attack of the floating surface with deflection of the split flap are compared with estimated variations of floating angles of triangular wings having a split flap (reference 6) and a plain flap (reference 2), assuming the wings to be free to pivot about an axis at 30 percent of the mean aerodynamic chord. The split flap was rectangular in plan form, but the plain-flap plan form was trapezoidal and extended to the wing tips. Corrections to the data have been made to account for the small differences in the relative flap areas for the different models.

At low Mach number (less than 0.3), the characteristics of the flap on the canard surface at a Reynolds number of 1.9 million (based upon the mean aerodynamic chord of the surface) are compared with the characteristics of the split flap on a wing at a Reynolds number of 1.8 million, and with the characteristics of the plain flap at a Reynolds number of 15 million. In the same figure the data for the canard surface are compared with the plain-flap data at Mach numbers of 0.9 and 0.95. At these Mach numbers the Reynolds number of the wing with the plain flap was 5.3 million, and the canard surface was at a Reynolds number of 0.72 million.

The data presented in figure 32 indicate about the same effectiveness for the plain flap on a wing as for the split flap on a wing, and, at all of the Mach numbers shown, the plain flap had considerably greater effectiveness than the flap on the canard surface. Since the Reynolds number of the present tests of the canard surface at low Mach number was approximately the same as that of the wing with a split flap, the low measured effectiveness of the flap on the canard surface was apparently not due to the smallness of the Reynolds number. Some of the loss in effectiveness of the flap on the canard can be attributed to the air leakage at the inner ends of the flap where a clearance gap remained between the movable surface and the fuselage boom.

APPLICATION OF THE DATA

The results of the tests described in this report have been used to calculate some of the characteristics of a hypothetical airplane employing a canard surface free to trim at the angle of zero aerodynamic moment about its hinge axis and an airplane with the canard surface controlled by the pilot independently of the aerodynamic hinge moment. The latter, or irreversible, type of control would ordinarily be combined with a means of artificially introducing the desired stick-force characteristics.

[redacted]

The angle of attack of the free horizontal surface was assumed to be controlled by means of a pilot-actuated servo tab which would have the same effect on the canard surface as the split flap used in the model tests. The canard airplanes are compared with an airplane composed of a triangular wing and fuselage and employing a constant-chord, plain, trailing-edge flap to provide longitudinal control. (See reference 2.) The center-of-gravity location assumed for the airplane with a free-floating canard surface and for the tailless airplane was 32 percent of the mean aerodynamic chord, and, for the airplane with an irreversible control, the center of gravity was assumed to be at 0.20 $\bar{c}$. A wing loading of 50 pounds per square foot was assumed.

Low-Speed Characteristics

In figure 33, the angles of attack and control-surface deflection for longitudinal balance in level flight are presented as functions of forward velocity at conditions corresponding to the approach and landing. Because of the wing lift characteristics, the angles of attack of all the airplanes are large at low speed. As a result of the loss in lift on the tailless airplane as the elevon is deflected upward to provide balance, this airplane requires the largest angle of attack at any given speed.

For the center-of-gravity locations selected, the predicted incidence of the irreversible canard surface and the deflections of the elevon required for balance of the tailless airplane vary by less than 6° within the speed range shown. The variation with forward speed of the angle of the servo tab on the floating canard surface was more than three times the variation of the elevon angle within the same speed range, and about twice the variation of incidence for the irreversible control.

Also shown in figure 33 are the calculated variations with forward speed of the increment of drag coefficient that result from the various means of providing longitudinal balance. For the tailless airplane, this increment is the increase in drag due to the deflection of the trailing-edge flap on the wing. For the canard airplanes, this drag increment is the difference in the drag coefficient of the airplane in the trimmed condition and the drag coefficient at the same lift coefficient but without the canard surface and boom. Figure 33 shows that the largest increment in drag coefficient (about 0.02) would result from deflecting the trailing-edge flap to balance the tailless airplane at low speed. The incremental drag data for the canard airplane with the free-floating control surface show that the drag of the airplane in the balanced condition is not significantly greater than that of the airplane without the trim and balancing devices. Results of calculations

for the canard-type airplane with the control surface restrained in pitch show at the lower speeds an increment of drag due to the control surface equal to about half that for the tailless airplane, and, at speeds between 260 and 300 miles per hour, practically no drag increment due to the addition of the control surface.

Mach Number Effects

Figures 34, 35, and 36 present the predicted angular deflections of the control surfaces as functions of Mach number for the three triangular-wing airplanes in level and accelerated flight at an altitude of 30,000 feet. The same wing loadings and center-of-gravity locations have been assumed as in the calculations of the low-speed characteristics.

With the canard surface free, large deflections of the servo tab are needed to balance the airplane at low Mach numbers. The variation of control angle with Mach number up to a Mach number of 0.80 indicates static longitudinal stability. As the Mach number is increased above 0.80, the variation of control-surface angle with speed indicates that the airplane would be generally neutrally stable up to a Mach number of 0.90 and unstable at higher Mach numbers. The instability is generally more severe at the higher normal accelerations. The variation of control position with normal acceleration indicates stick-fixed stability at all Mach numbers under the conditions investigated. The calculations at the lower Mach numbers were limited to normal acceleration factors less than 3.0 by the maximum angles of attack and lift coefficients for which data were obtained in the model tests.

The characteristics of the model with the irreversible canard control were not investigated in the wind-tunnel tests at Mach numbers between 0.25 and 0.80, therefore the calculations for this configuration are limited to the Mach number range from 0.8 to 0.95 (fig. 35). The predicted variations with Mach number of control-surface angle of incidence for longitudinal balance are similar to the variations of the servo-tab angles presented in figure 34, except that the angle-of-incidence variations are smaller (and of opposite sign). Also, the longitudinal instability indicated by the variation of control angle with Mach number at high Mach number is relatively independent of normal acceleration.

Figure 35 shows that for normal acceleration factors up to 3.0 the variation of control angle with normal acceleration factor corresponds to stick-fixed stability. The maximum control-surface incidence required for the assumed airplane at a normal acceleration factor of 3.0 is less than 10°. The effect of a further increase in the incidence is indicated

by the variation of trim lift coefficient with control-surface incidence shown in figure 16. Increasing the incidence above 10° first produces a slightly higher normal-acceleration factor until a maximum value is reached; further increases in incidence then result in trim at lower normal accelerations. While the calculations have not been extended to encompass this condition, it is obvious that the assumed airplane would be unstable in maneuvers at normal acceleration factors above about 3.5 at Mach numbers from 0.80 to 0.95.

The variations with Mach number of the elevon deflection required for balance of the assumed tailless airplane are shown in figure 36. The data for these calculations were obtained from reference 2. The variation of elevon angle with Mach number up to 0.85 indicates static longitudinal stability at constant normal-acceleration factors. At higher Mach numbers, the variations differ somewhat, depending upon the normal acceleration. With a normal-acceleration factor near unity, the variation indicates first almost neutral static longitudinal stability, and then instability as the Mach number increases up to 0.95. For the higher normal-acceleration factors, the variations indicate that the airplane would be statically unstable within a small Mach number range, and then stable again at the highest Mach numbers.

The incremental drag coefficients attributable to the addition of the horizontal control surface (and supporting boom) at the angles of incidence to balance the canard airplanes in level flight are shown as functions of Mach number in figure 37. The same figure shows the increase in drag coefficient due to the deflection of the elevon on the tailless airplane. The data indicate that in balancing the tailless airplane, there would be a significant increase in drag coefficient at the lower Mach numbers. Calculations for the canard airplane with the free-floating control surface indicated no large increase in drag at any Mach number, and at all Mach numbers considered the drag increments were lower than those of the other two configurations. For the airplane with the irreversible canard control, calculations showed that the drag increments due to the canard surface were very small at a Mach number of 0.80, but exceeded the increments for the tailless airplane in the Mach number range from 0.85 to 0.93. At the highest Mach number of the tests (0.95), however, the data indicate that the incremental drag coefficient of this canard was slightly less than that for the tailless airplane.

CONCLUSIONS

Tests of a canard model with a triangular wing and a triangular horizontal control surface have indicated the following conclusions:

1. With an irreversible control and the assumed center-of-gravity location, the variation of control-surface angle of incidence with lift coefficient for balance at a Mach number of 0.25 indicated stick-fixed stability but, for Mach numbers of 0.8 and higher, this variation indicated increasing instability as the angle of incidence exceeded 10°.

2. For small angles of incidence, the effectiveness of the irreversible control increased with angle of attack of the model in the range between 0° and 12°. This characteristic did not depend upon the presence of the wing on the model.

3. When the control surface was free to pivot on an axis at 30 percent of its mean aerodynamic chord, a rectangular split flap on the control surface effectively varied the angle of attack of the control surface at all model angles of attack and all Mach numbers of the test but, for the larger flap deflections, the effectiveness decreased somewhat with increasing Mach number.

4. With the control surface free and the assumed center-of-gravity location, variations with split-flap angle of the lift coefficient for balance indicated stick-fixed stability at all the test Mach numbers and angles of attack, but the lift coefficient for balance with any given flap angle decreased considerably with increasing Mach number.

Calculated characteristics of two hypothetical triangular-winged canard airplanes, one employing a free-floating canard control surface with a servo tab having the same aerodynamic characteristics as the split flap on the model, and the other employing an irreversible horizontal surface control, indicated the following:

1. At low Mach numbers, both airplanes would have stick-fixed stability in level flight at sea level.

2. In level flight at 30,000 feet, the variations of control angle with Mach number indicated neutral static longitudinal stability at Mach numbers near 0.85, and instability above 0.90 Mach number.

3. The variations of control angle with normal acceleration corresponded to stick-fixed stability under the conditions investigated, but with the irreversible control, a further increase of the angle of incidence of the horizontal control surface to angles exceeding 10° would lead to instability.

4. Adding the free-floating canard surface to the wing-body combination entailed no significant drag increase to obtain longitudinal balance. Calculations for a tailless airplane indicated that the drag

[redacted]

coefficient would increase at low speed by about 0.02 as the elevons were deflected for balance. At the same speed, the drag increment attributable to the addition of an irreversible canard control to balance the airplane was about half that of the tailless airplane.

Ames Aeronautical Laboratory,
National Advisory Committee for Aeronautics,
Moffett Field, Calif.

REFERENCES

1. Graham, David, and Koenig, David G.: Tests in the Ames 40- by 80-Foot Wind Tunnel of an Airplane Configuration With an Aspect Ratio 2 Triangular Wing and an All-Movable Horizontal Tail - Longitudinal Characteristics. NACA RM A51B21, 1951.

2. Stephenson, Jack D., and Amuedo, Arthur R.: Tests of a Triangular Wing of Aspect Ratio 2 in the Ames 12-Foot Pressure Wind Tunnel. II - The Effectiveness and Hinge Moments of a Constant-Chord Plain Flap. NACA RM A8E03, 1948.

3. Smith, Donald W., and Heitmeyer, John C.: Lift, Drag, and Pitching Moment of Low-Aspect-Ratio Wings at Subsonic and Supersonic Speeds - Plane Triangular Wing of Aspect Ratio 2 With NACA 0008-63 Section. NACA RM A50K20, 1951.

4. Glauert, H.: The Elements of Aerofoil and Airscrew Theory. The University Press, Cambridge, England, 1947.

5. Herriot, John G.: Blockage Corrections for Three-Dimensional-Flow Closed-Throat Wind Tunnels, With Consideration of the Effect of Compressibility. NACA Rep. 995, 1950. (Formerly issued as NACA RM A7B28.)

6. Rose, Leonard M.: Low-Speed Investigation of a Small Triangular Wing of Aspect Ratio 2.0. I - The Effect of Combination with a Body of Revolution and Height Above a Ground Plane. NACA RM A7K03, 1948.

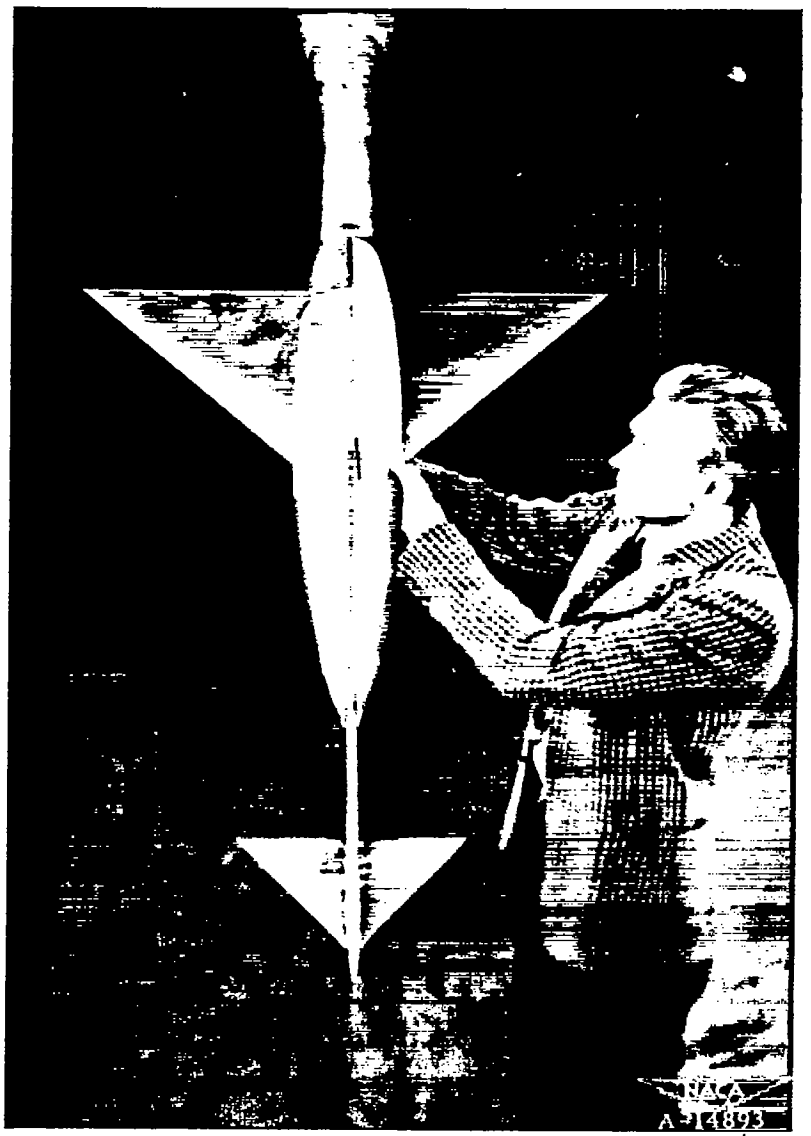

Figure 1.- The canard model in the 12-foot pressure wind tunnel.

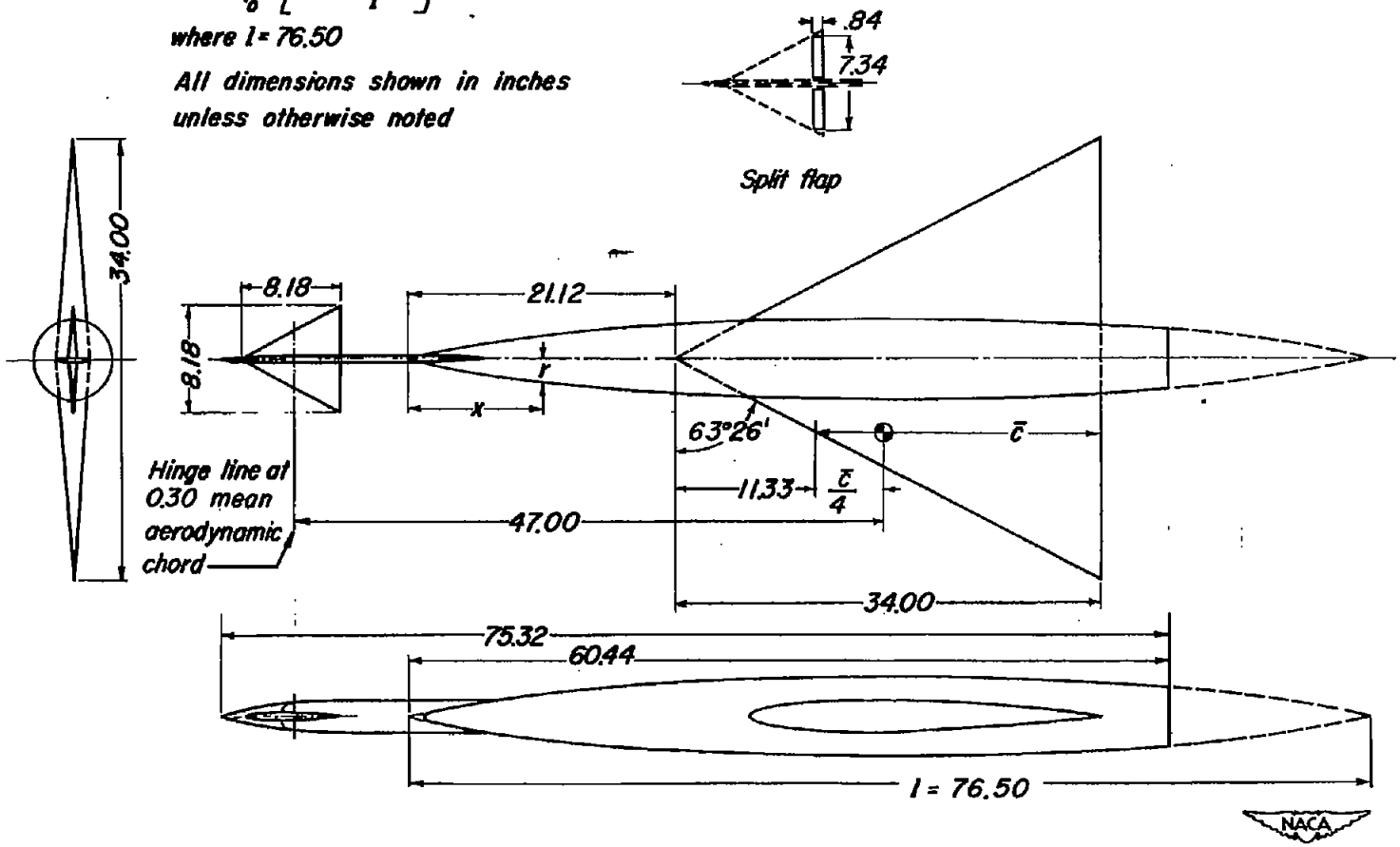

Figure 2.- Three-view drawing of the canard model.

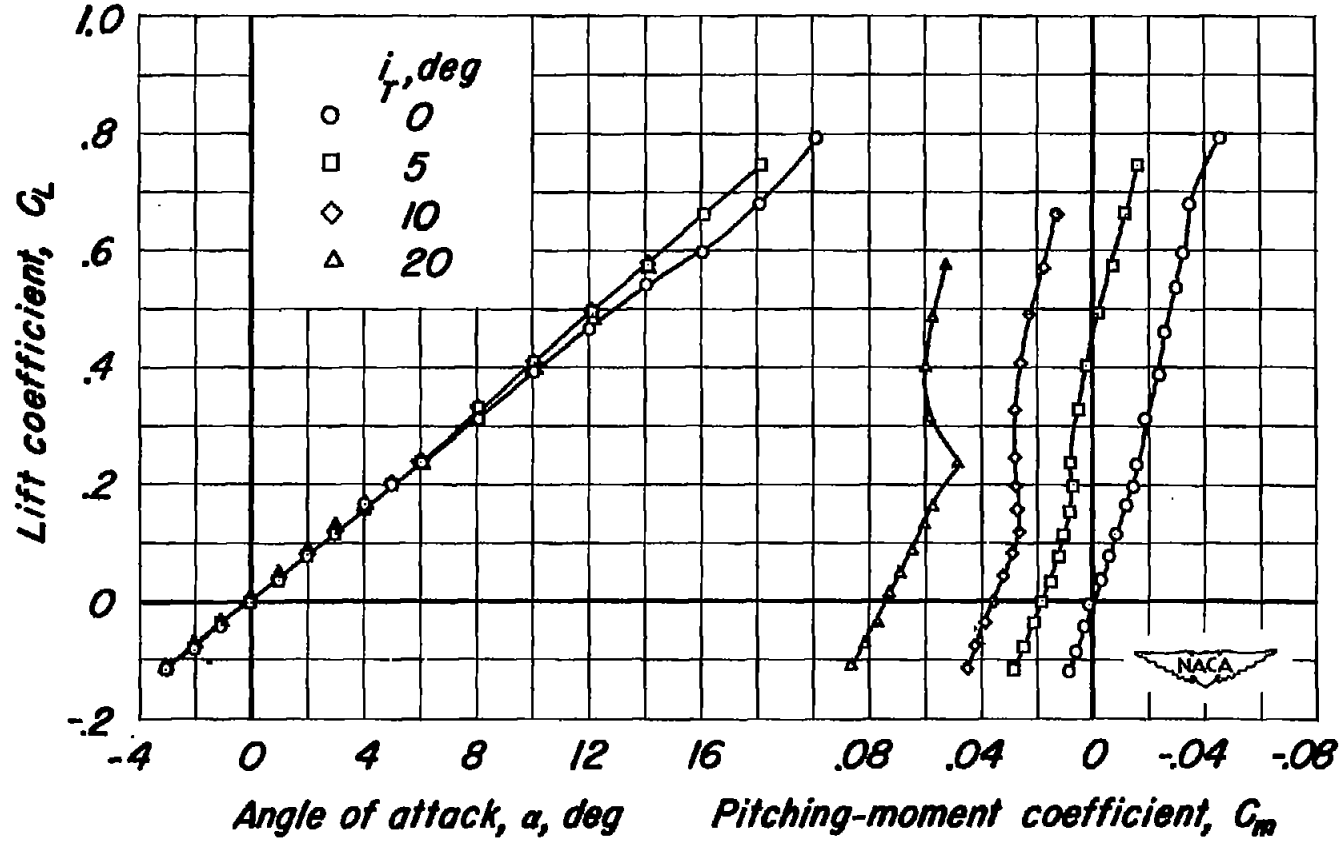

(a) C_L vs α, C_L vs C_m

Figure 3.- The aerodynamic characteristics of the canard model with the horizontal control surface fixed. Mach number, 0.25; Reynolds number, 8.0 million.

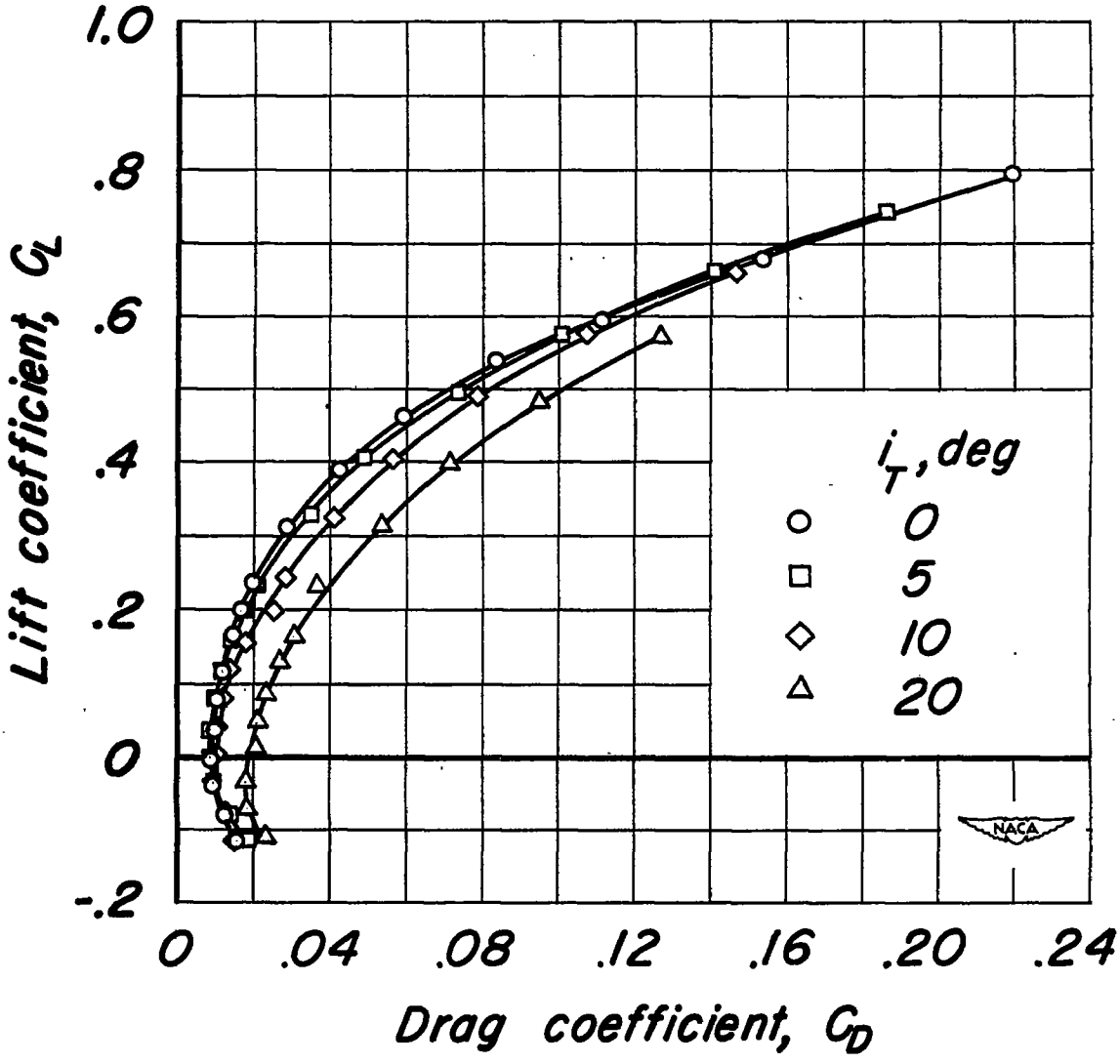

(b) C_L vs C_D

Figure 3.- Concluded.

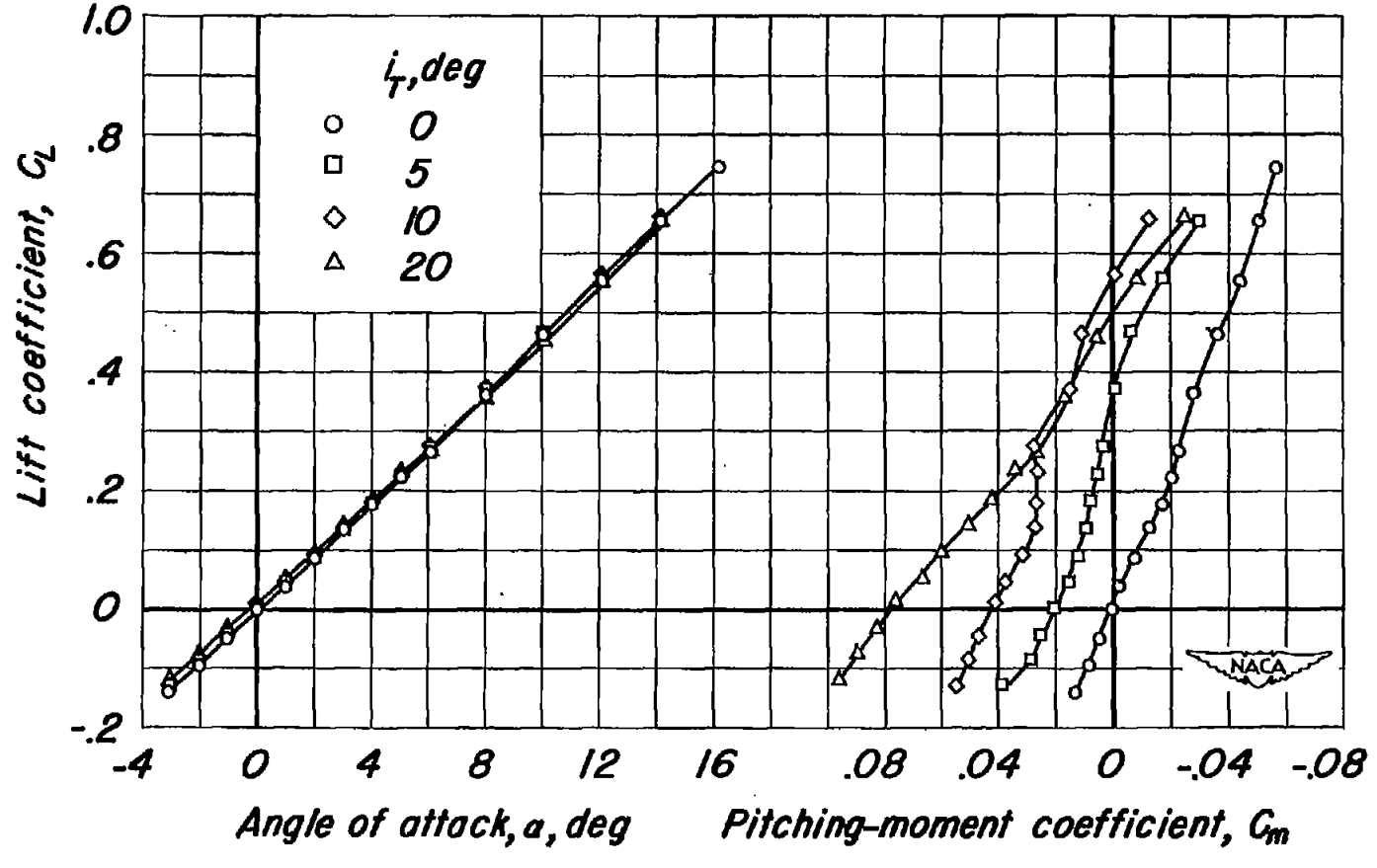

(a) C_L vs α, C_L vs C_m

Figure 4.-The aerodynamic characteristics of the canard model with the horizontal control surface fixed. Mach number, 0.80; Reynolds number, 3.0 million.

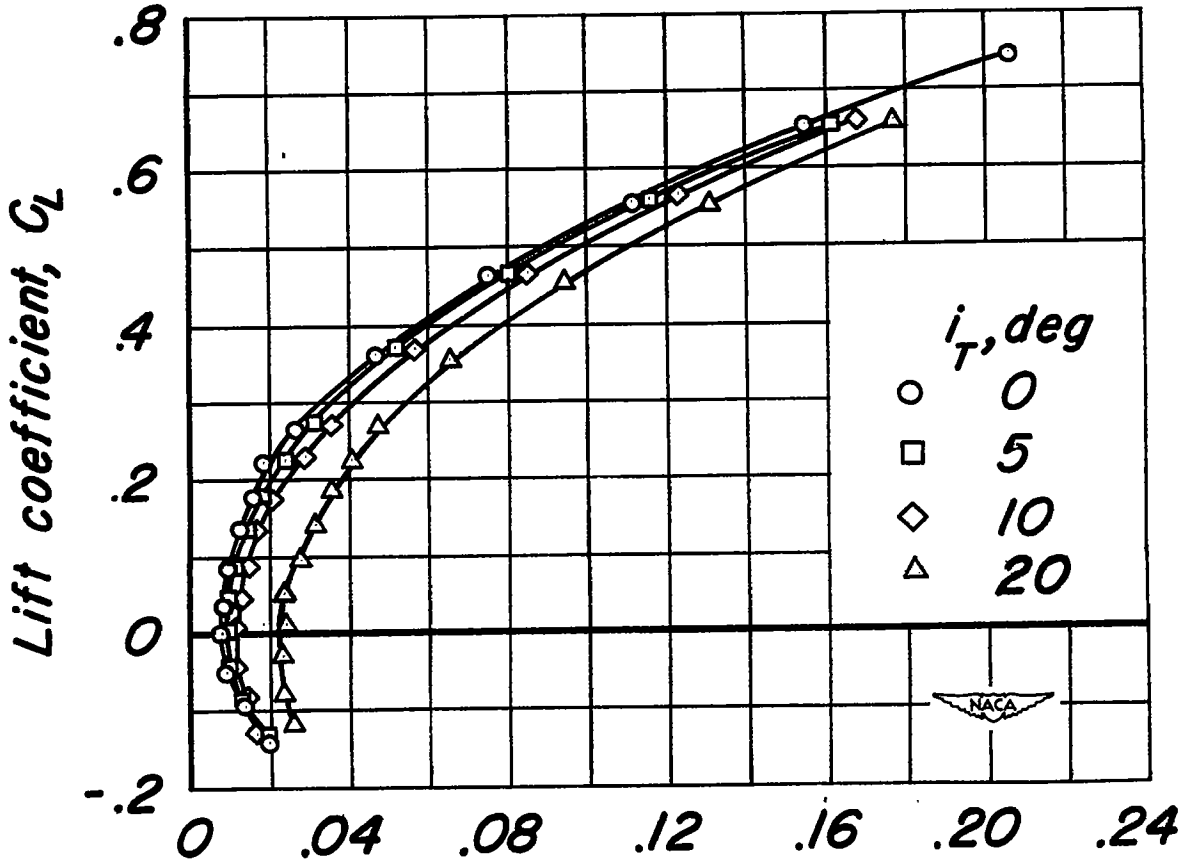

(b) C_L vs C_D

Figure 4.- Concluded.

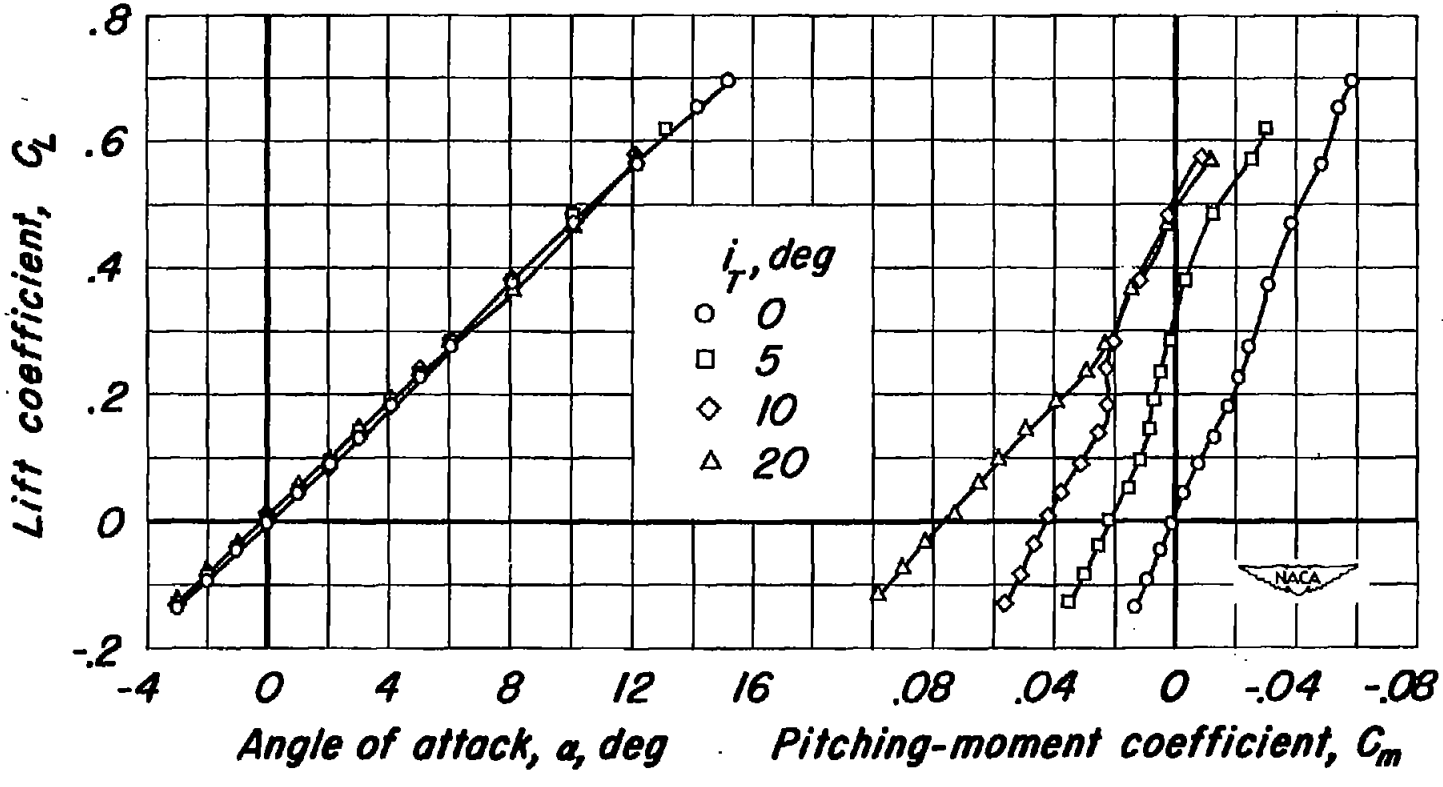

(a) C_L vs α, C_L vs C_m

Figure 5.- The aerodynamic characteristics of the canard model with the horizontal control surface fixed. Mach number, 0.85; Reynolds number, 3.0 million.

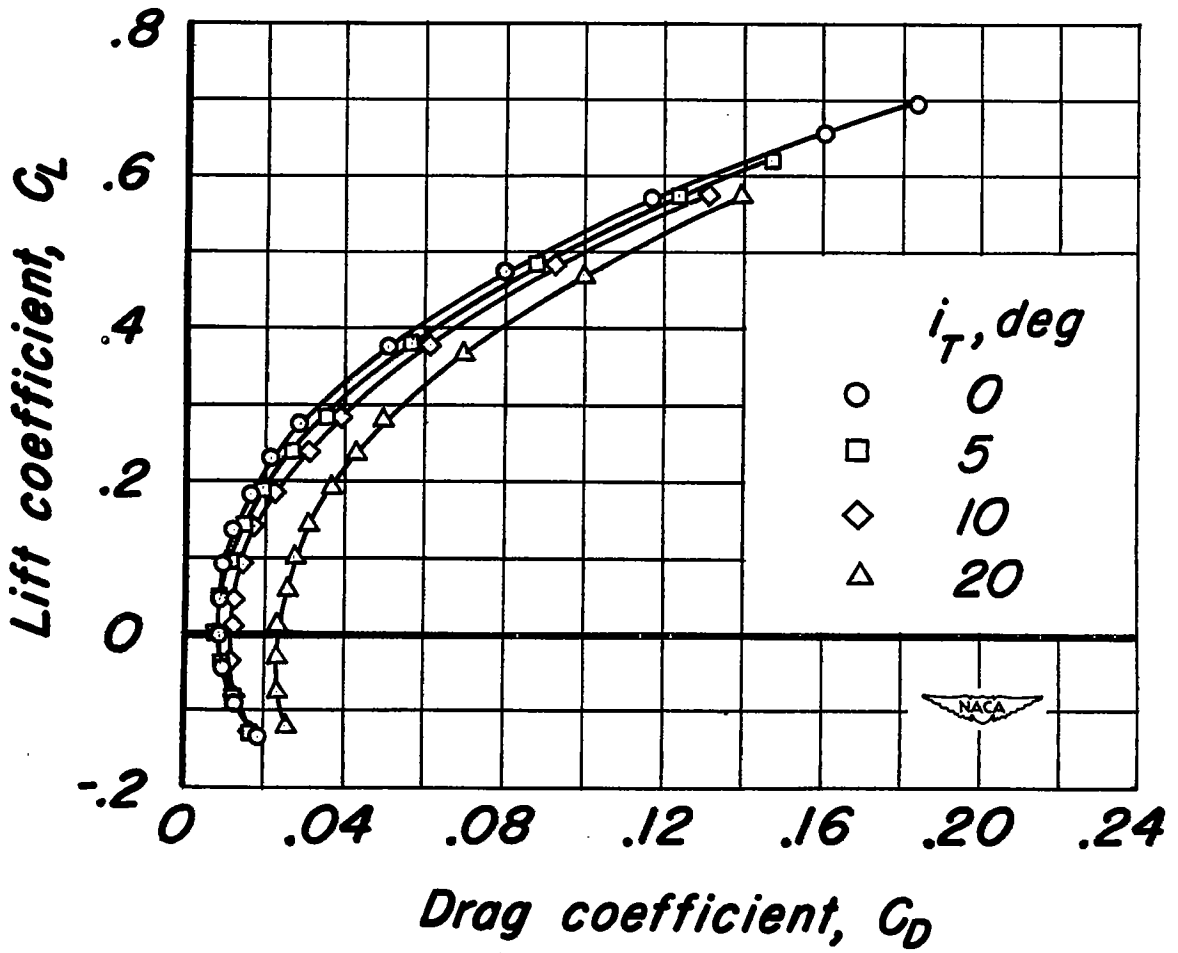

(b) C_L vs C_D

Figure 5.- Concluded.

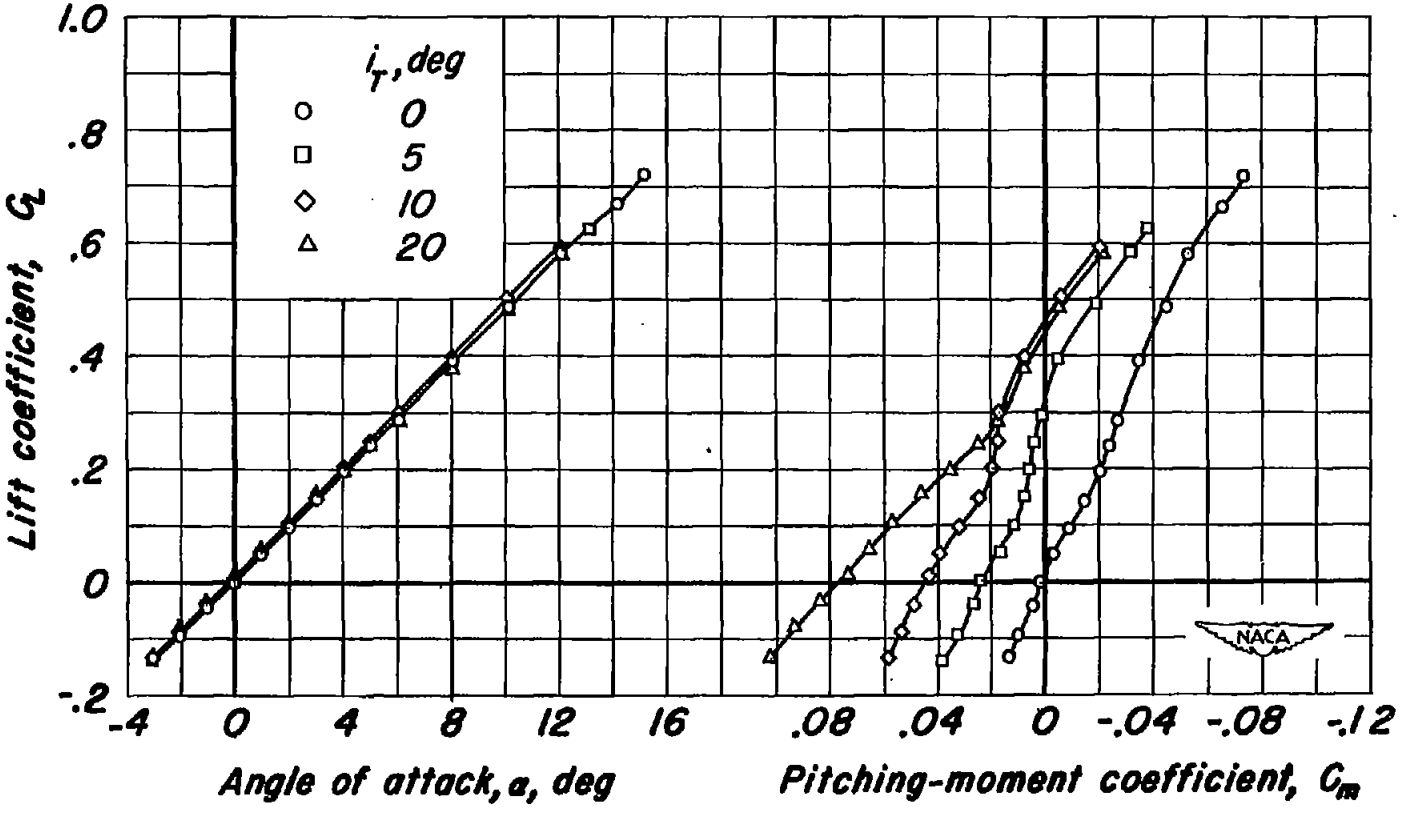

(a) C_L vs α, C_L vs C_m

Figure 6.- The aerodynamic characteristics of the canard model with the horizontal control surface fixed. Mach number, 0.90; Reynolds number, 3.0 million.

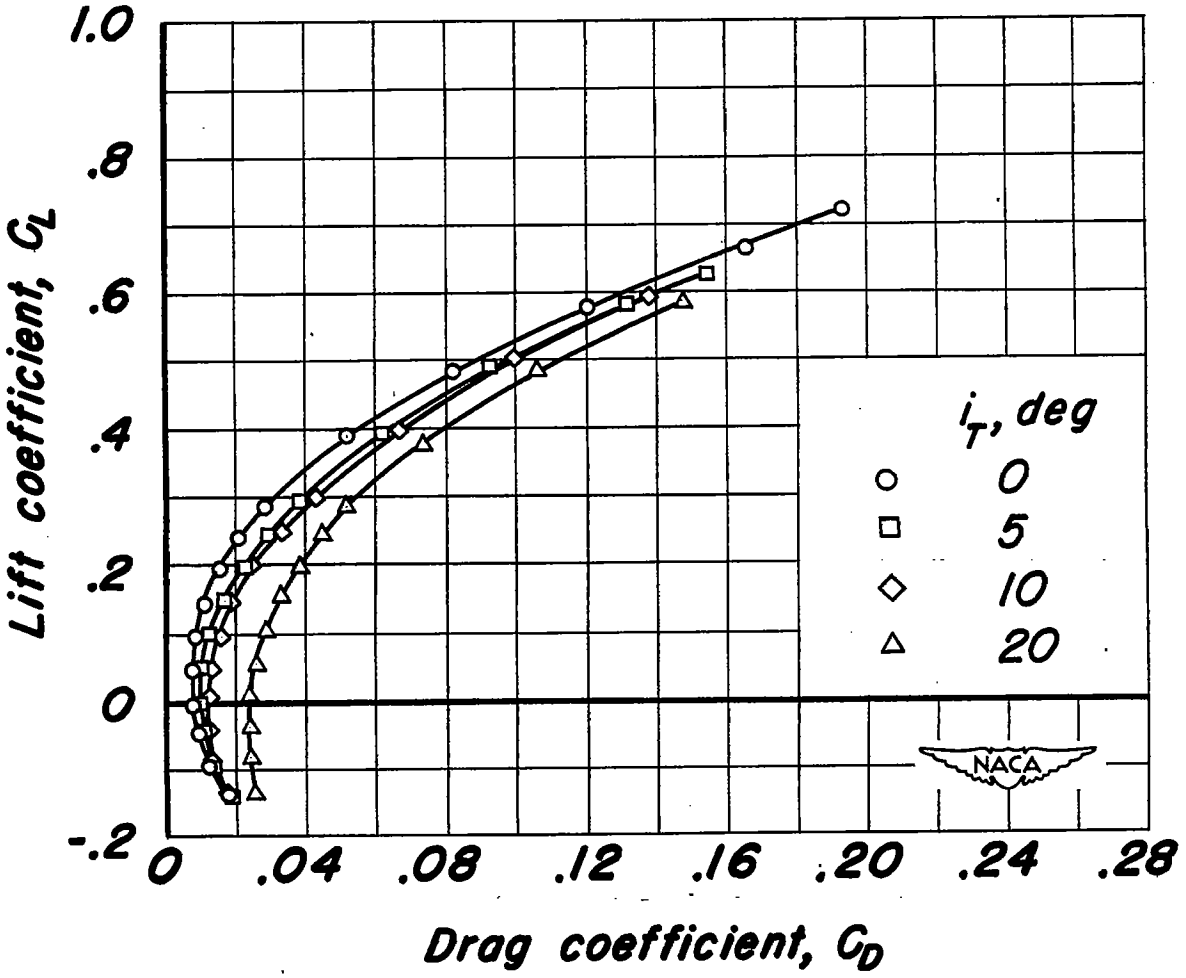

(b) C_L vs C_D

Figure 6.- Concluded.

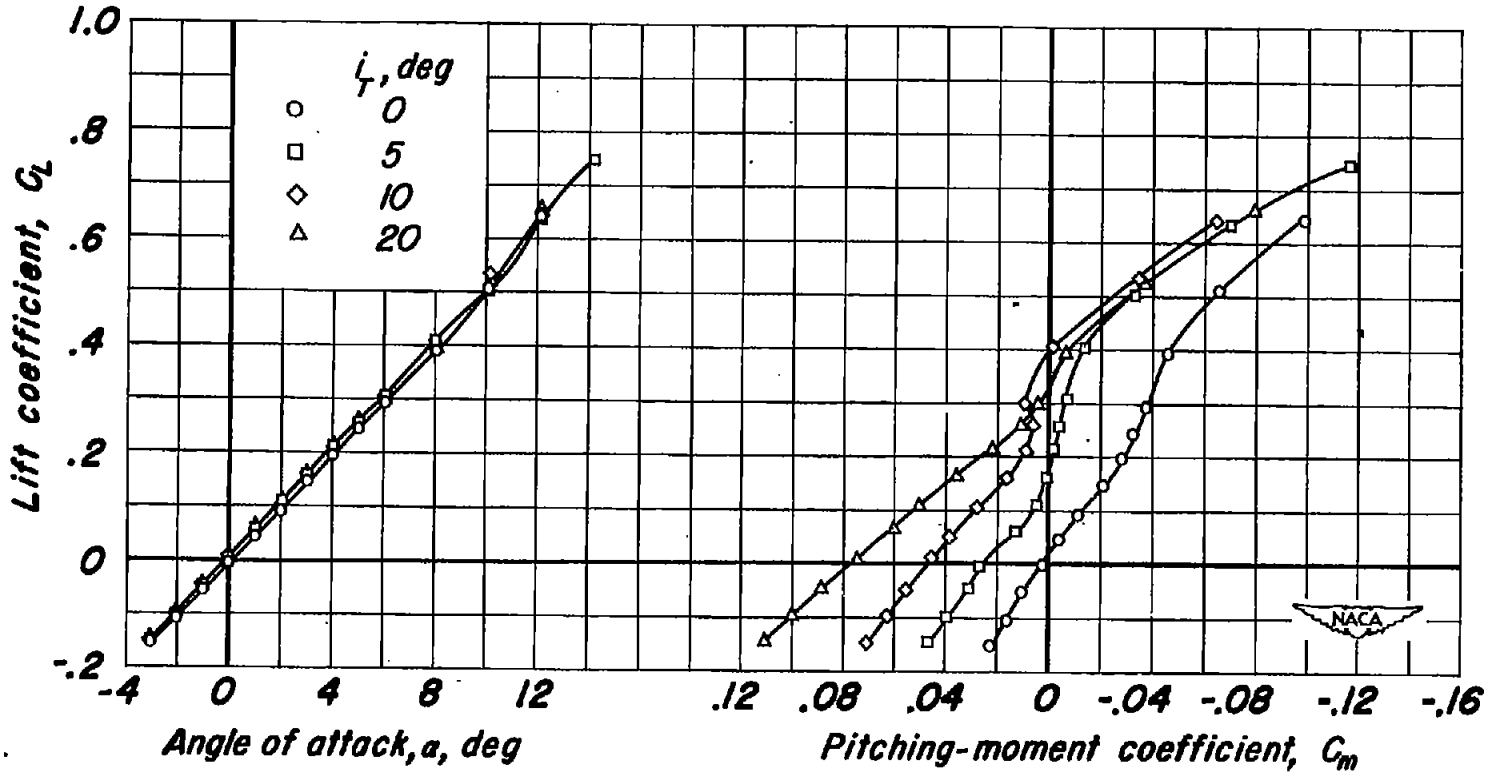

(a) C_L vs α, C_L vs C_m

Figure 7.- The aerodynamic characteristics of the canard model with the horizontal control surface fixed. Mach number, 0.95; Reynolds number, 3.0 million.

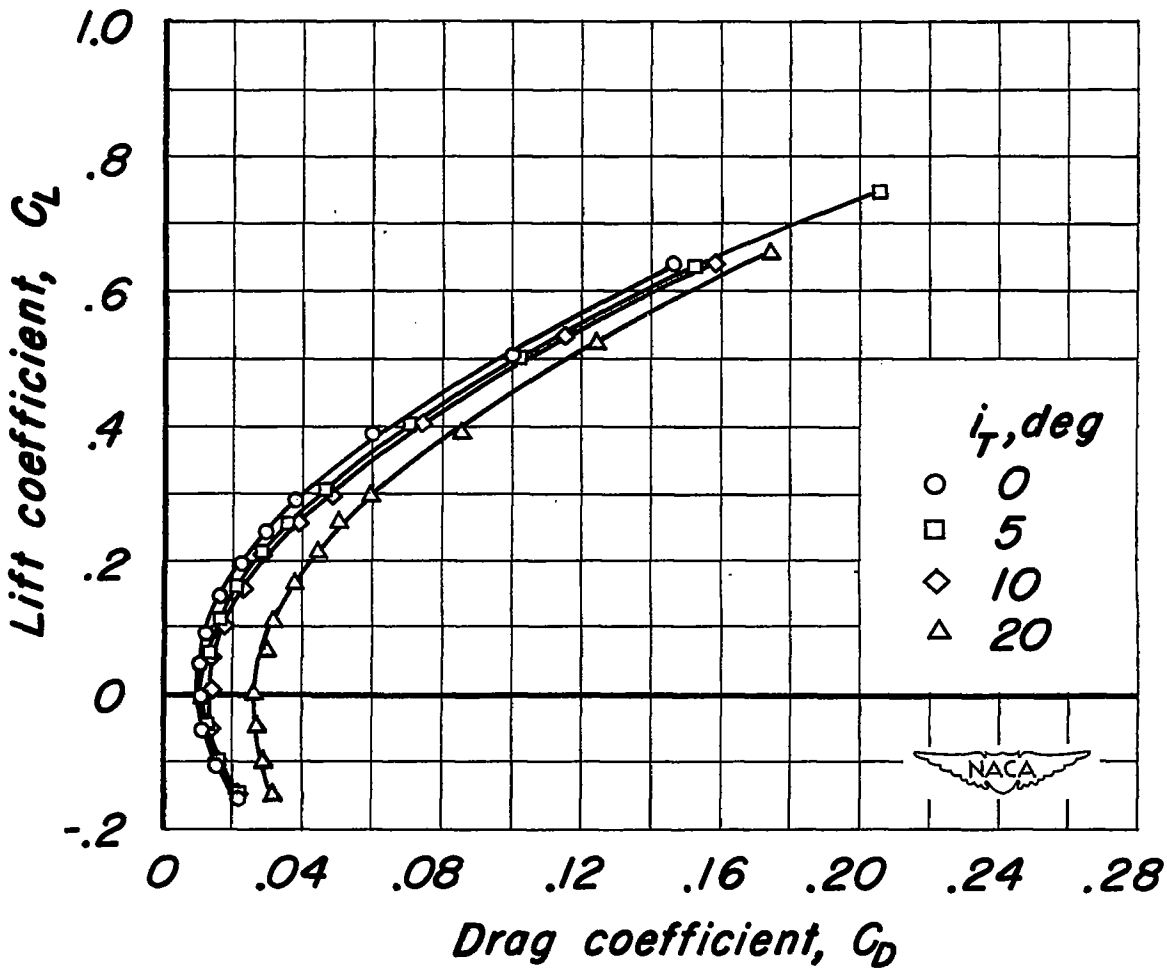

(b) C_L vs C_D

Figure 7.- Concluded.

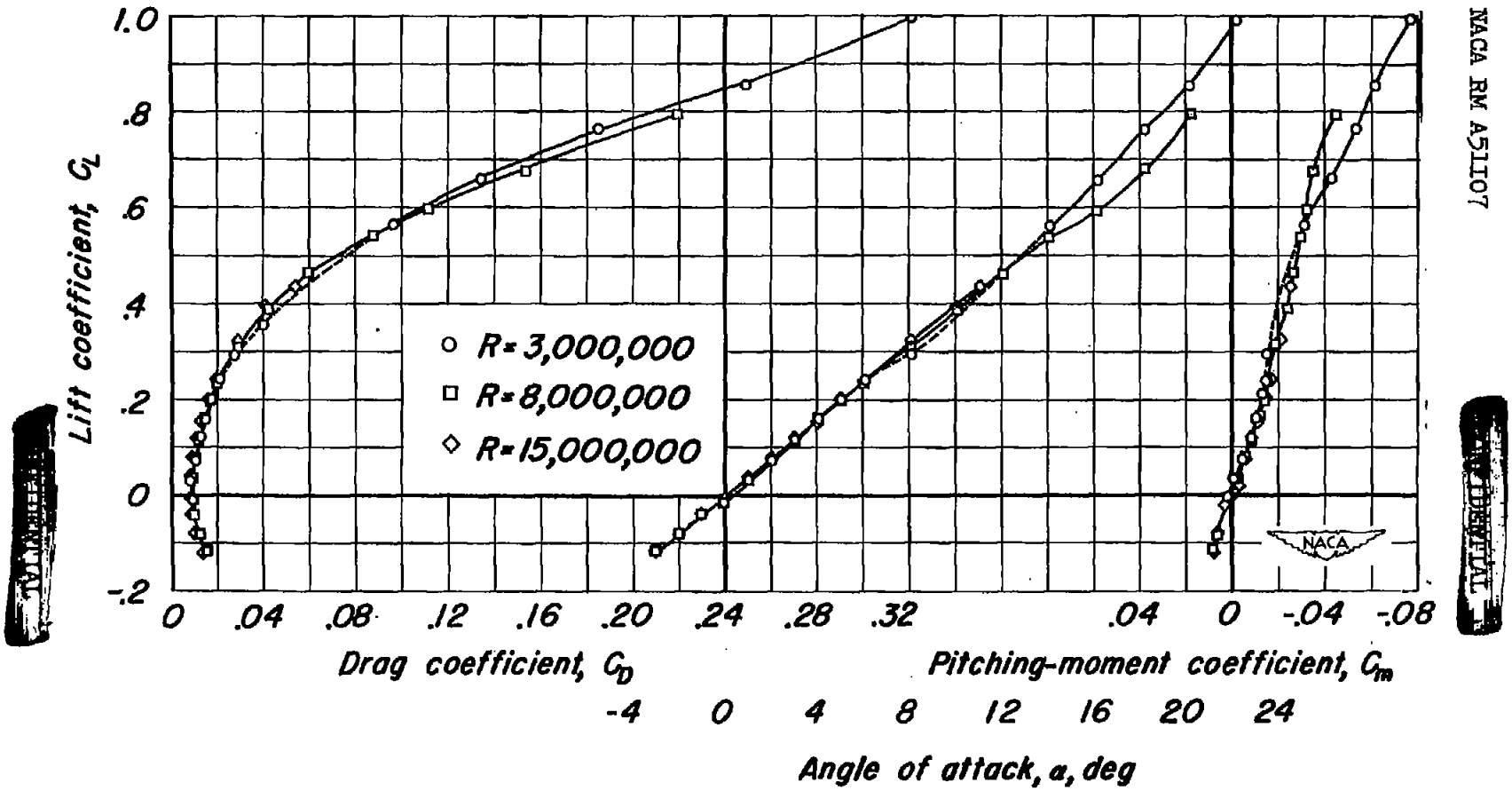

(a) i_t, 0°

Figure 8.- The effects of Reynolds number on the aerodynamic characteristics of the canard model with the horizontal control surface fixed. Mach number, 0.25.

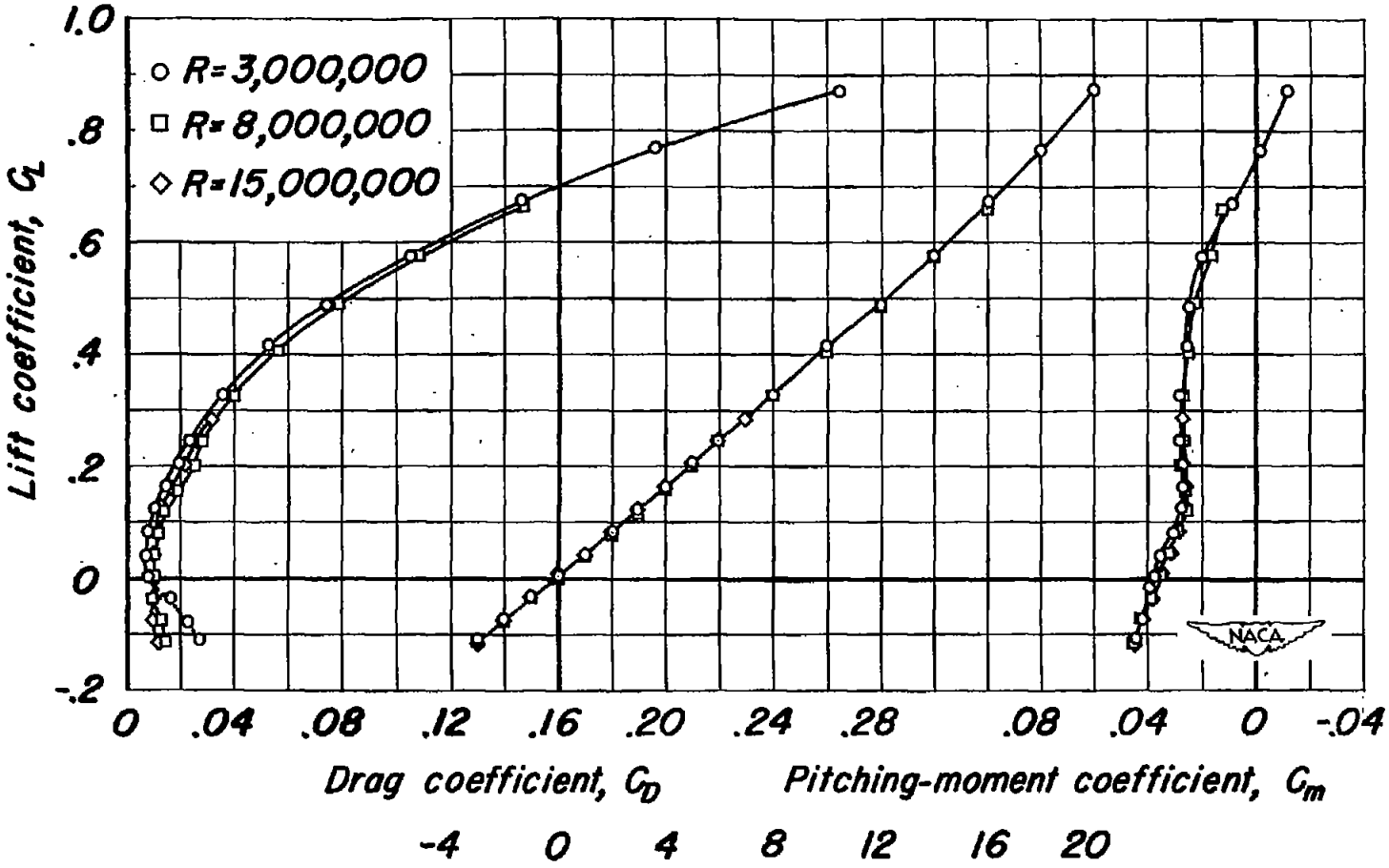

(b) i_T, 10°

Figure 8.- Concluded.

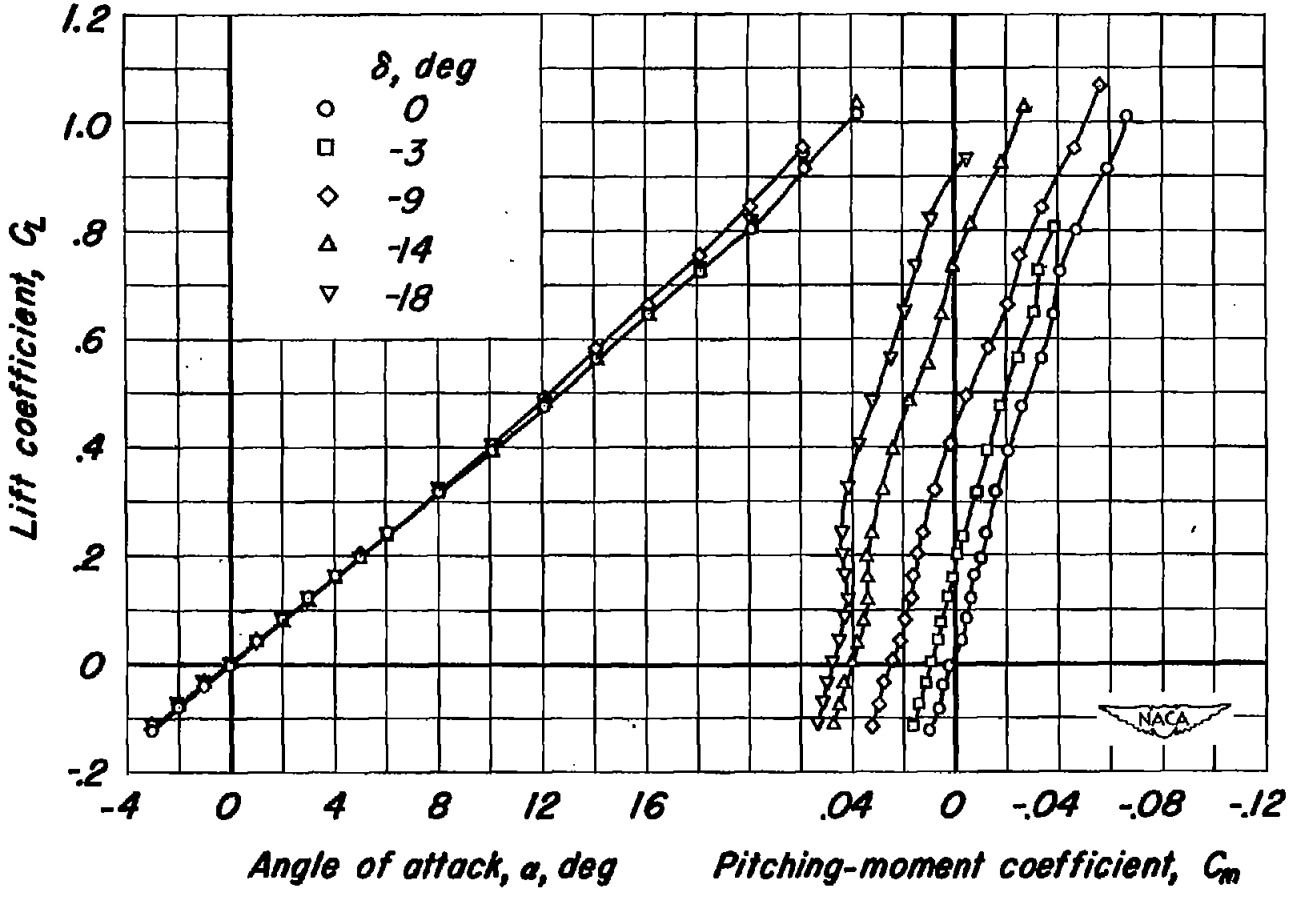

(a) C_L vs α, C_L vs C_m

Figure 9.- The aerodynamic characteristics of the canard model with the horizontal control surface free. Mach number, 0.25; Reynolds number, 8.0 million.

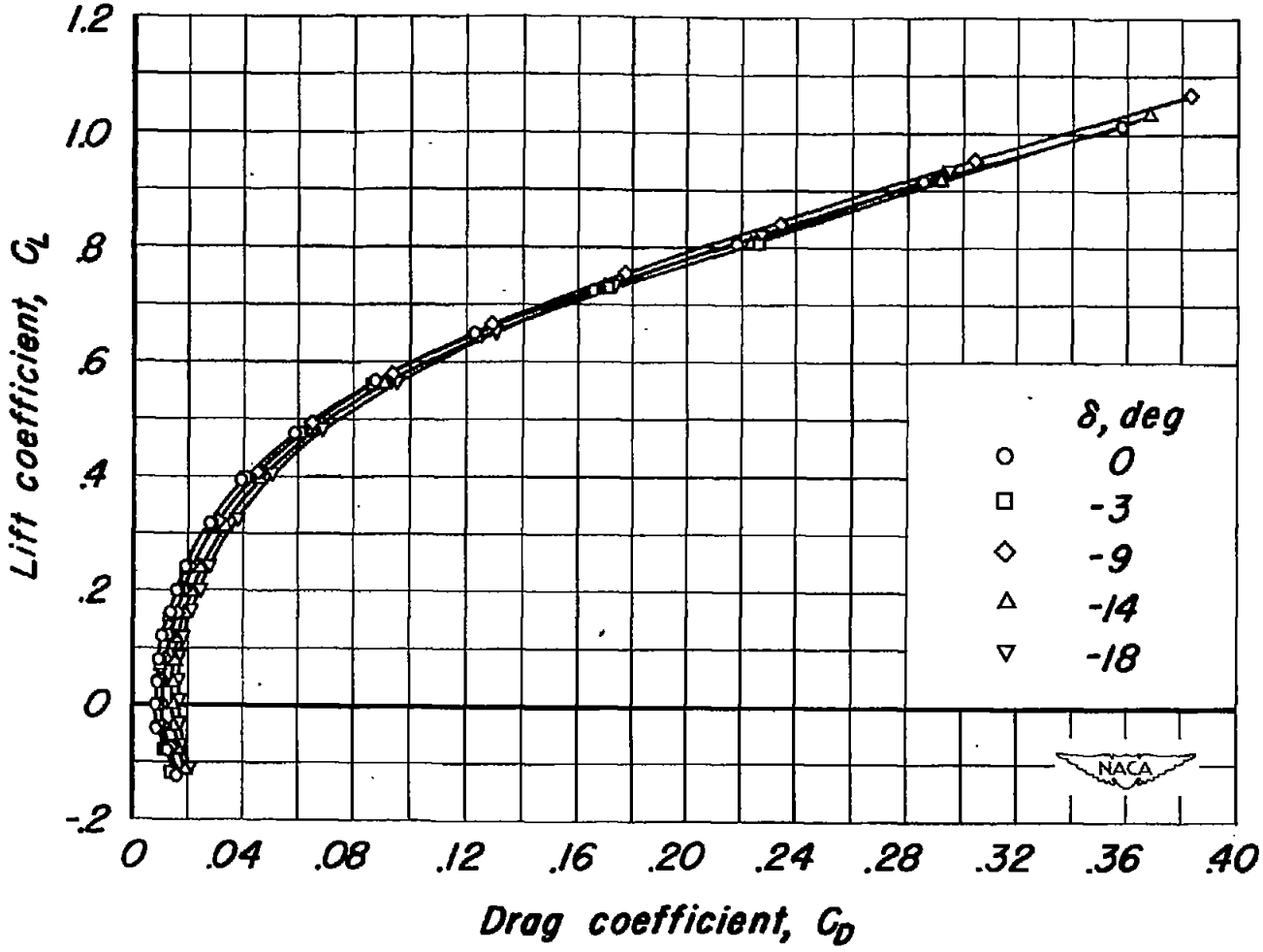

(b) C_L vs C_D

Figure 9.- Concluded.

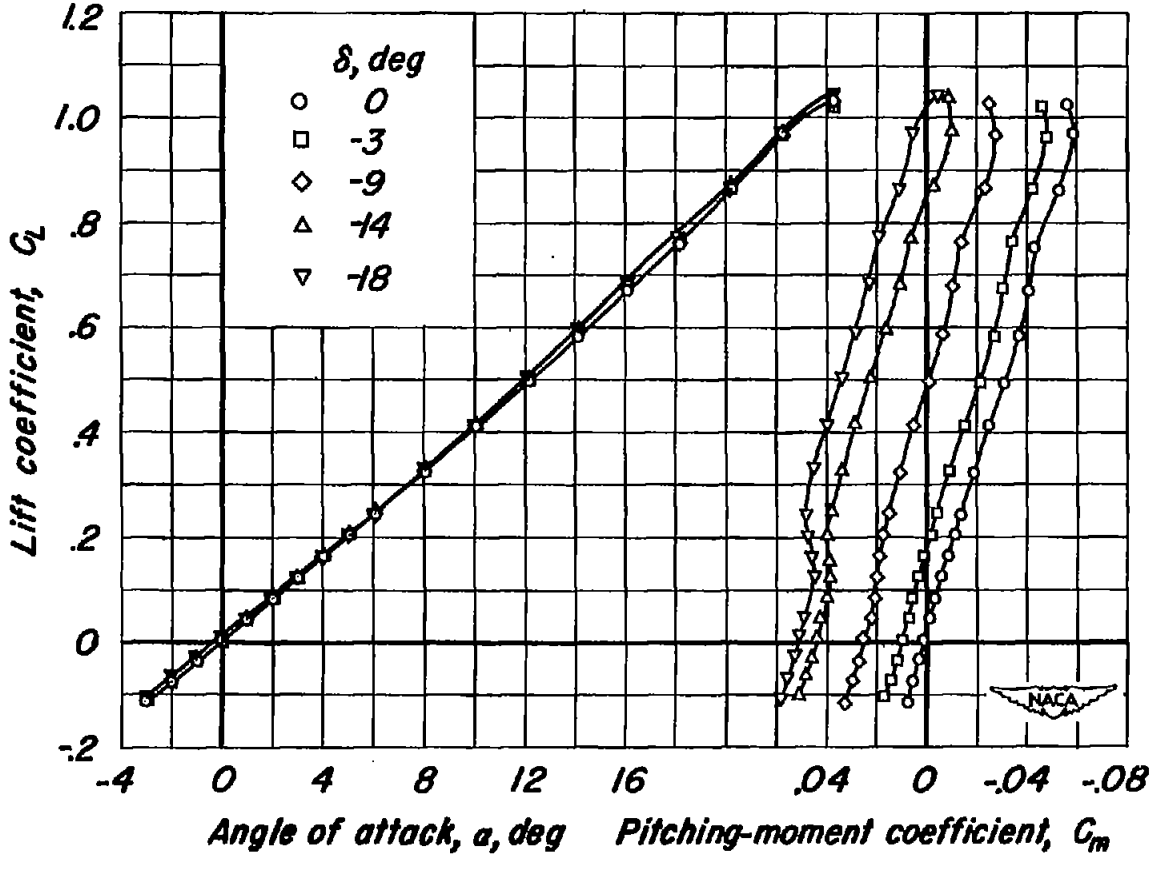

(a) C_L vs α, C_L vs C_m

Figure 10.- The aerodynamic characteristics of the canard model with the horizontal control surface free. Mach number, 0.40; Reynolds number, 3.0 million.

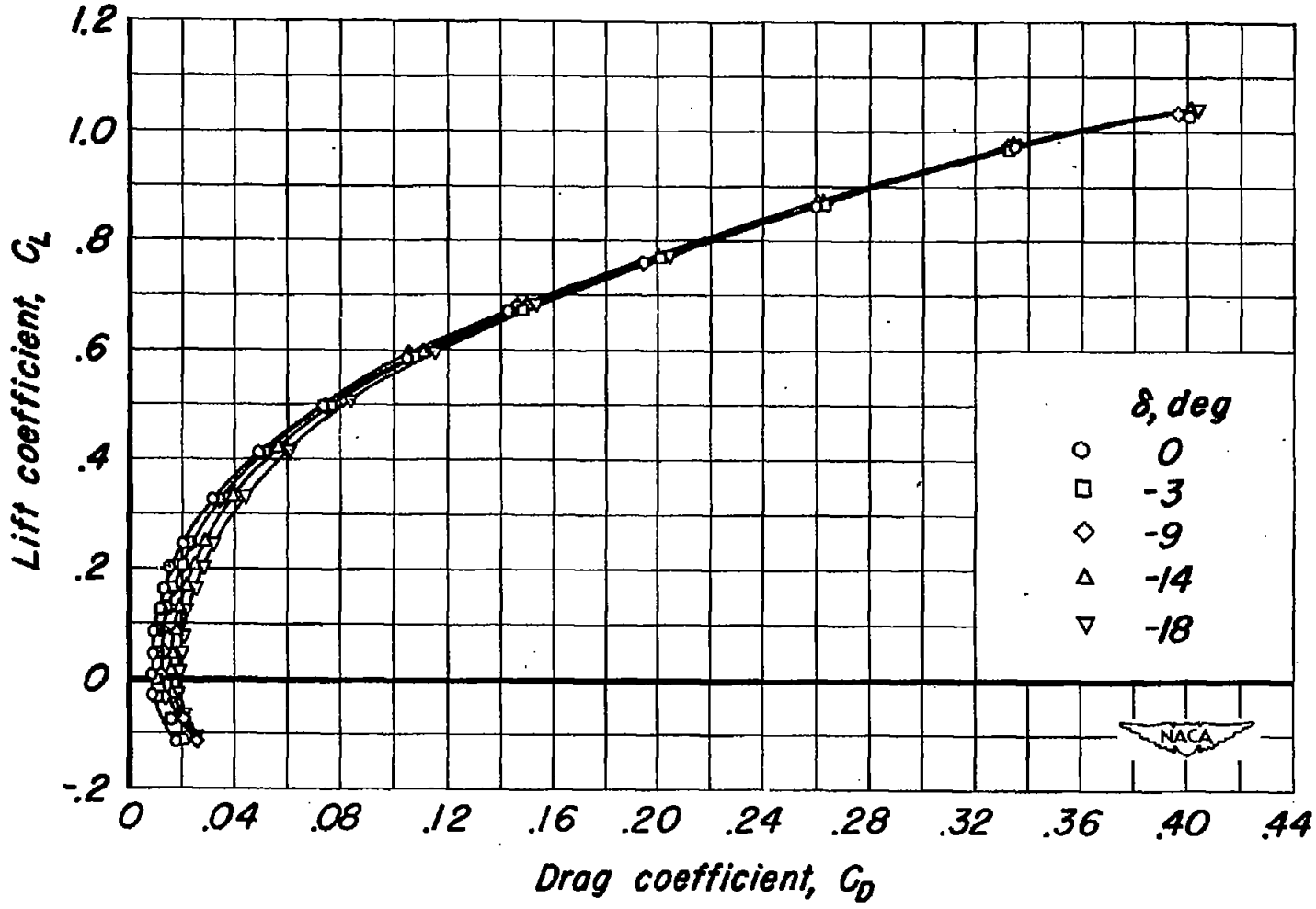

(b) C_L vs C_D

Figure 10.- Concluded.

CONFIDENTIAL

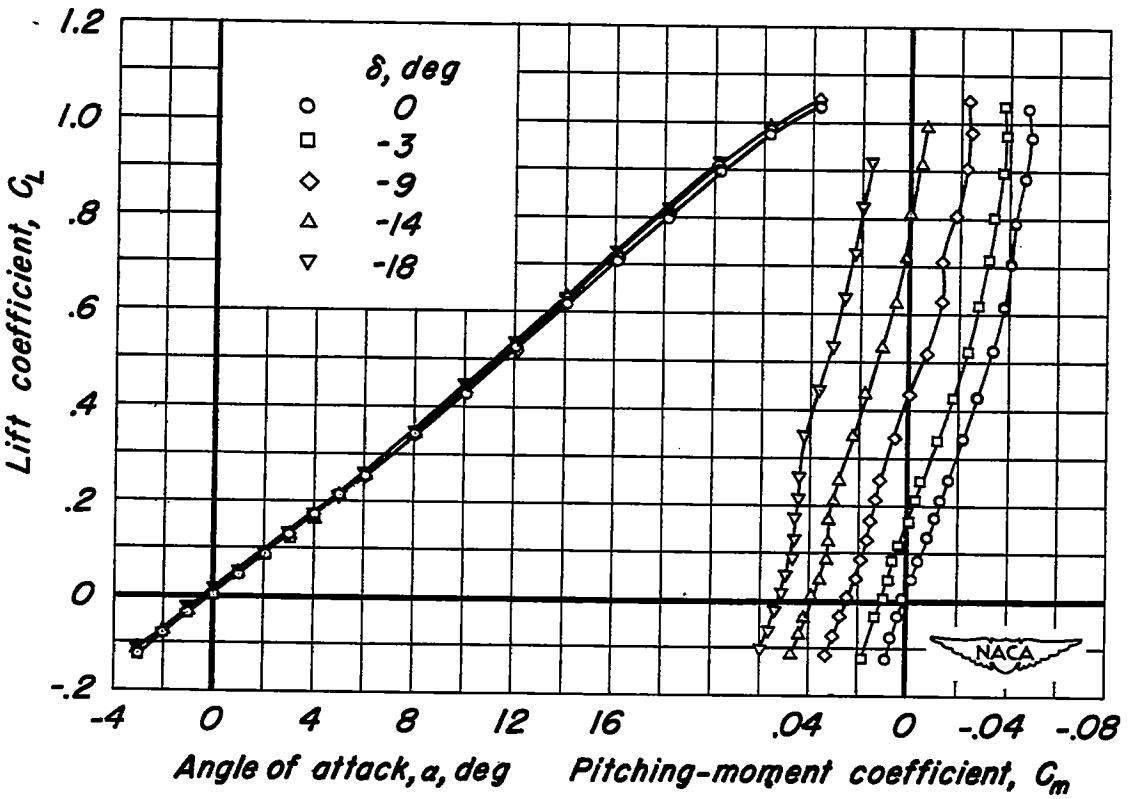

(a) C_L vs a, C_L vs C_m

Figure 11.-The aerodynamic characteristics of the canard model with the horizontal control surface free. Mach number, 0.60; Reynolds number, 3.0 million.

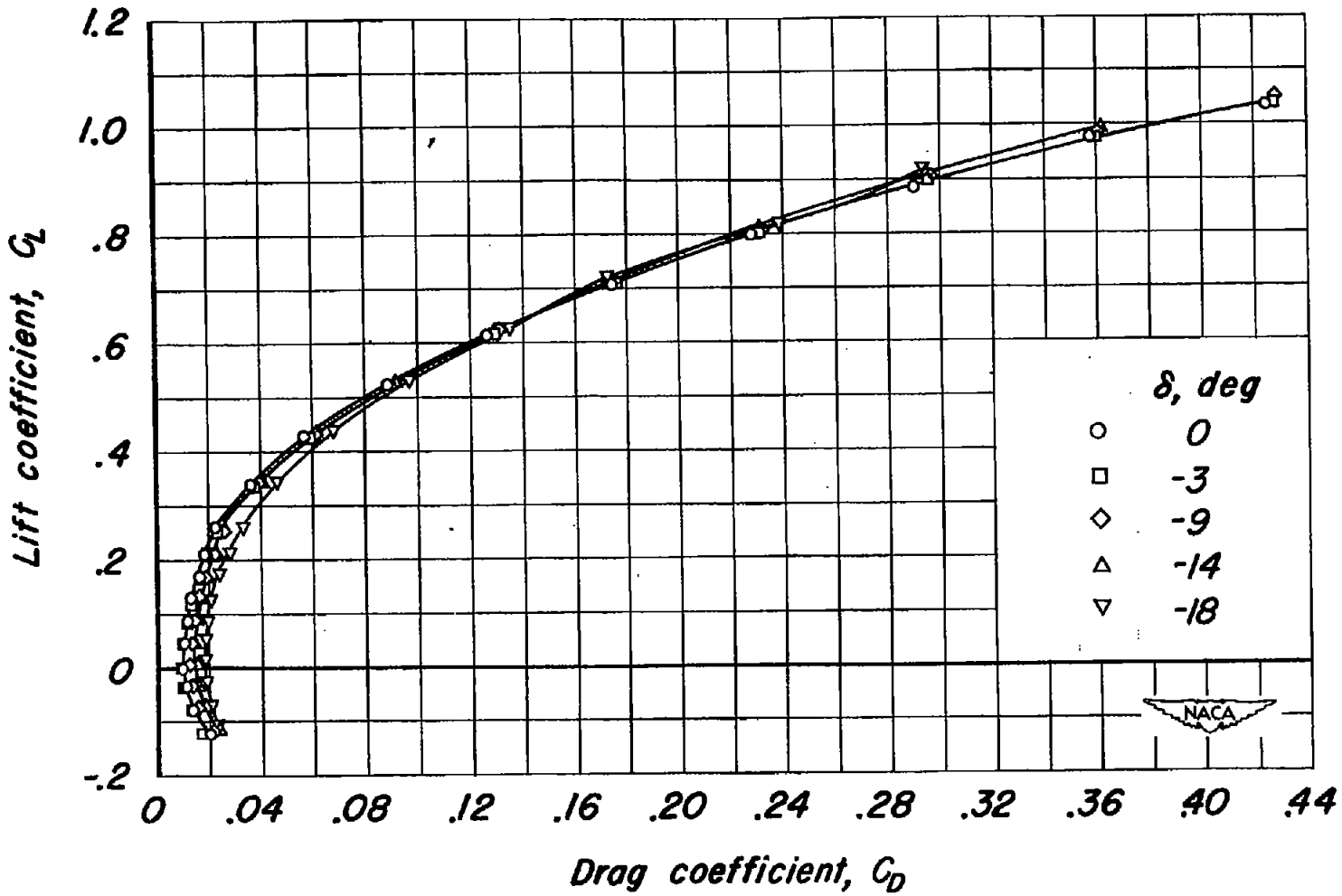

(b) C_L vs C_D

Figure 11.- Concluded.

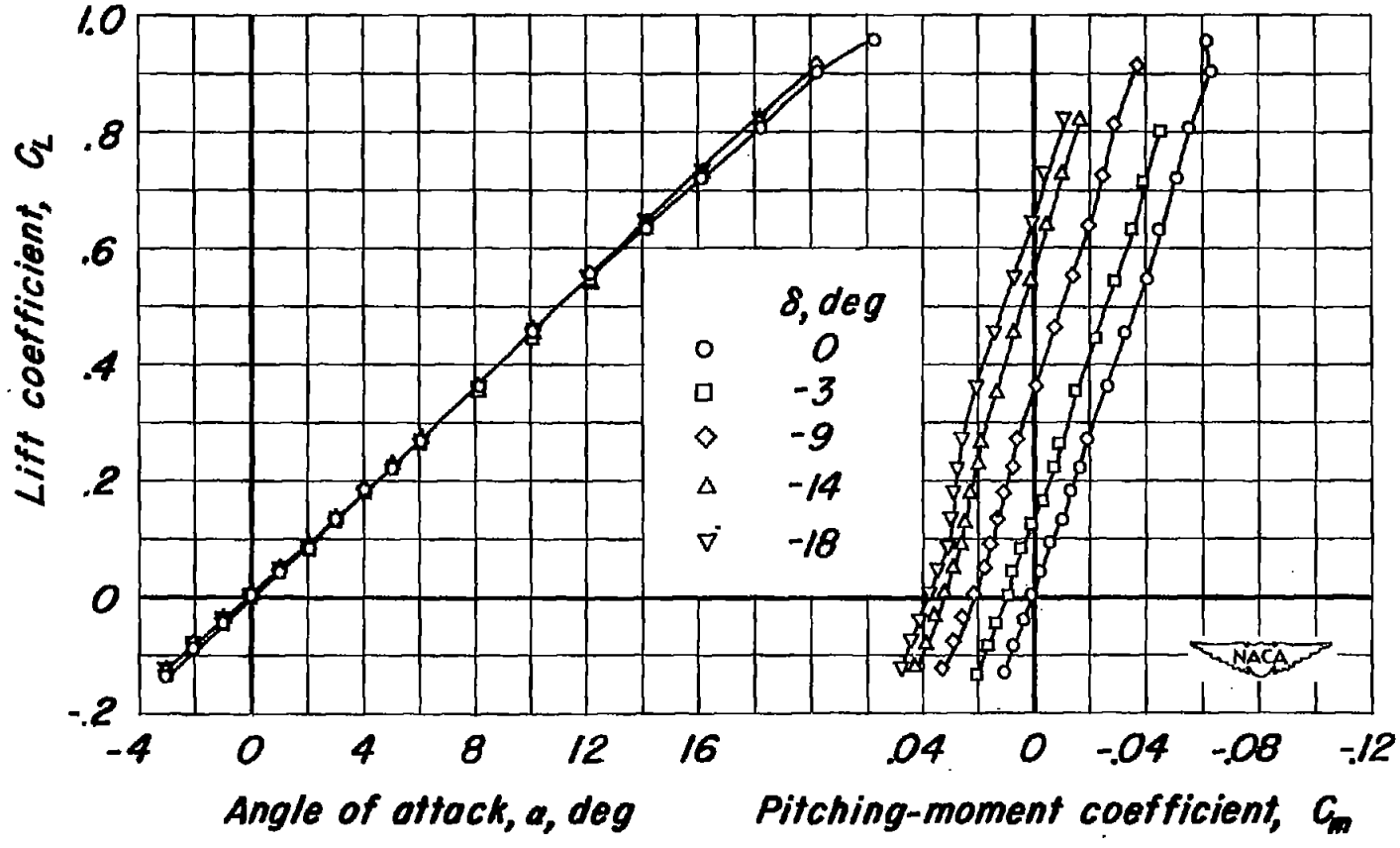

(a) C_L vs α, C_L vs C_m

Figure 12.- The aerodynamic characteristics of the canard model with the horizontal control surface free. Mach number, 0.80; Reynolds number, 3.0 million.

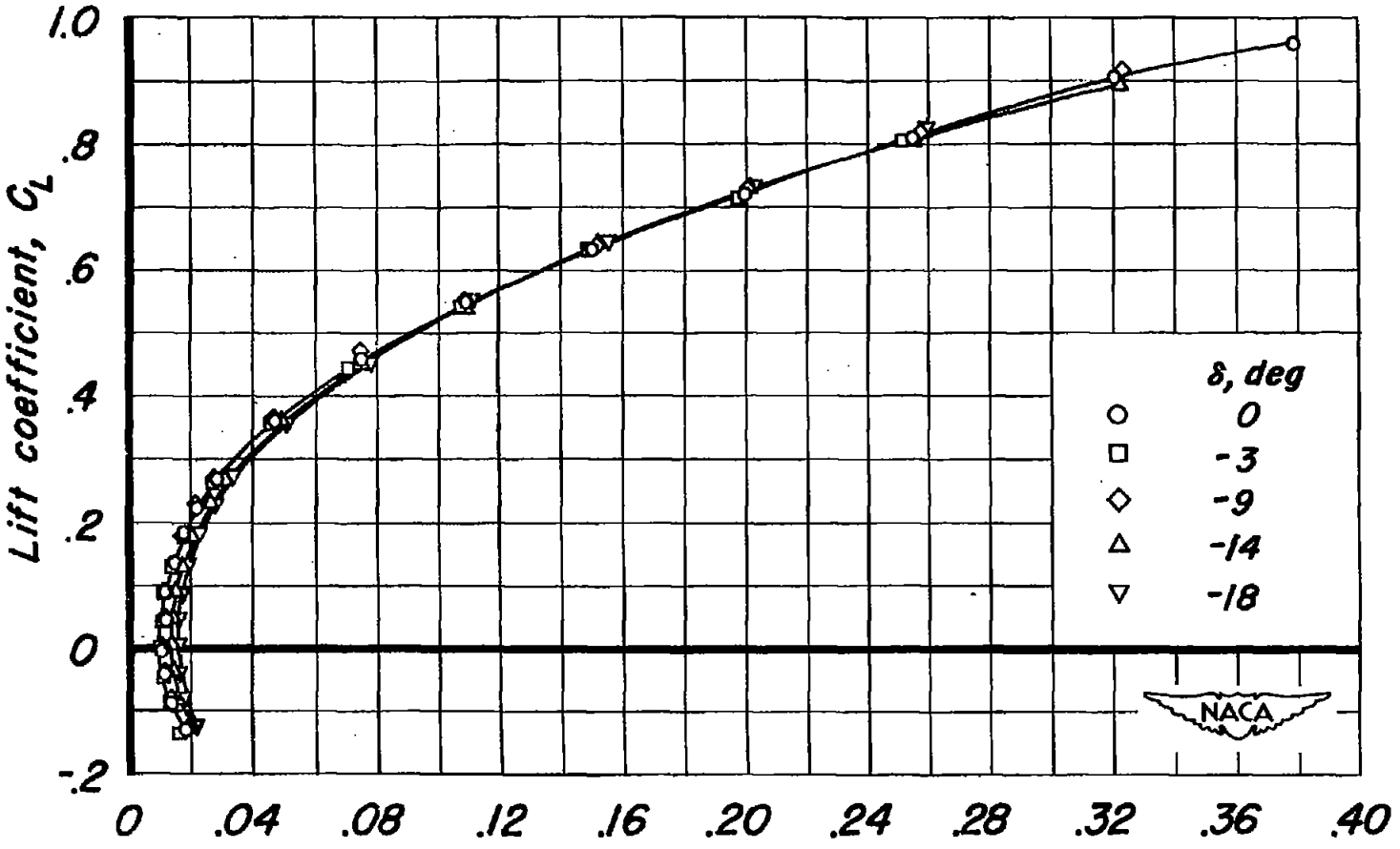

(b) C_L vs C_D

Figure 12.- Concluded.

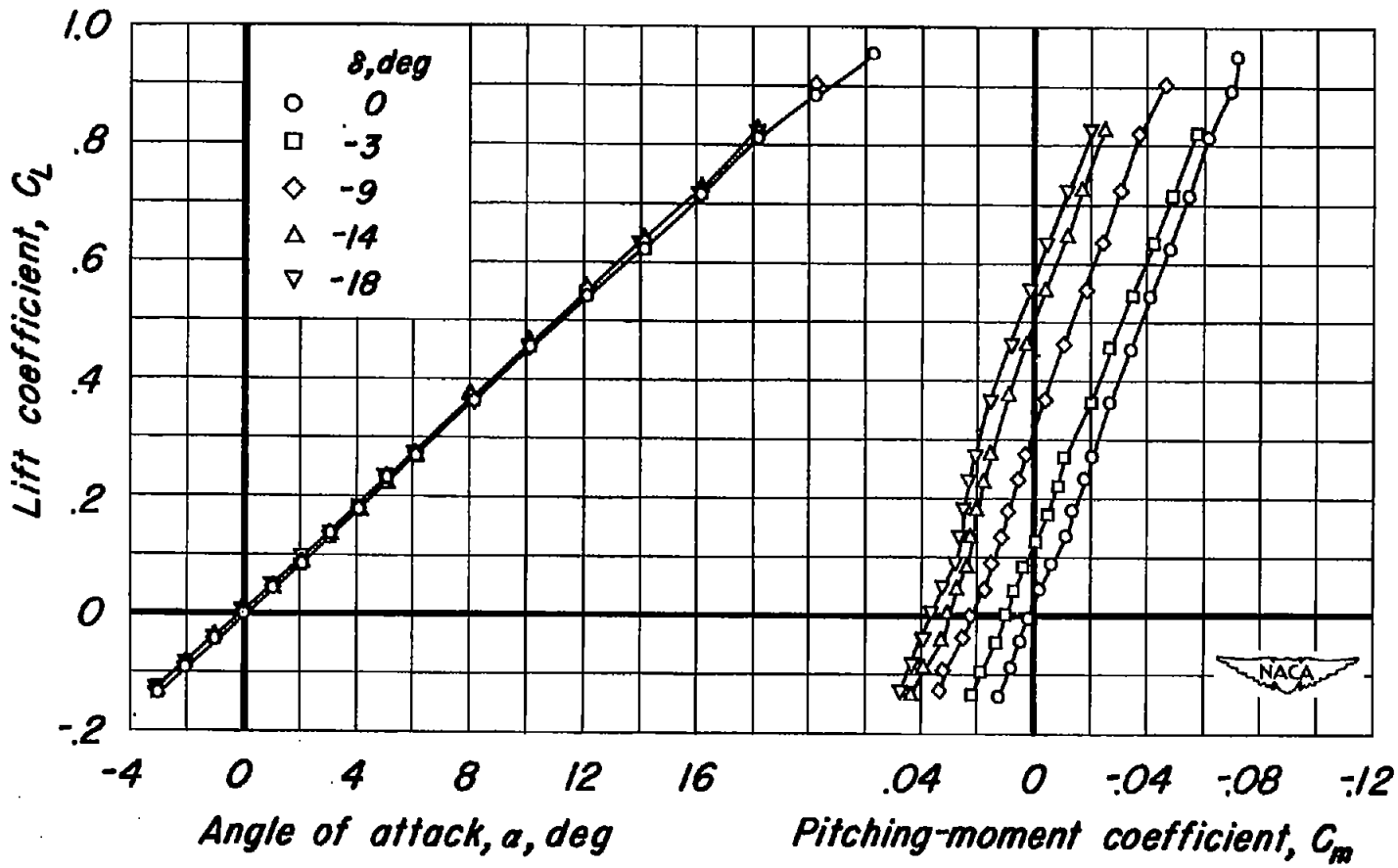

(a) C_L vs α, C_L vs C_m

Figure 13.-The aerodynamic characteristics of the canard model with the horizontal control surface free. Mach number, 0.85; Reynolds number, 3.0 million.

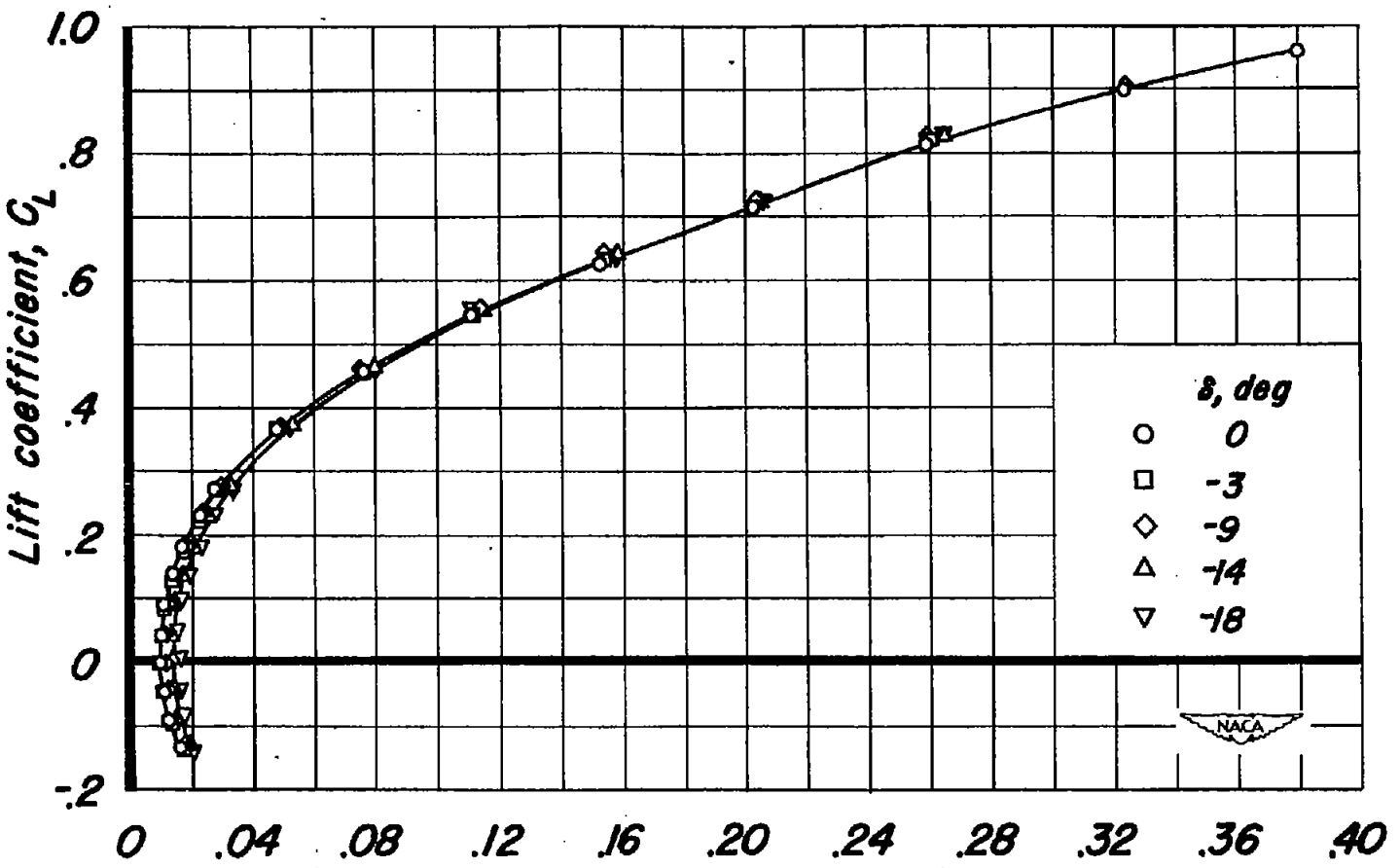

(b) C_L vs C_D

Figure 13.- Concluded.

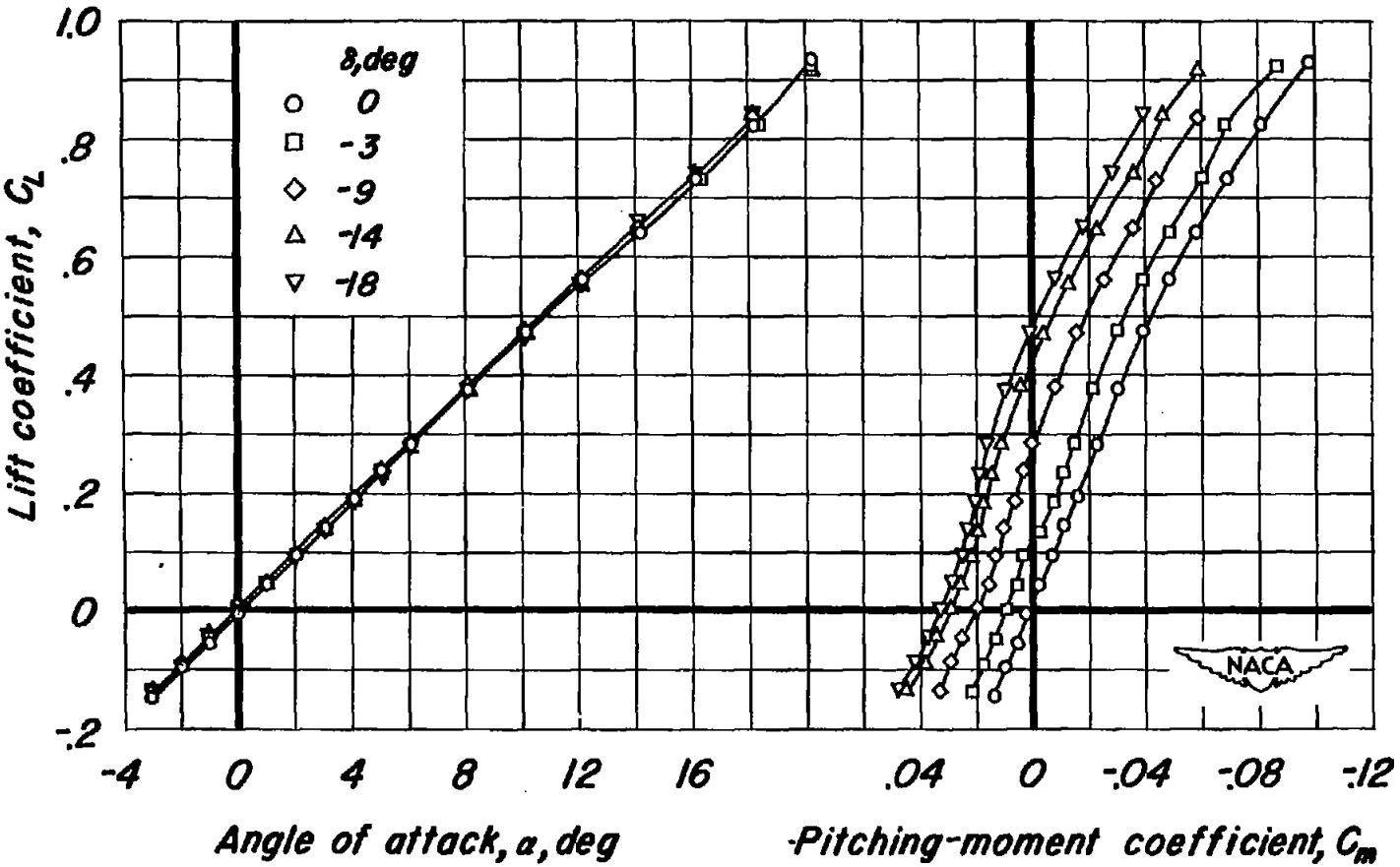

(a) C_L vs α, C_L vs C_m

Figure 14.-The aerodynamic characteristics of the canard model with the horizontal control surface free. Mach number, 0.90; Reynolds number, 3.0 million.

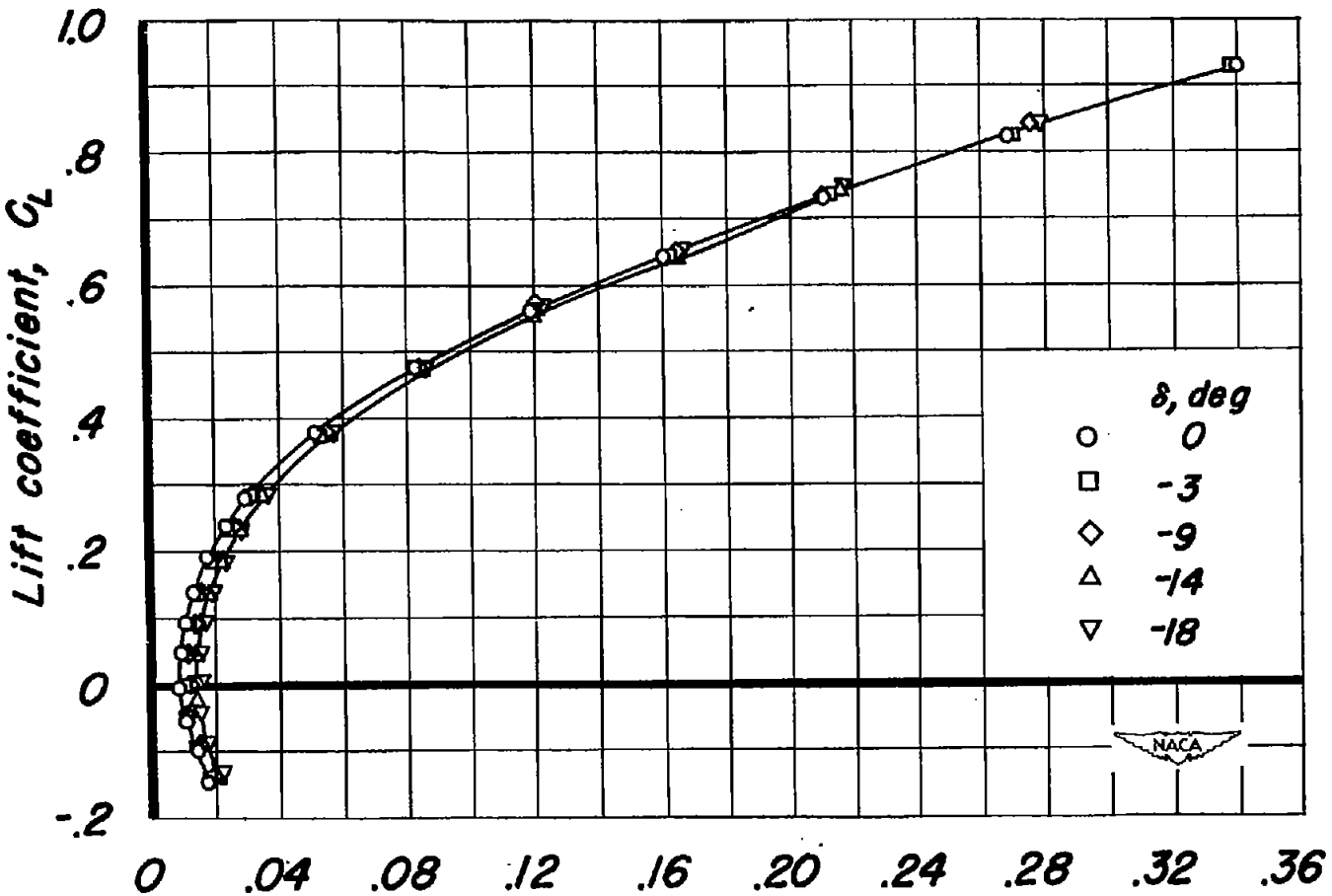

(b) C_L vs C_D

Figure 14.- Concluded.

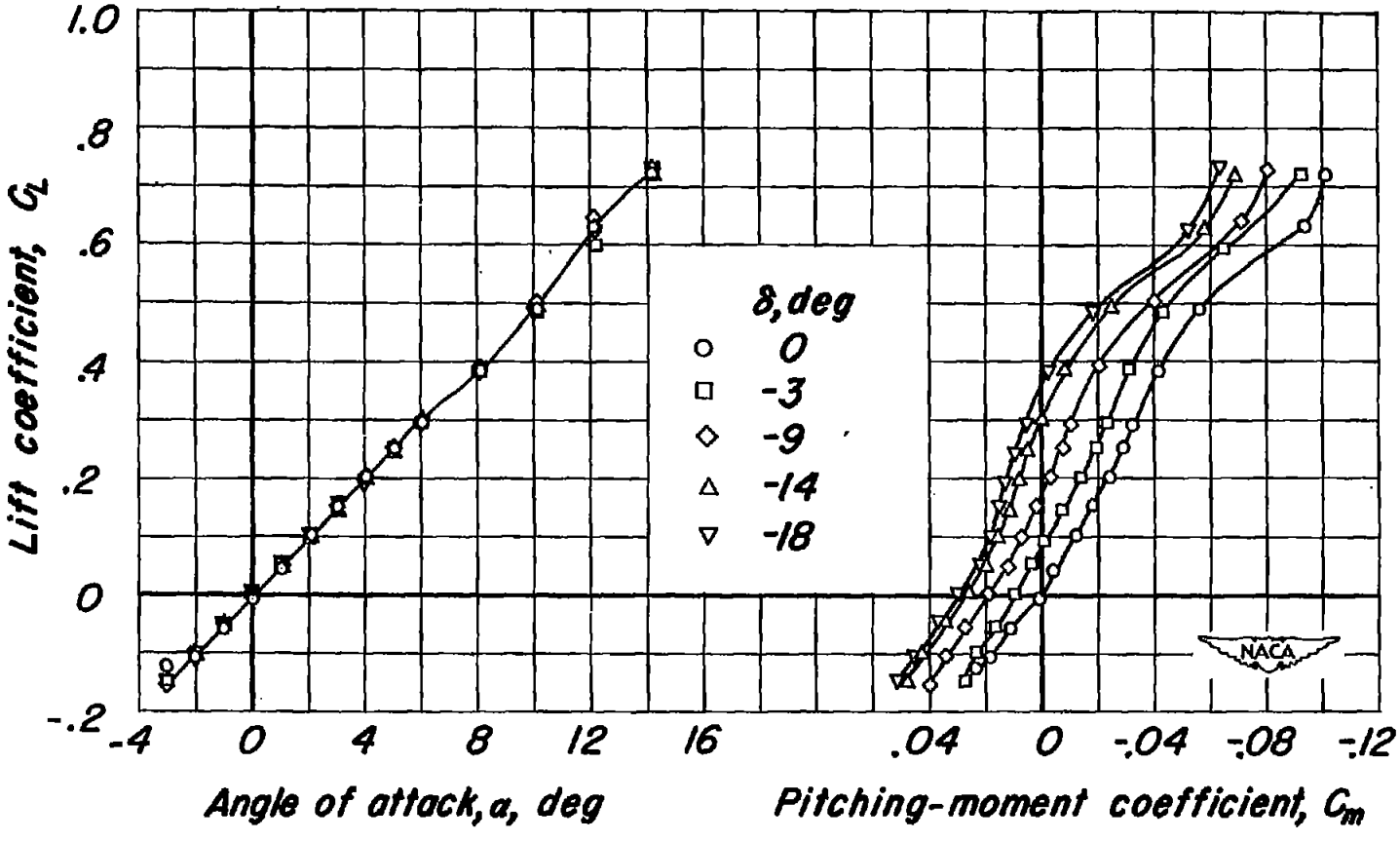

(a) C_L vs α, C_L vs C_m

Figure 15.-The aerodynamic characteristics of the canard model with the horizontal control surface free. Mach number, 0.95; Reynolds number, 3.0 million.

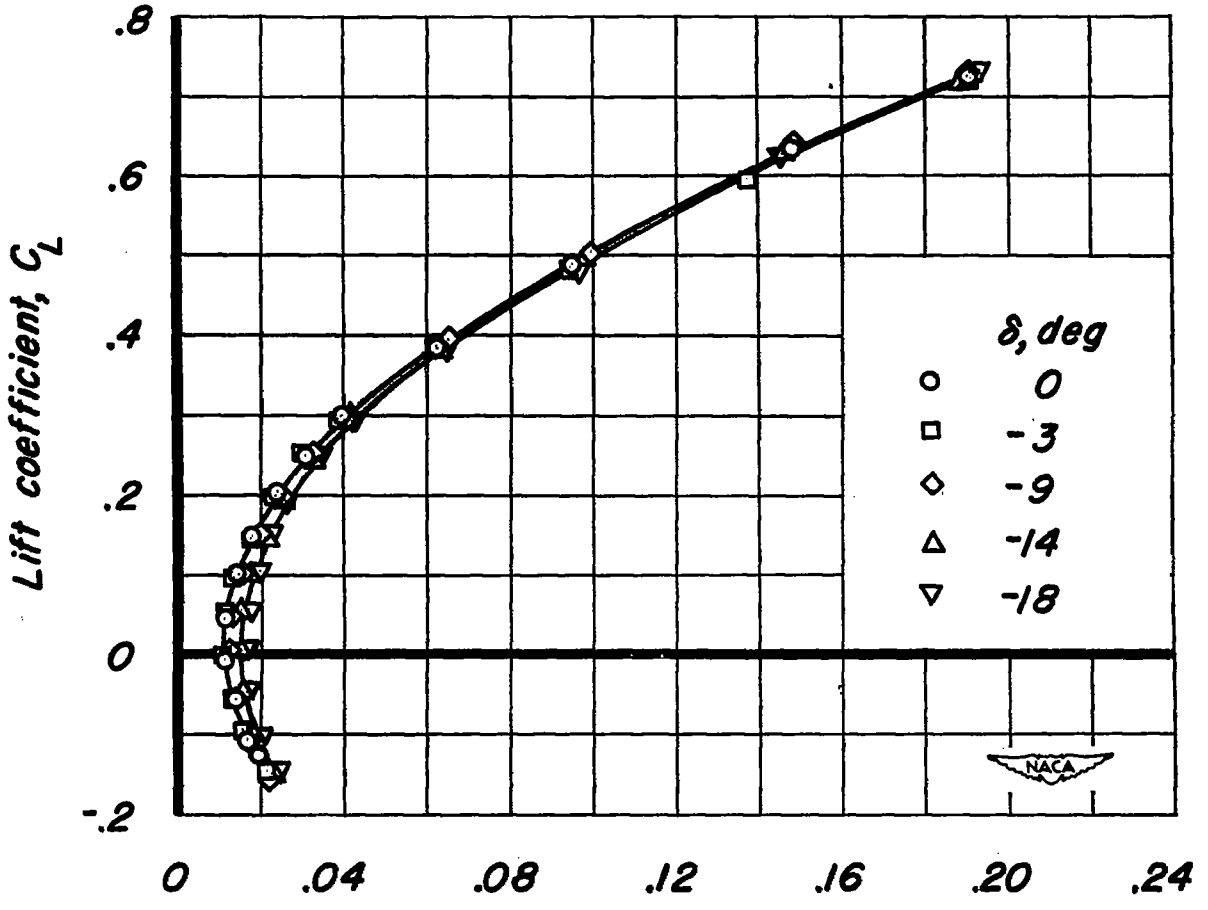

(b) C_L vs C_D

Figure 15.- Concluded.

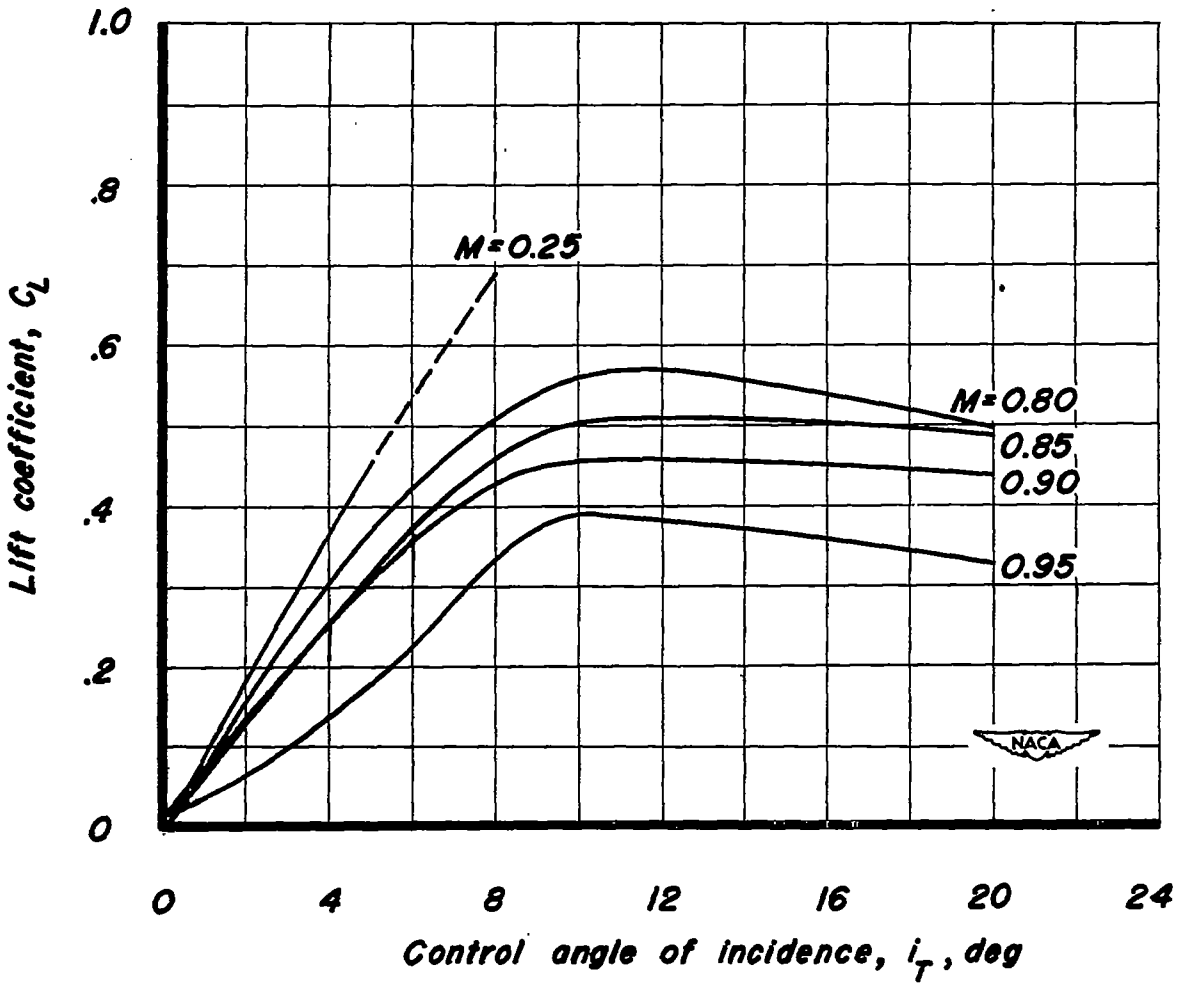

Figure 16.- The variation of the canard model lift coefficient for balance with control angle of incidence for several Mach numbers. Center of gravity at 0.20$\bar{c}$.

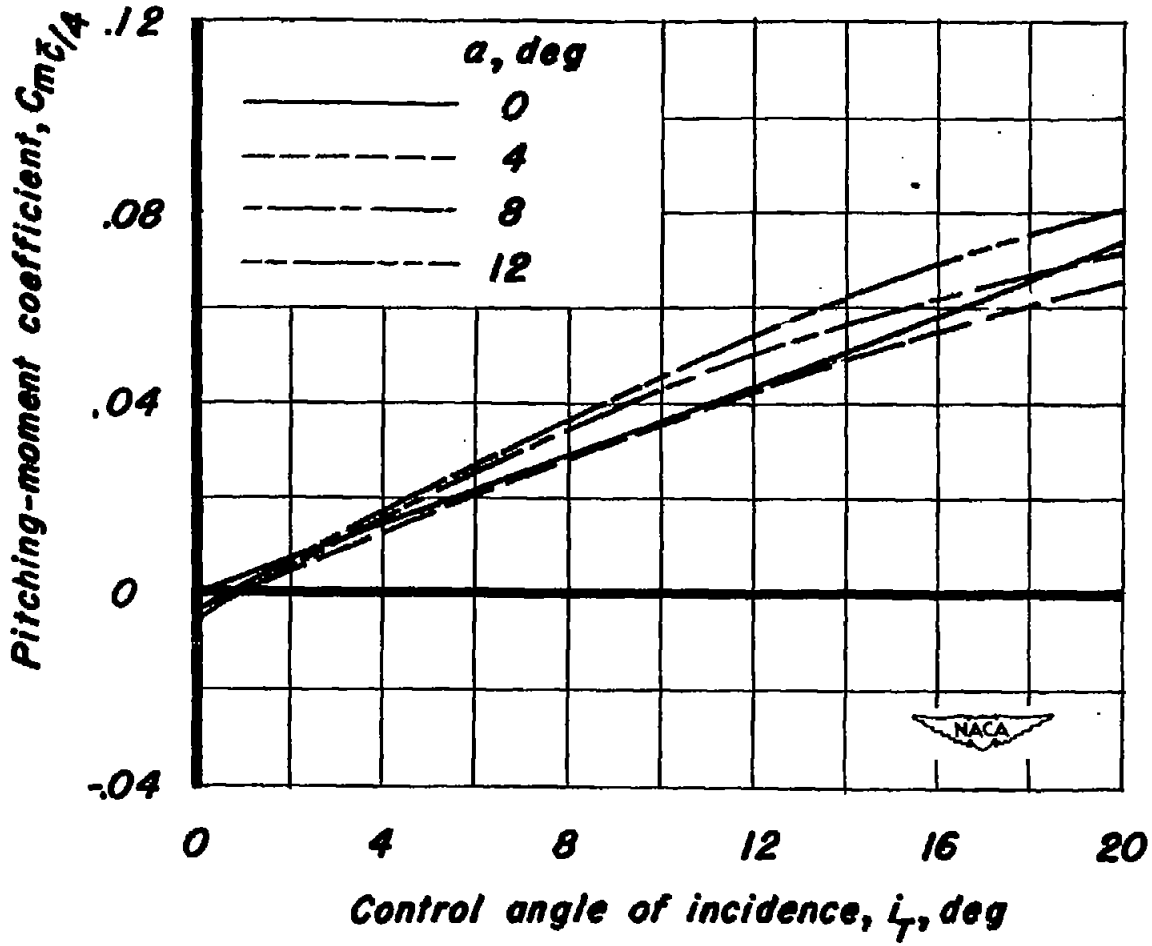

Figure 17.-The variation of pitching-moment coefficient with horizontal-control-surface angle of incidence at several model angles of attack. Mach number, 0.25; Reynolds number, 8.0 million.

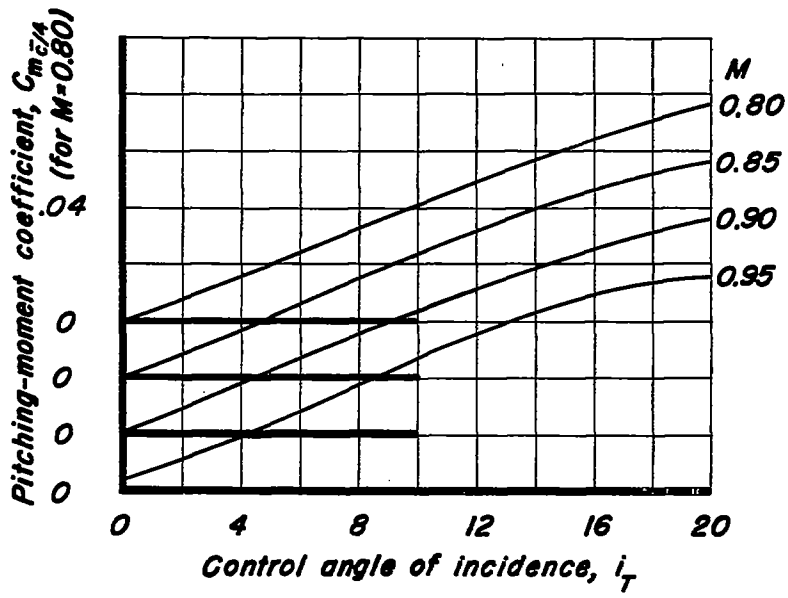

(a) α, 0°

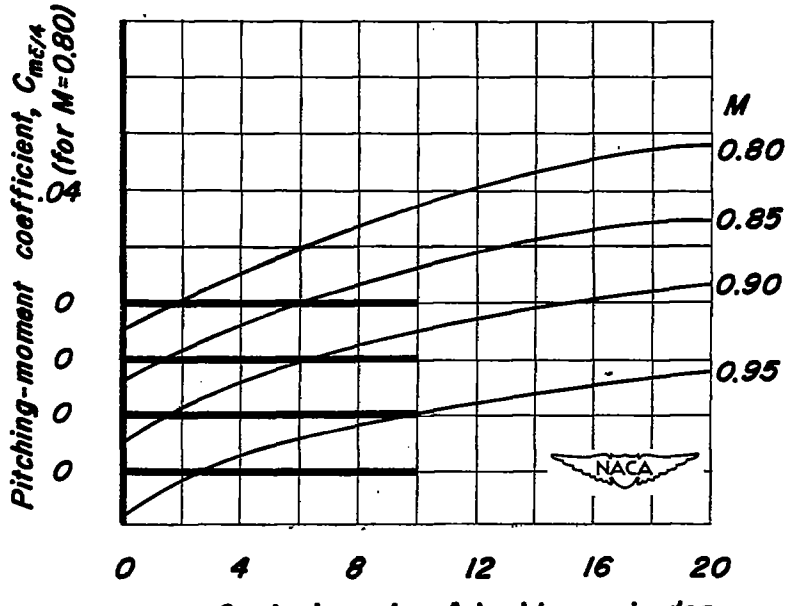

(b) α, 4°

Figure 18.-The variation of pitching-moment coefficient with horizontal-control-surface angle of incidence at various Mach numbers. Reynolds number, 3.0 million.

[redacted]

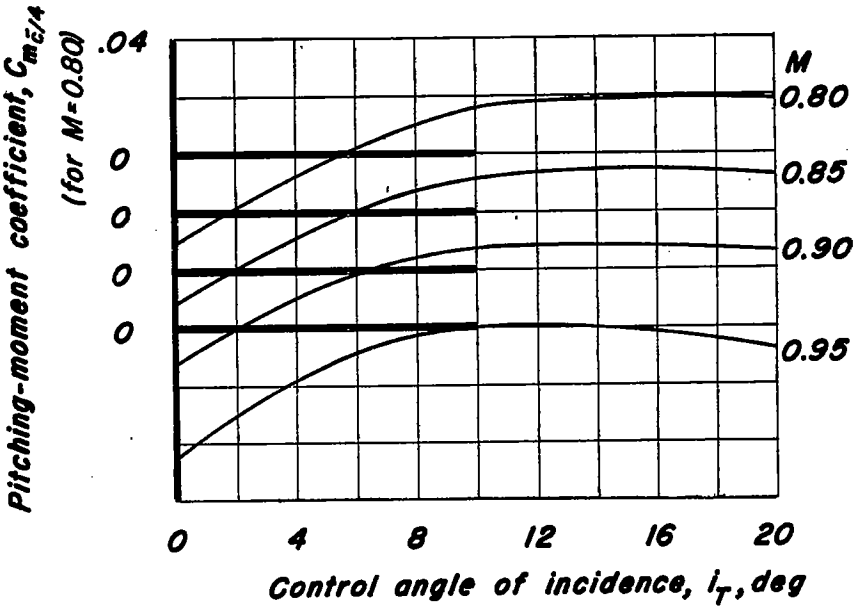

(c) α, 8°

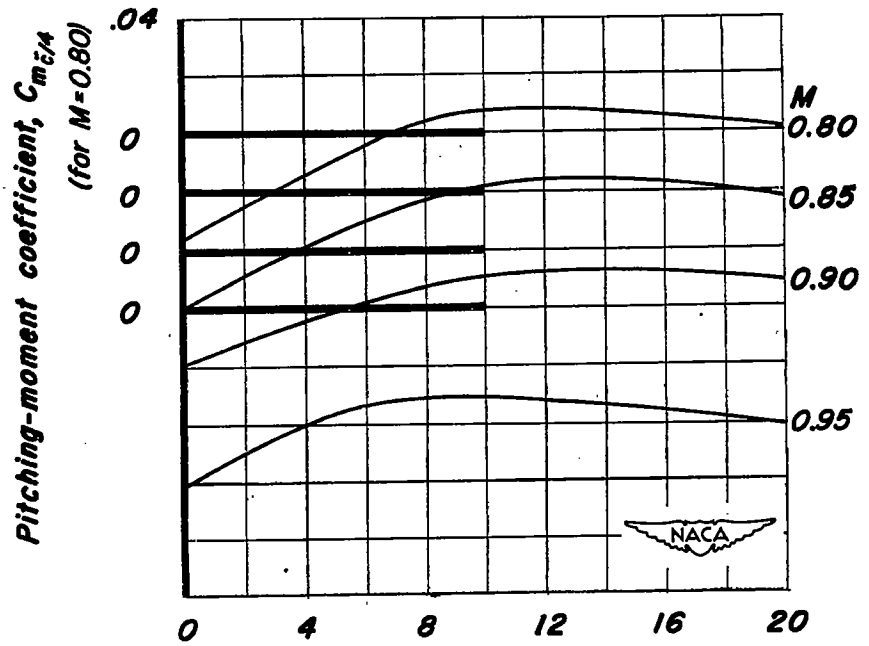

(d) α, 12°

Figure 18.- Concluded.

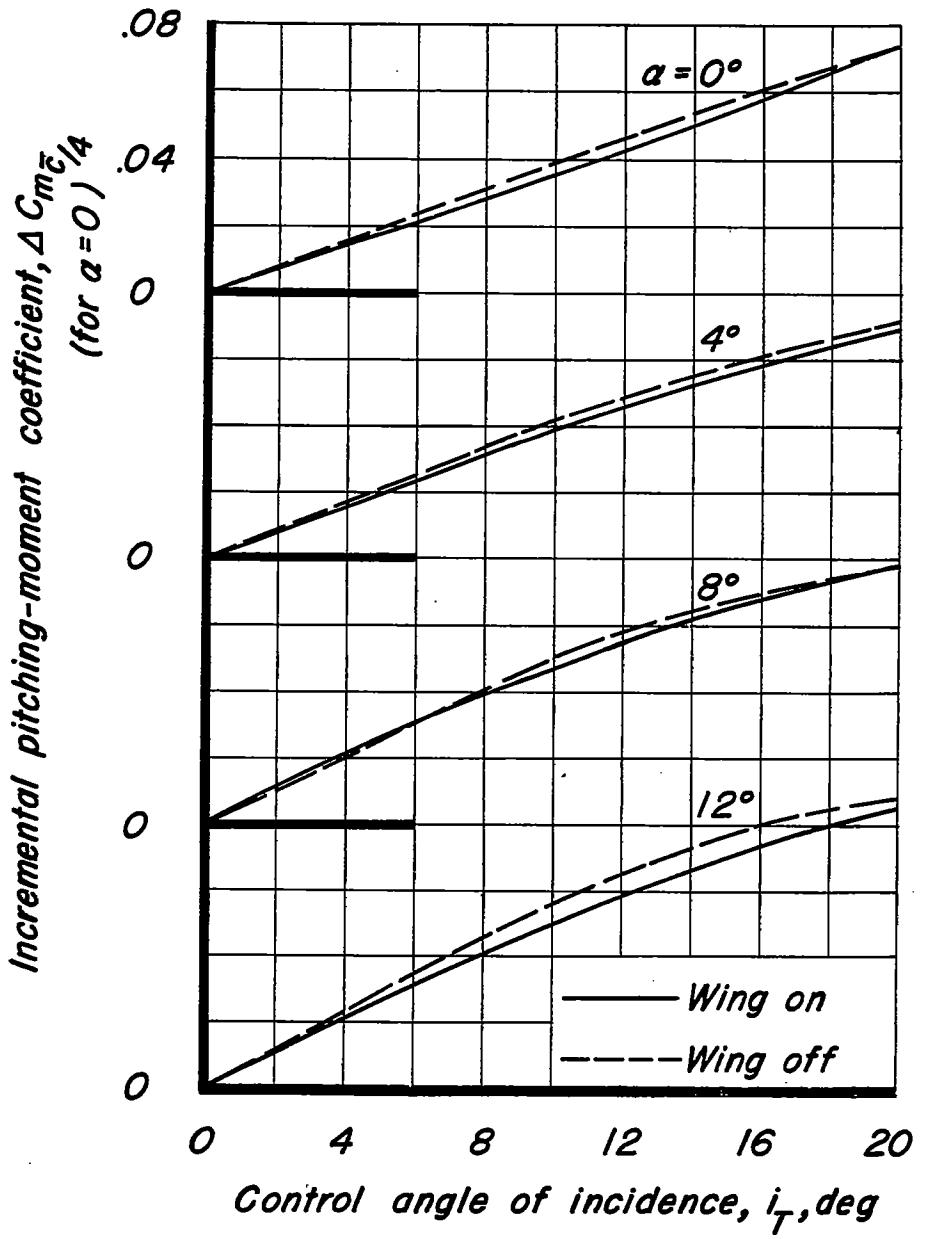

Figure 19.–Comparison of the effectiveness of the irreversible control surface for the canard model with the wing on and with the wing off. Mach number, 0.25; Reynolds number, 8.0 million.

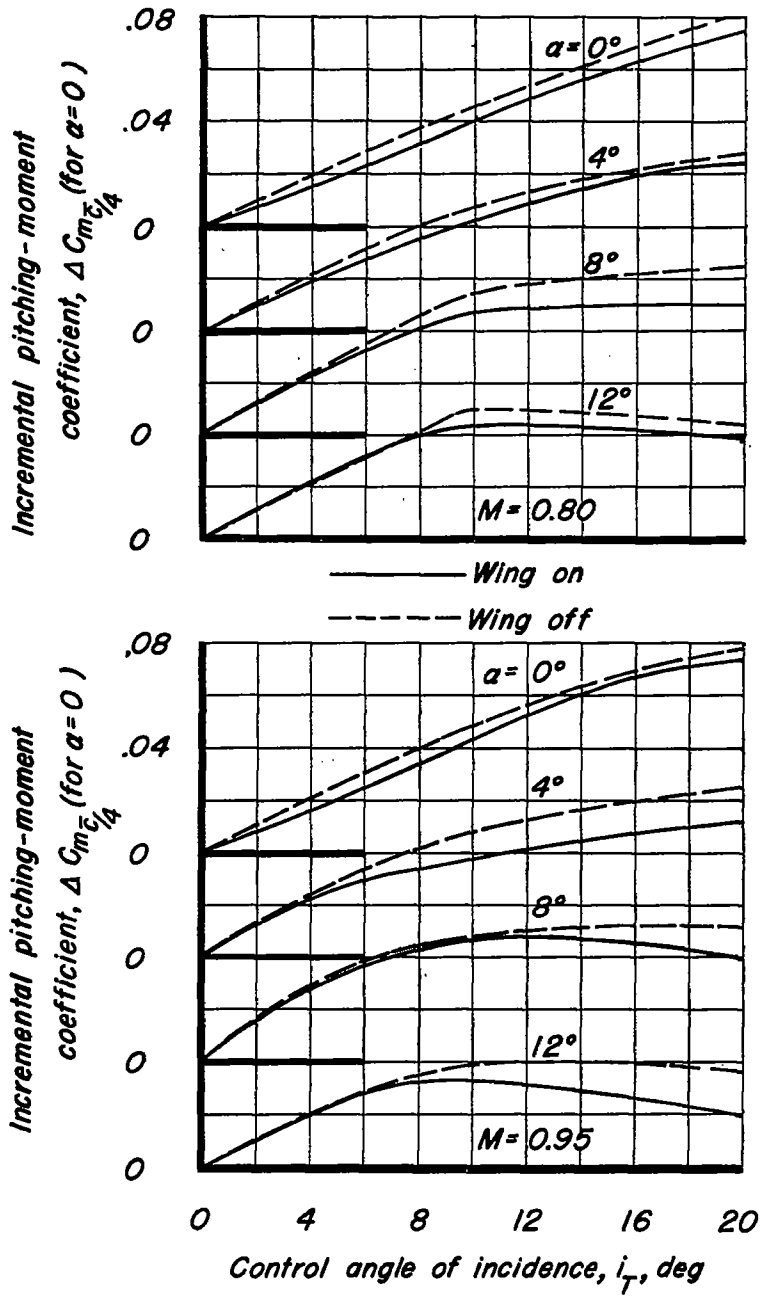

Figure 20.–Comparison of the effectiveness of the irreversible control surface for the canard model with the wing on and with the wing off. Reynolds number, 3.0 million.

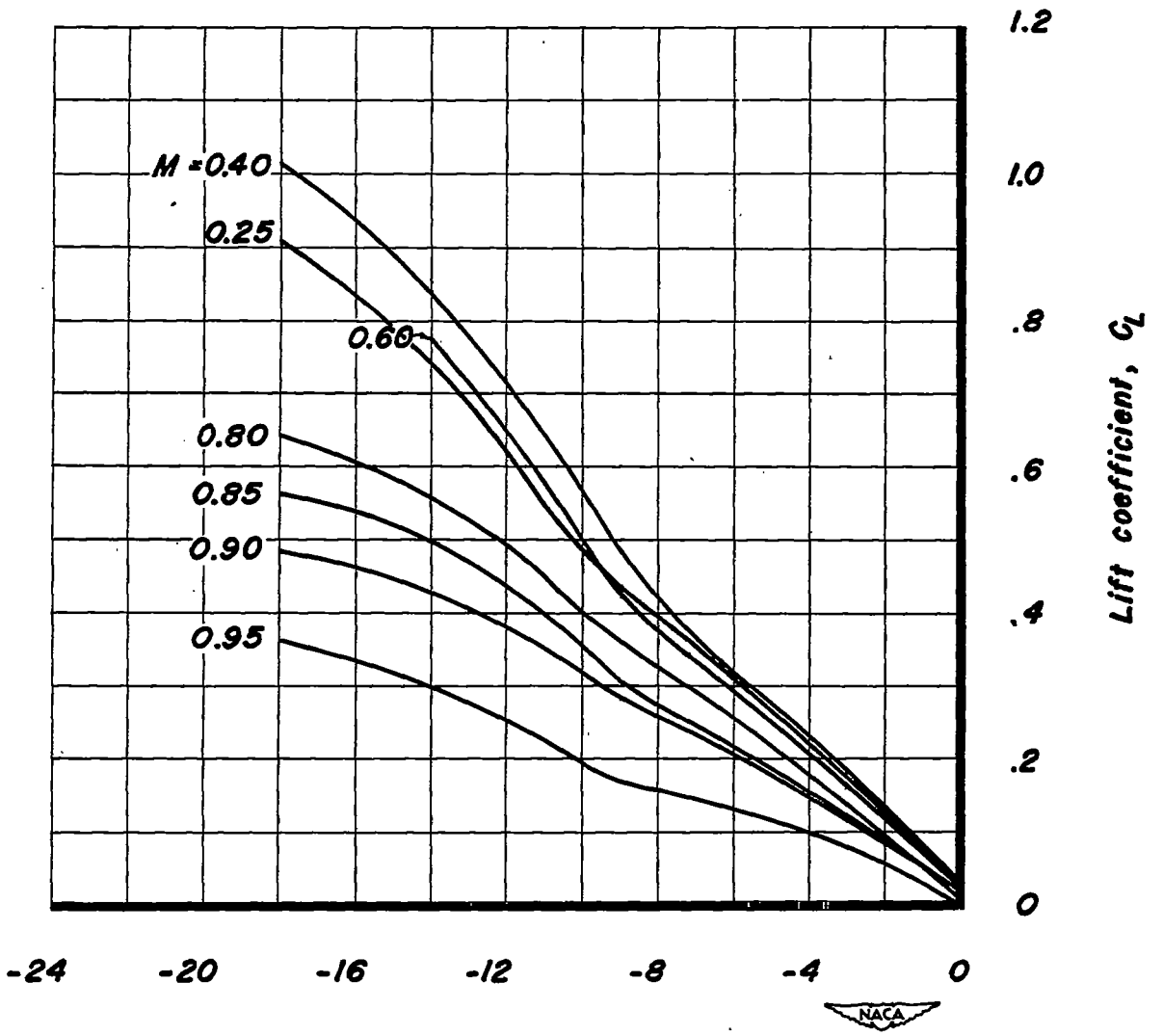

Figure 21.- The variation of the canard-model lift coefficient for balance with split-flap angle for several Mach numbers. Center of gravity at 0.32$\bar{c}$.

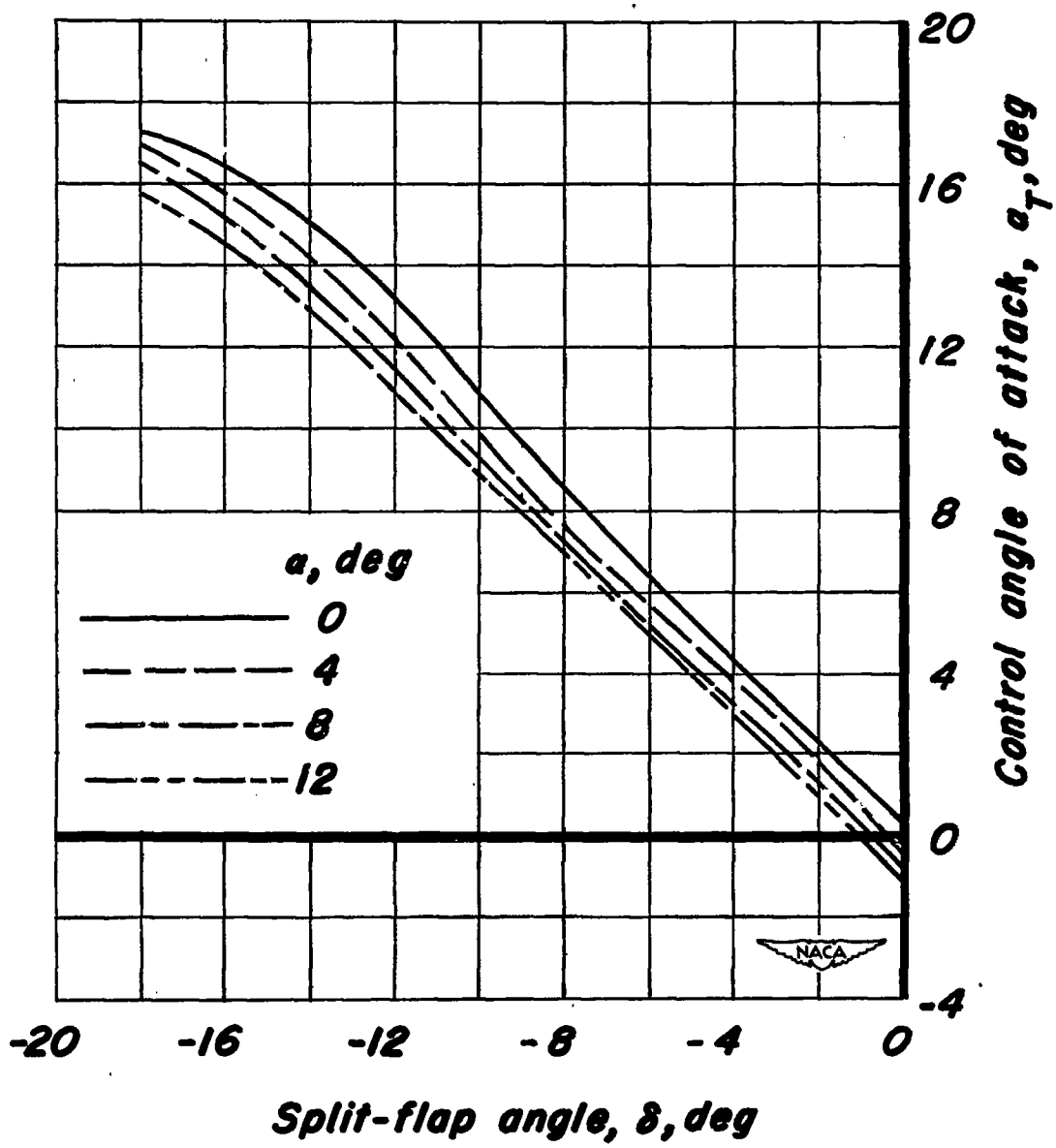

Figure 22.- The variation of the free-floating-control-surface angle of attack with split-flap angle at several model angles of attack. Mach number, 0.25; Reynolds number, 8.0 million.

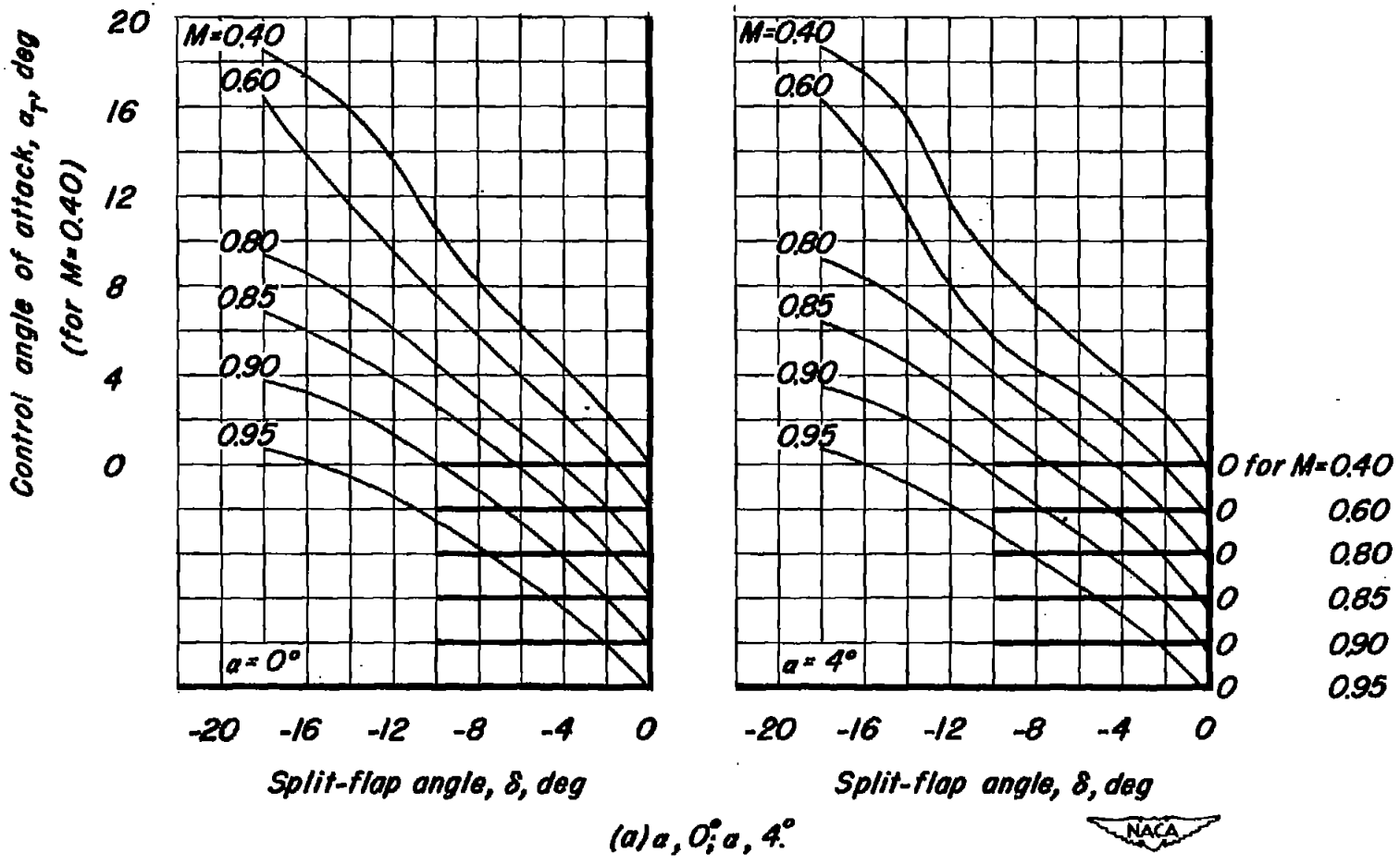

Figure 23.-The variation of the angle of attack of the free-floating control surface with split-flap angle at several Mach numbers. Reynolds number, 3.0 million.

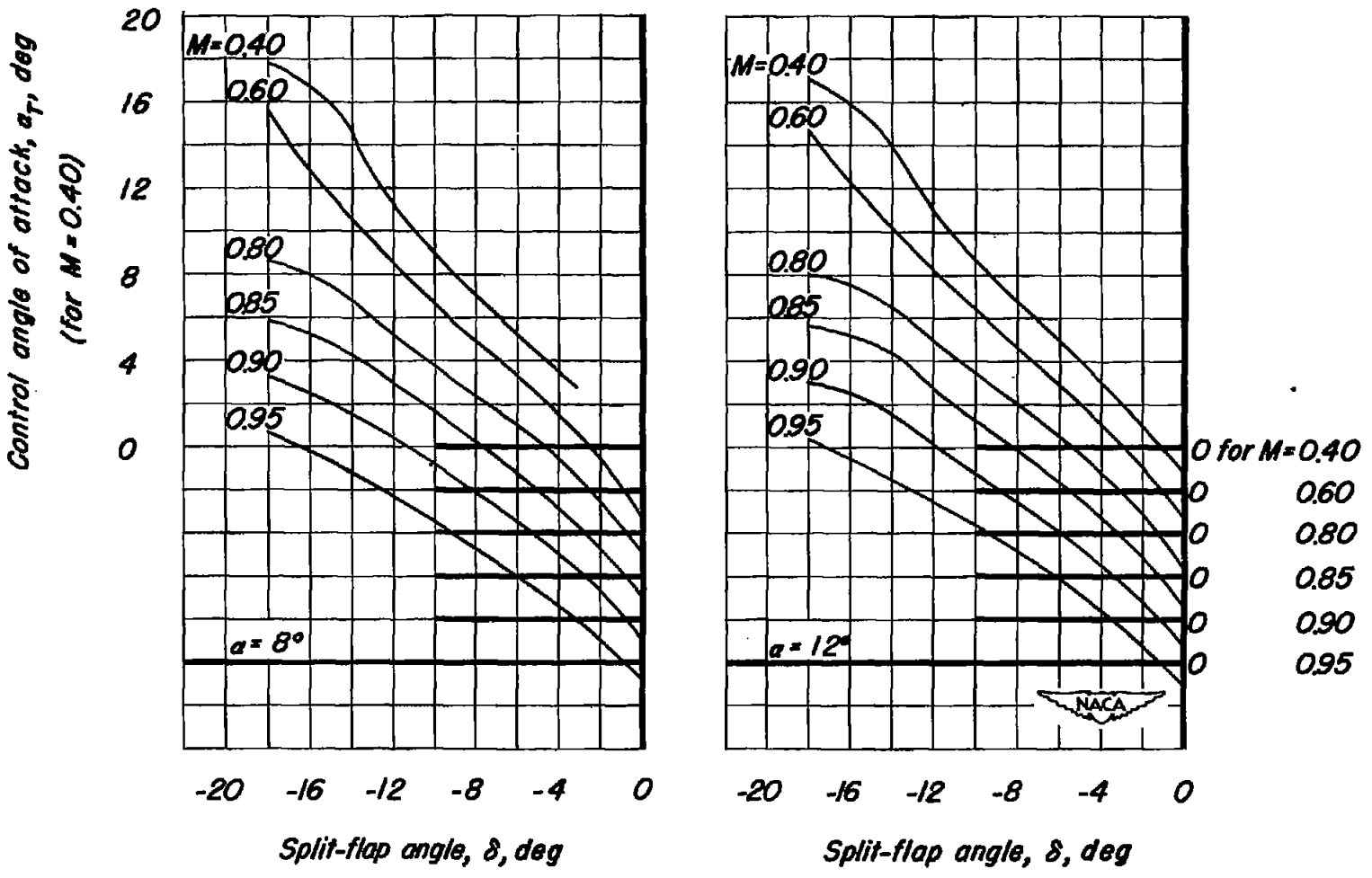

(b) α, 8°; α, 12°.

Figure 23.-Concluded.

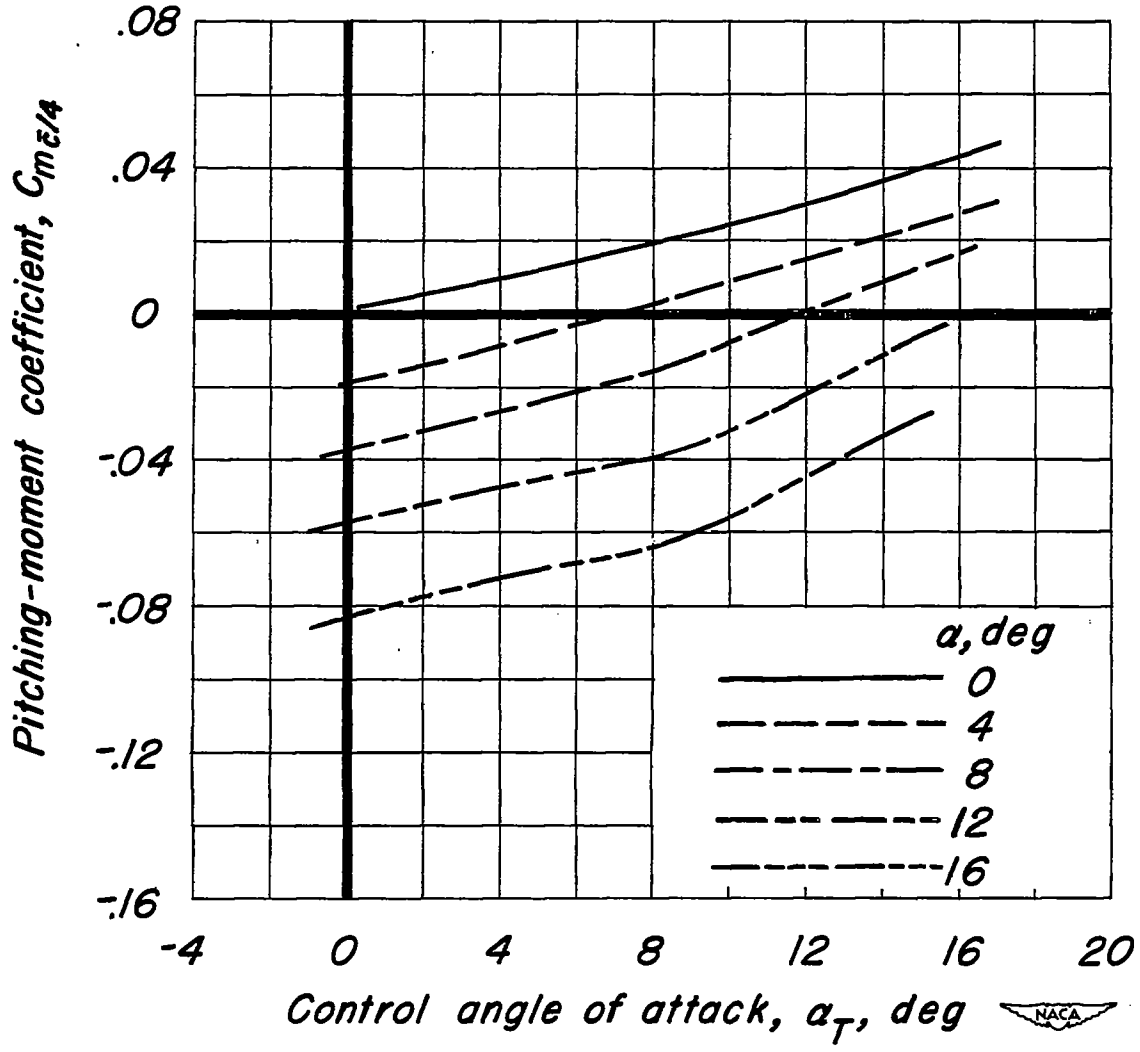

Figure 24.-The variation with horizontal-control-surface angle of attack of the pitching-moment coefficient of the canard model with the control surface free. Mach number, 0.25; Reynolds number, 8.0 million.

[redacted]

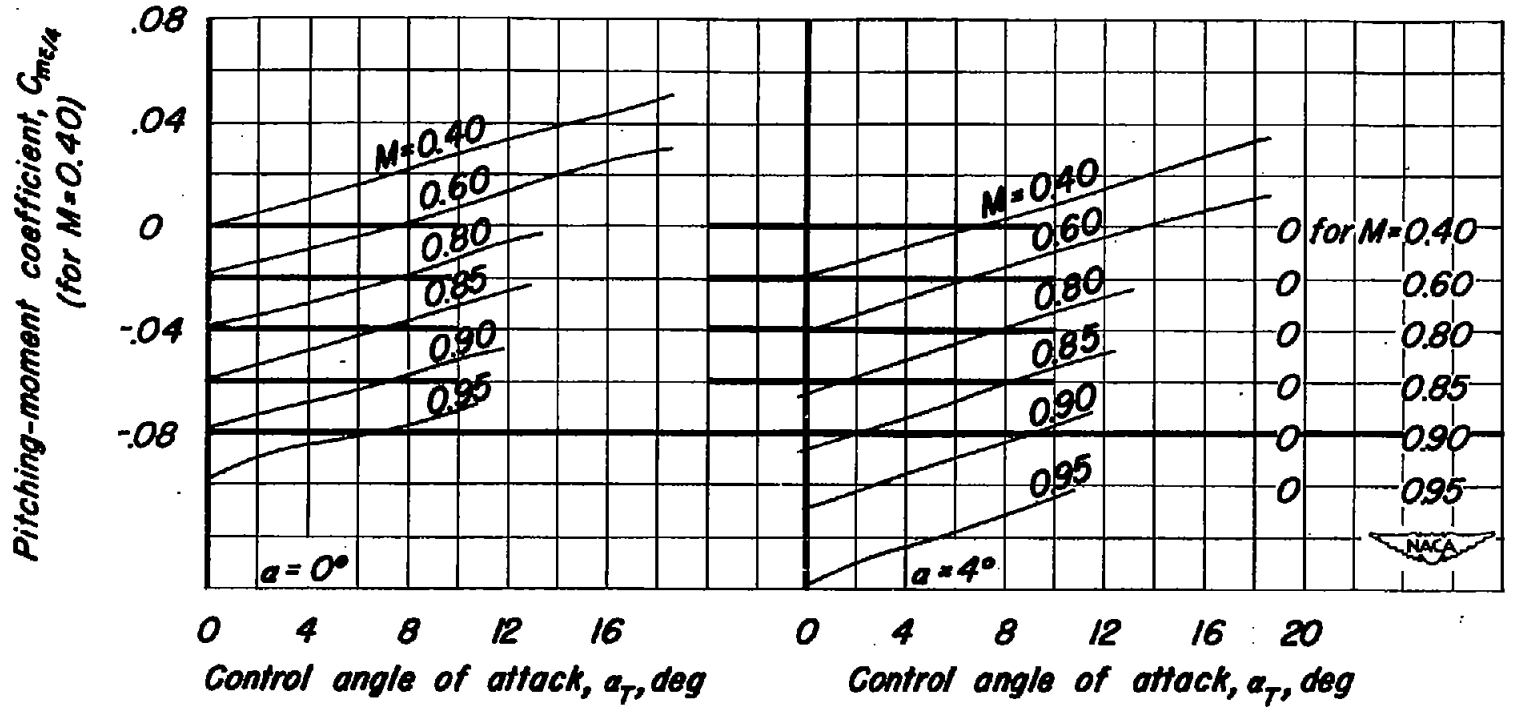

(a) α, 0°; α, 4°.

Figure 25.- The variation with horizontal-control-surface angle of attack of the pitching-moment coefficient of the canard model with the control-surface free. Reynolds number, 3.0 million.

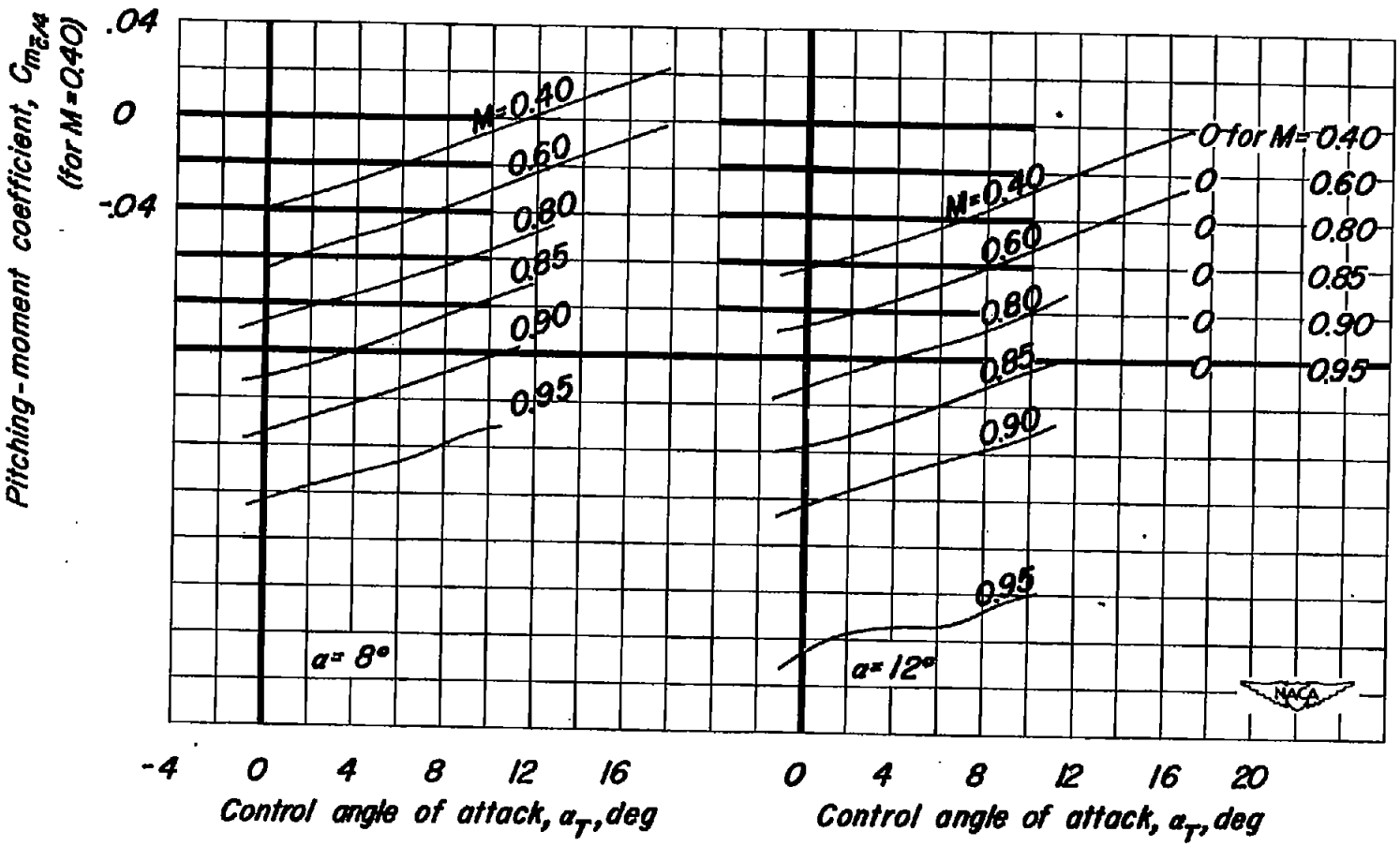

(b) a, 8°; a, 12°

Figure 25.-Continued.

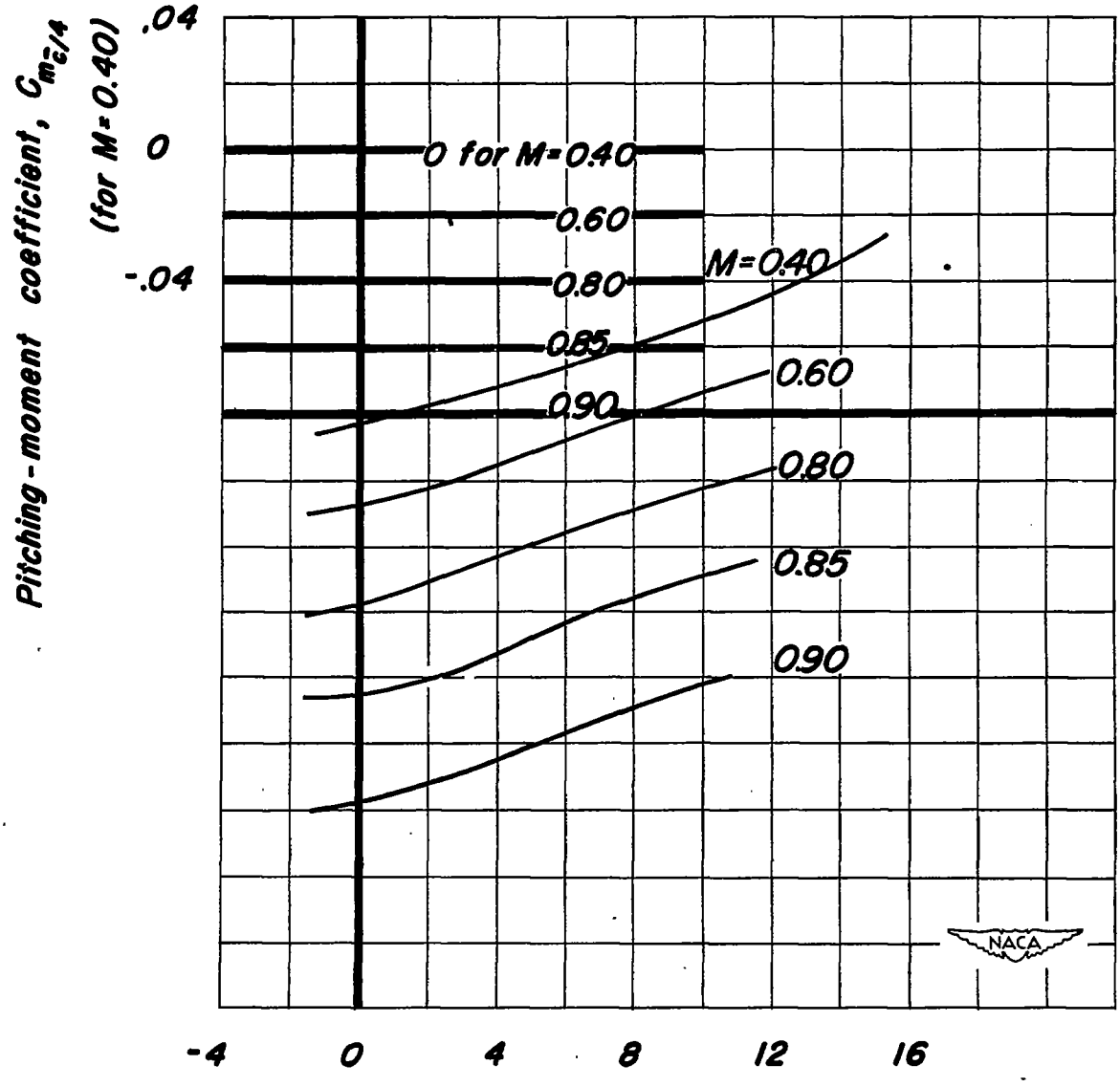

(c) α=16°

Figure 25.-Concluded.

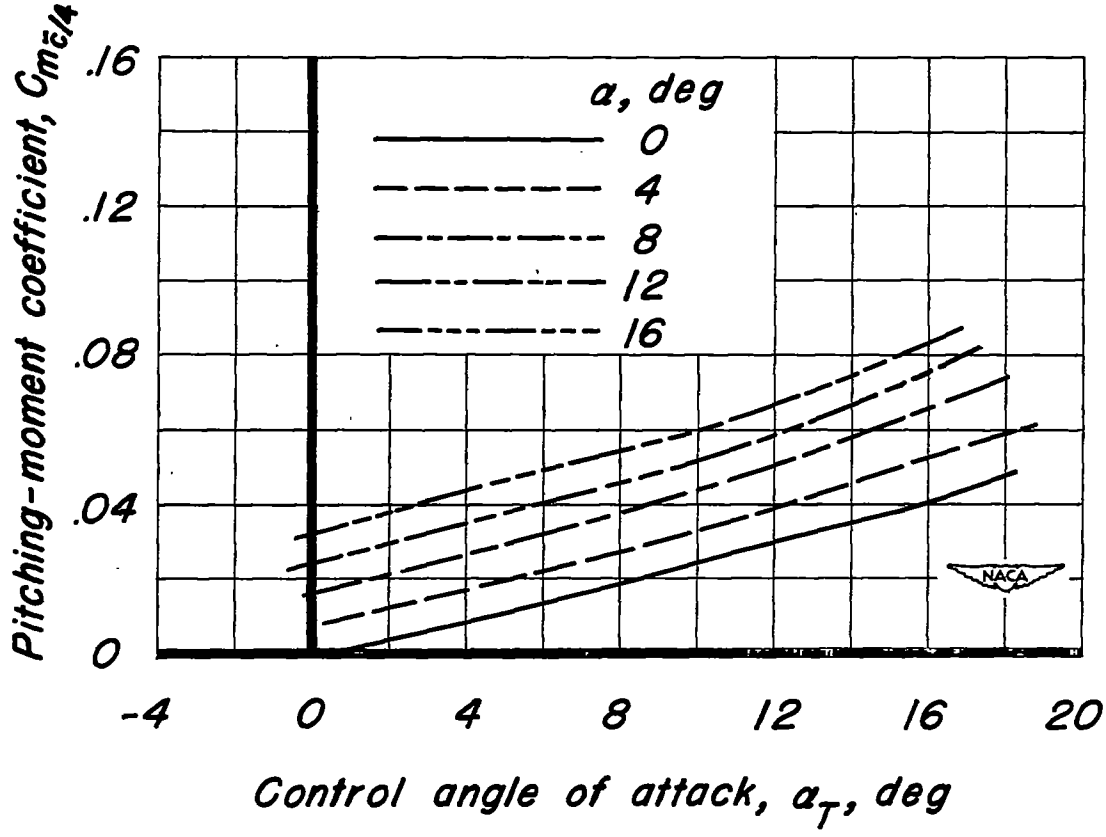

Figure 26.-The variation with horizontal-control-surface angle of attack of the pitching-moment coefficient of the canard model with the wing off and control surface free. Mach number, 0.25; Reynolds number, 8.0 million.

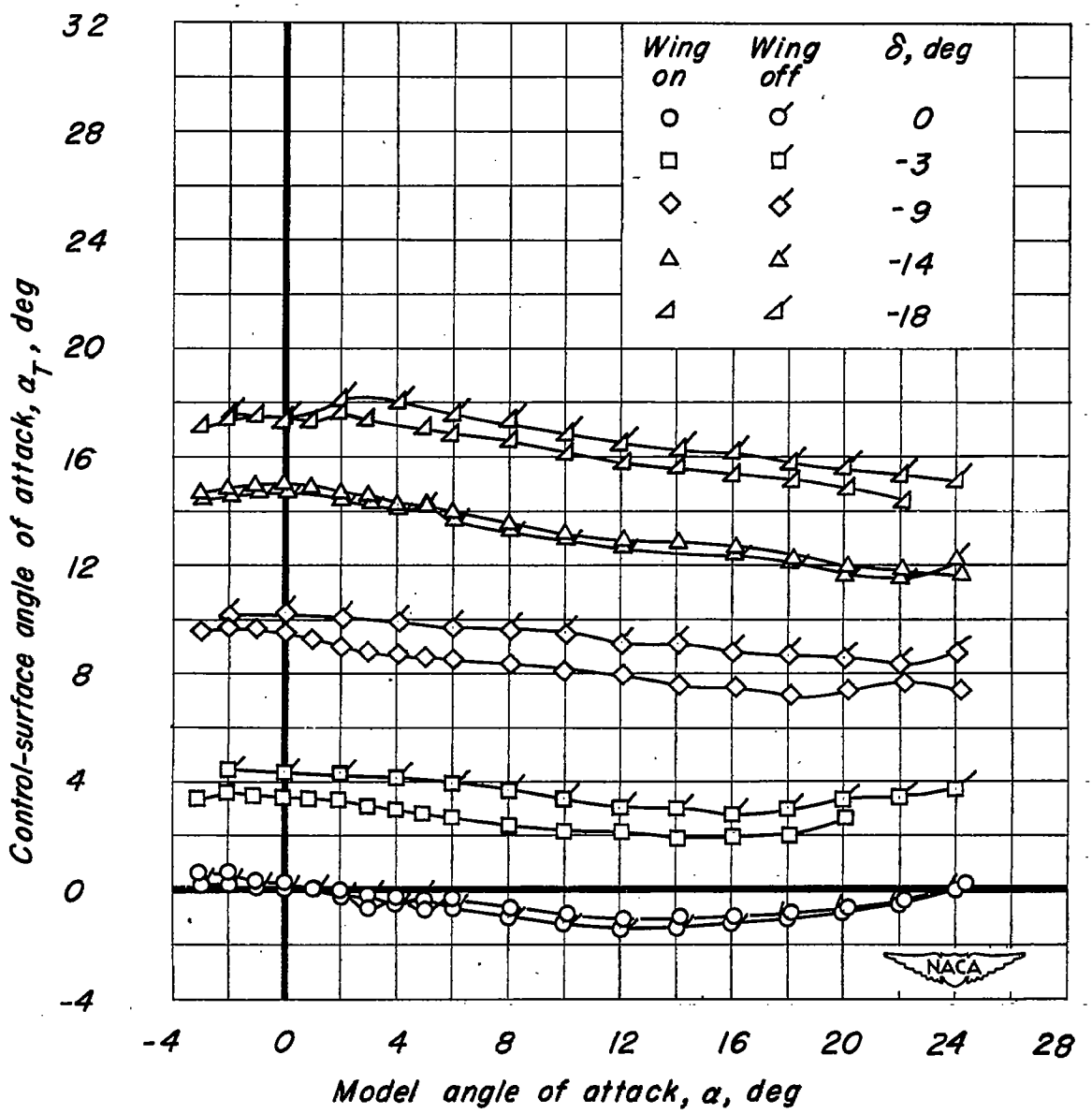

Figure 27.- The variation with model angle of attack of the control-surface angle of attack for several split-flap angles. Mach number, 0.25; Reynolds number, 8.0 million.

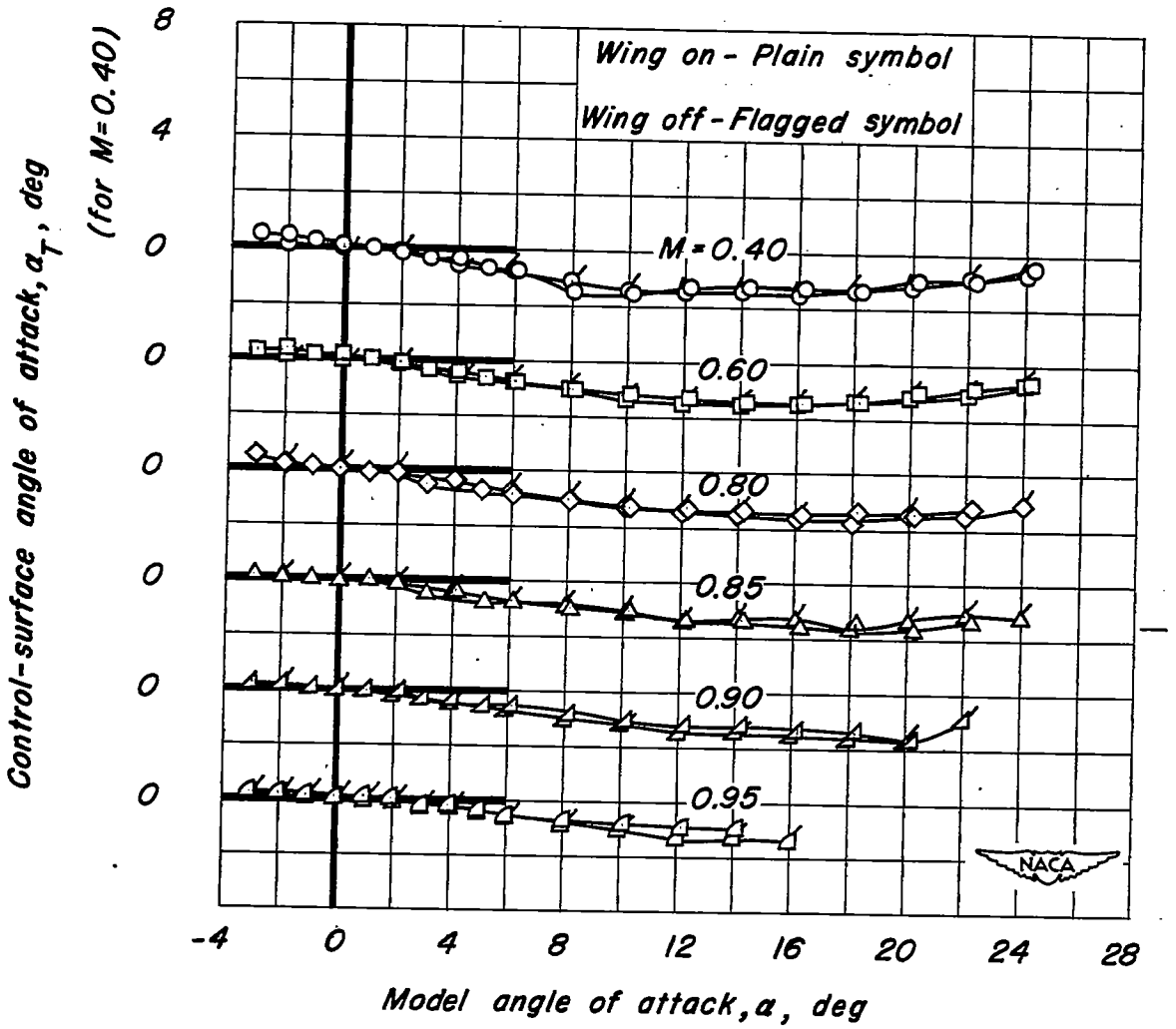

Figure 28.- The variation with model angle of attack of the control-surface angle of attack for several Mach numbers. Flap undeflected; Reynolds number, 3.0 million.

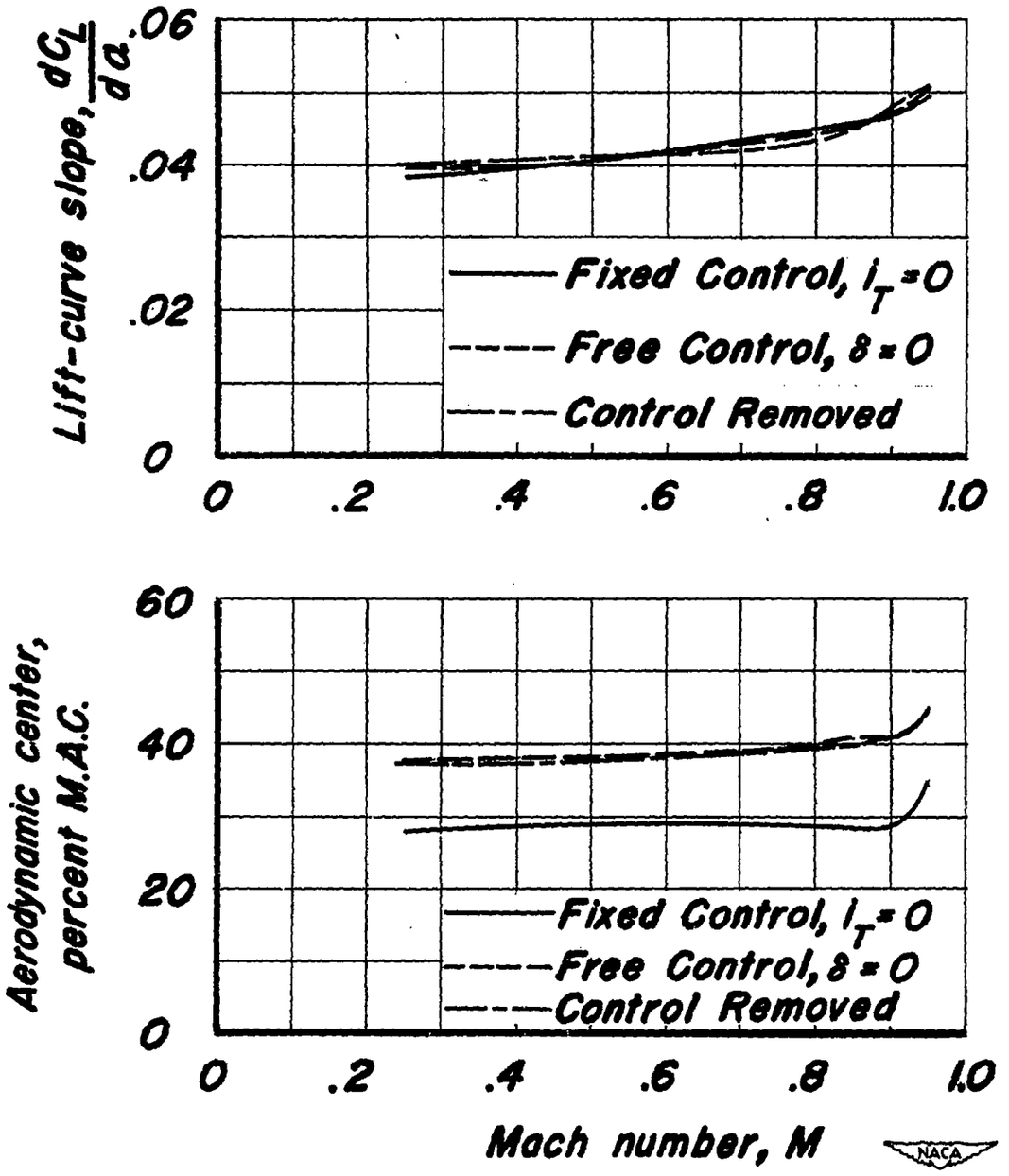

Figure 29.-The effect of Mach number on the lift-curve slope and aerodynamic center of the canard model. C_L, 0.

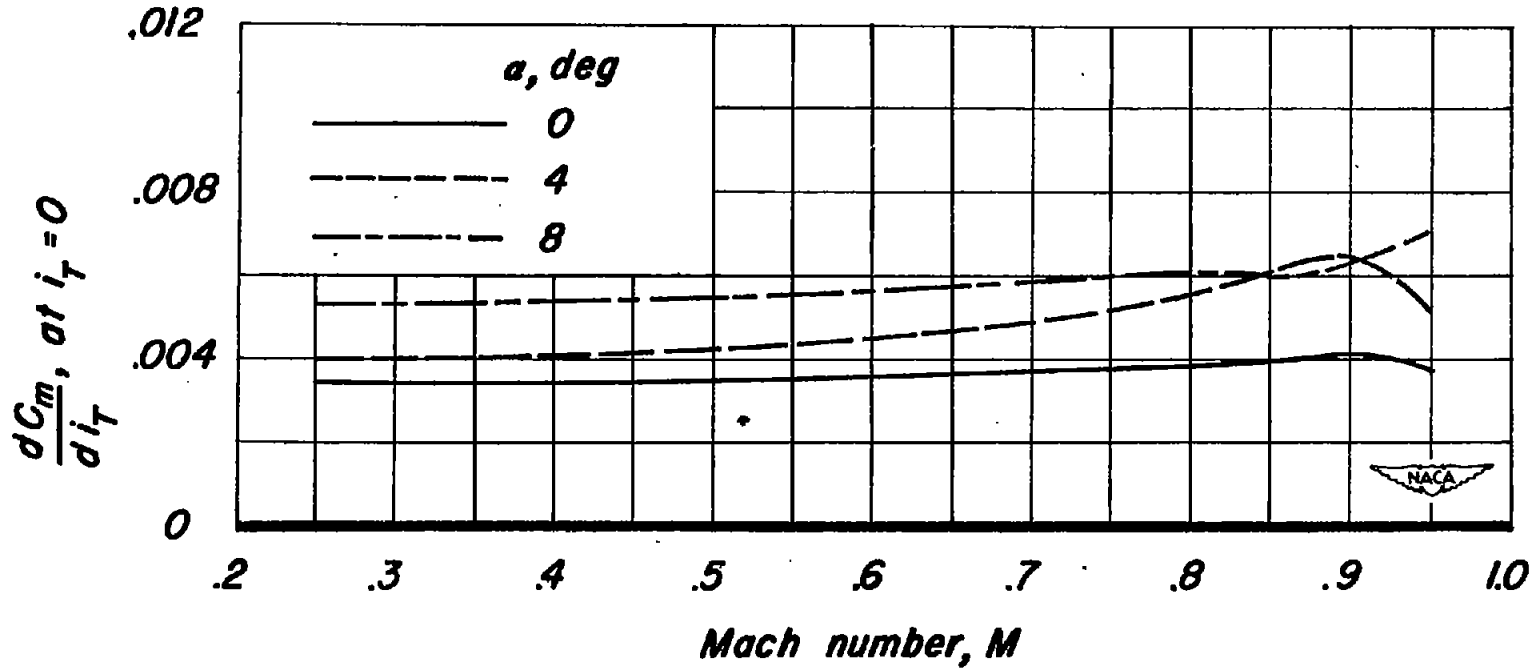

Figure 30.-The variation of horizontal-control-surface effectiveness with Mach number for several angles of attack.

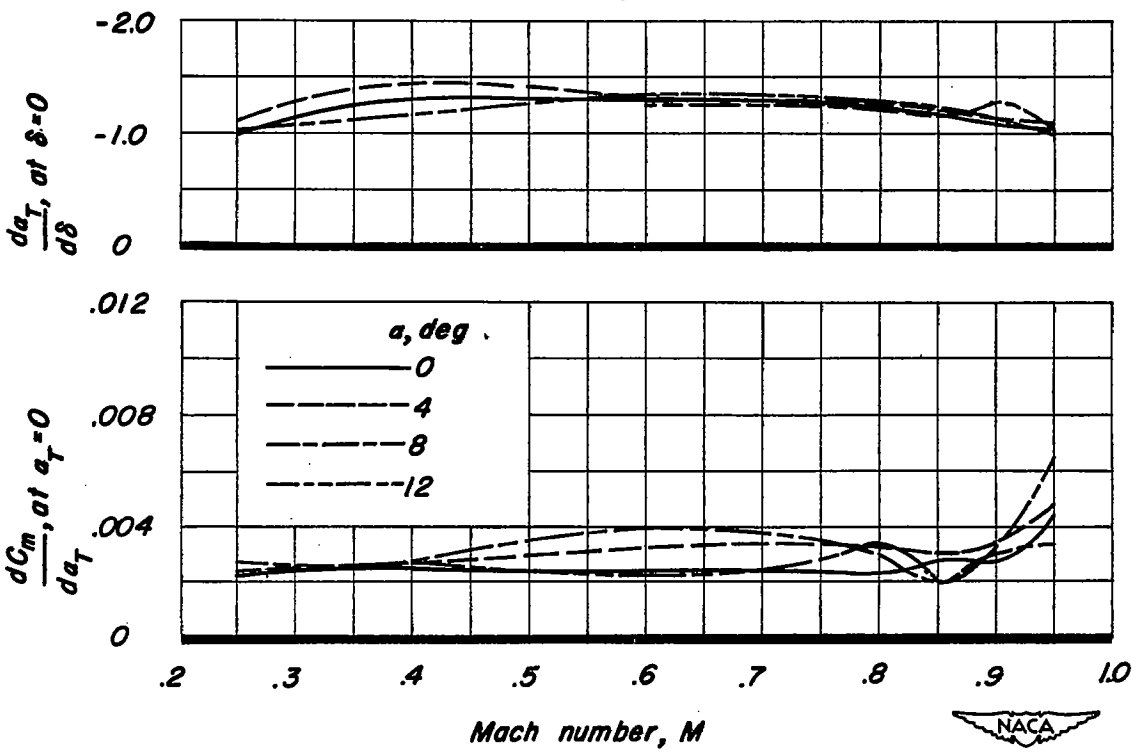

Figure 31.- The variation with Mach number of the split-flap effectiveness parameter $da_T/d\delta$ and the horizontal-control-surface effectiveness dC_m/da_T for the canard model with the control surface free.

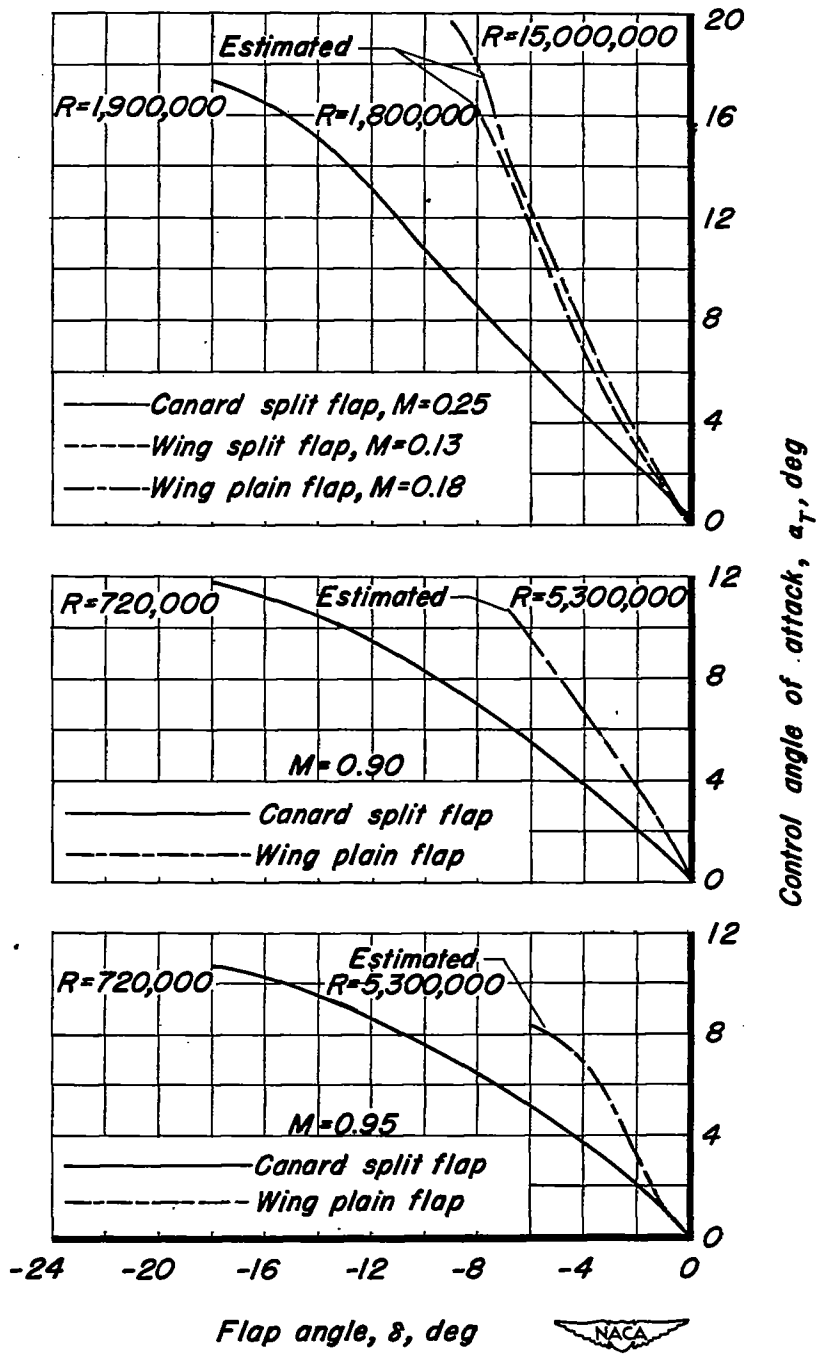

Figure 32.- Comparison of the control-surface floating angles of attack with estimated floating angles.

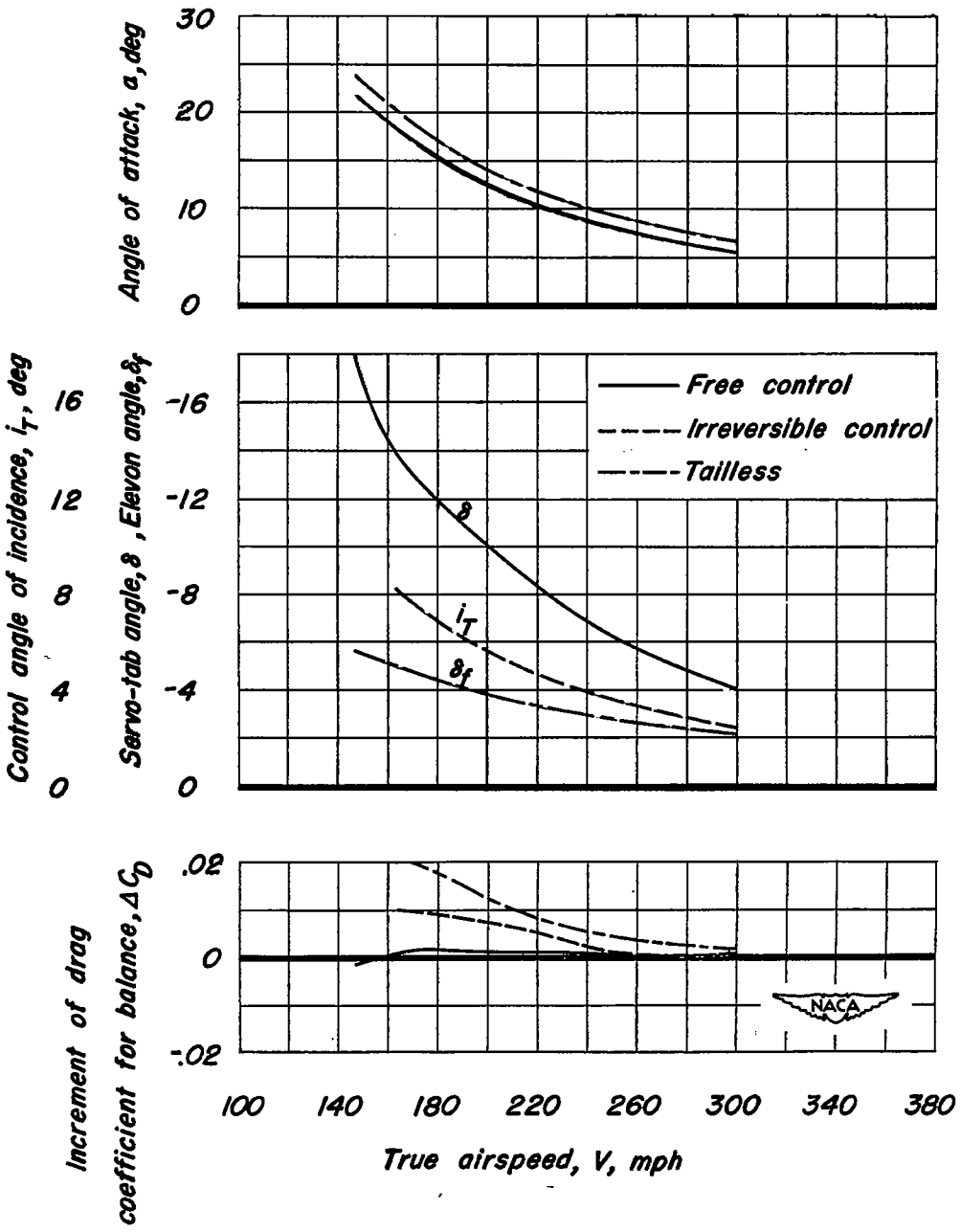

Figure 33-The low-speed characteristics of three airplanes with similar triangular wings and different types of longitudinal control. Wing loading, 50 lb per sq ft; sea level.

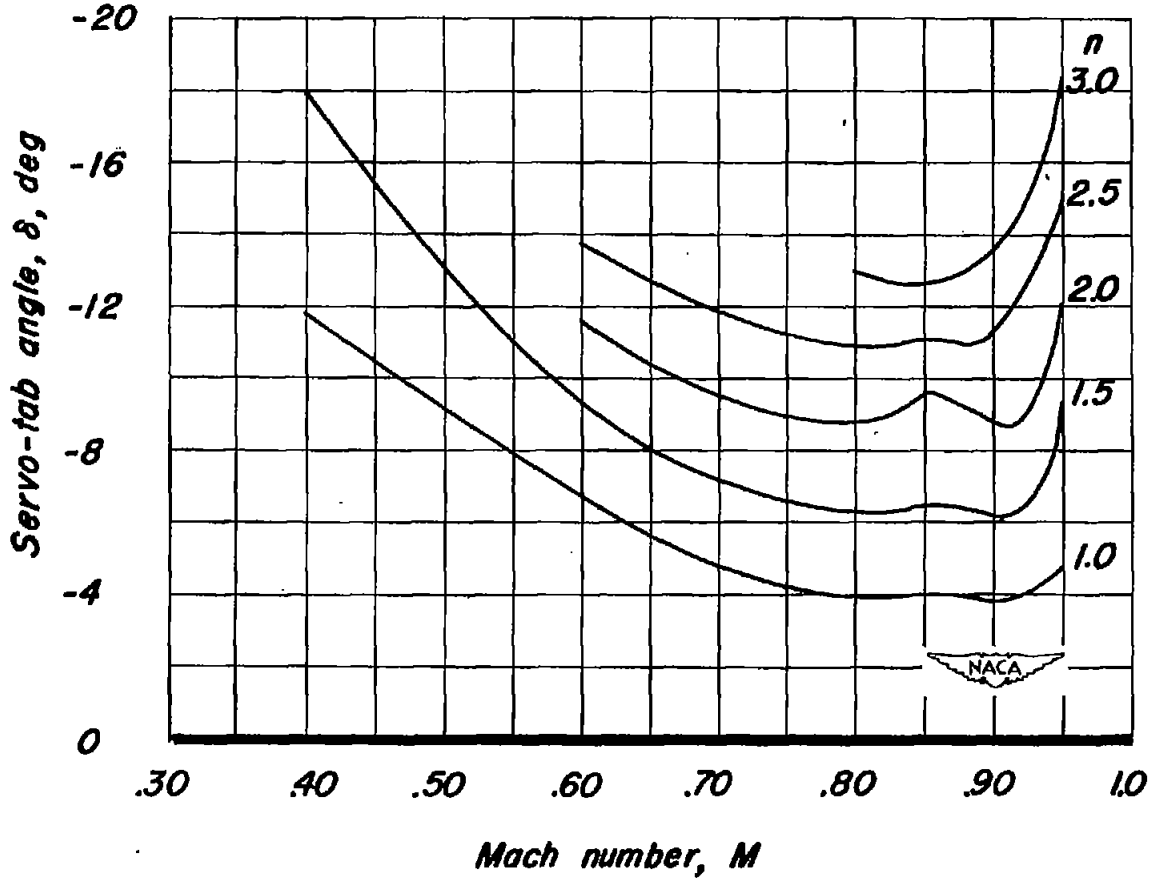

Figure 34-The variation with Mach number of the servo-tab angle to balance a canard airplane with a free-floating horizontal control surface. Wing loading, 50 lb per sq ft; c.g. at 0.32 $\bar{c}$; altitude, 30,000 ft.

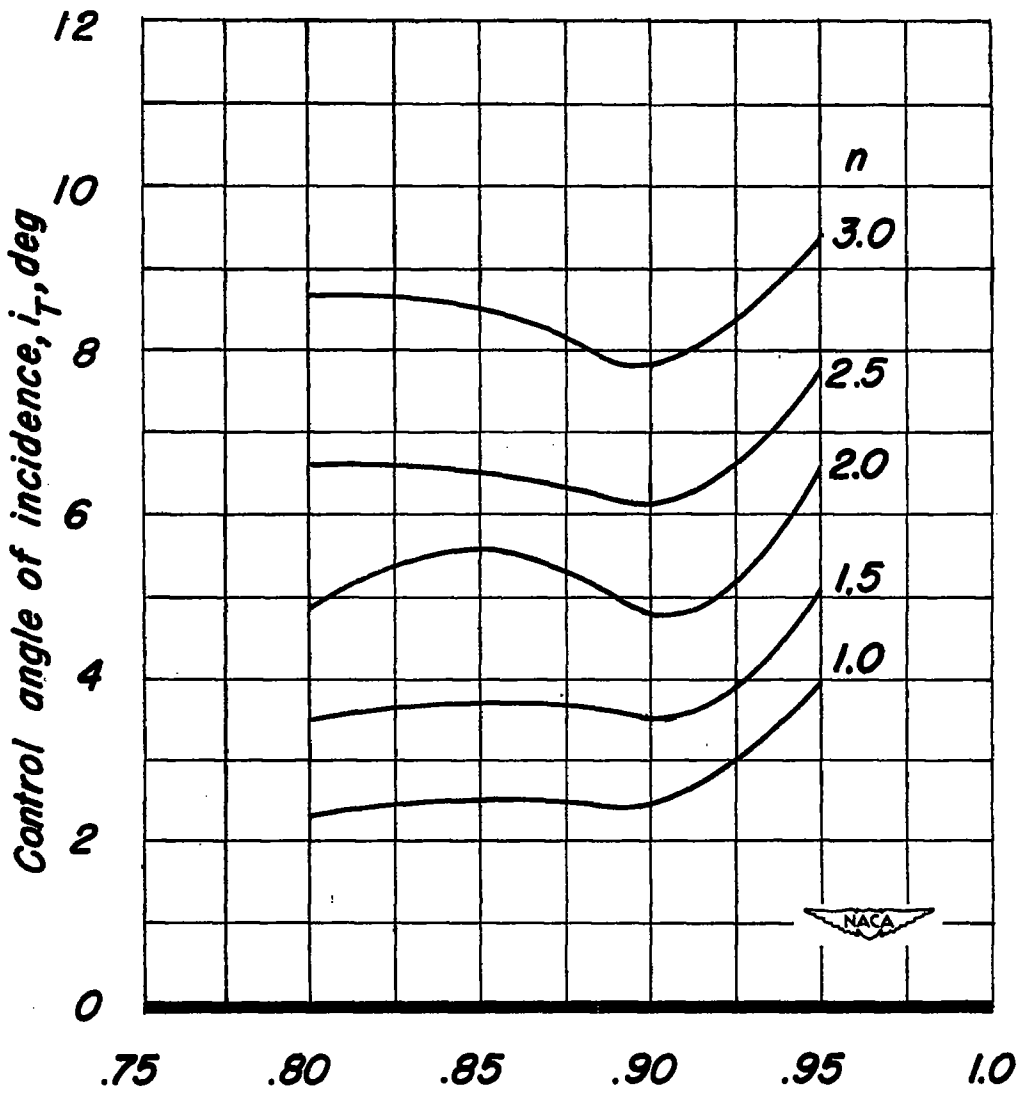

Figure 35.-The variation with Mach number of the control-surface incidence to balance a canard airplane with an irreversible control. Wing loading, 50 lb per sq ft; c.g. at 0.20$\bar{c}$; altitude, 30,000 ft.

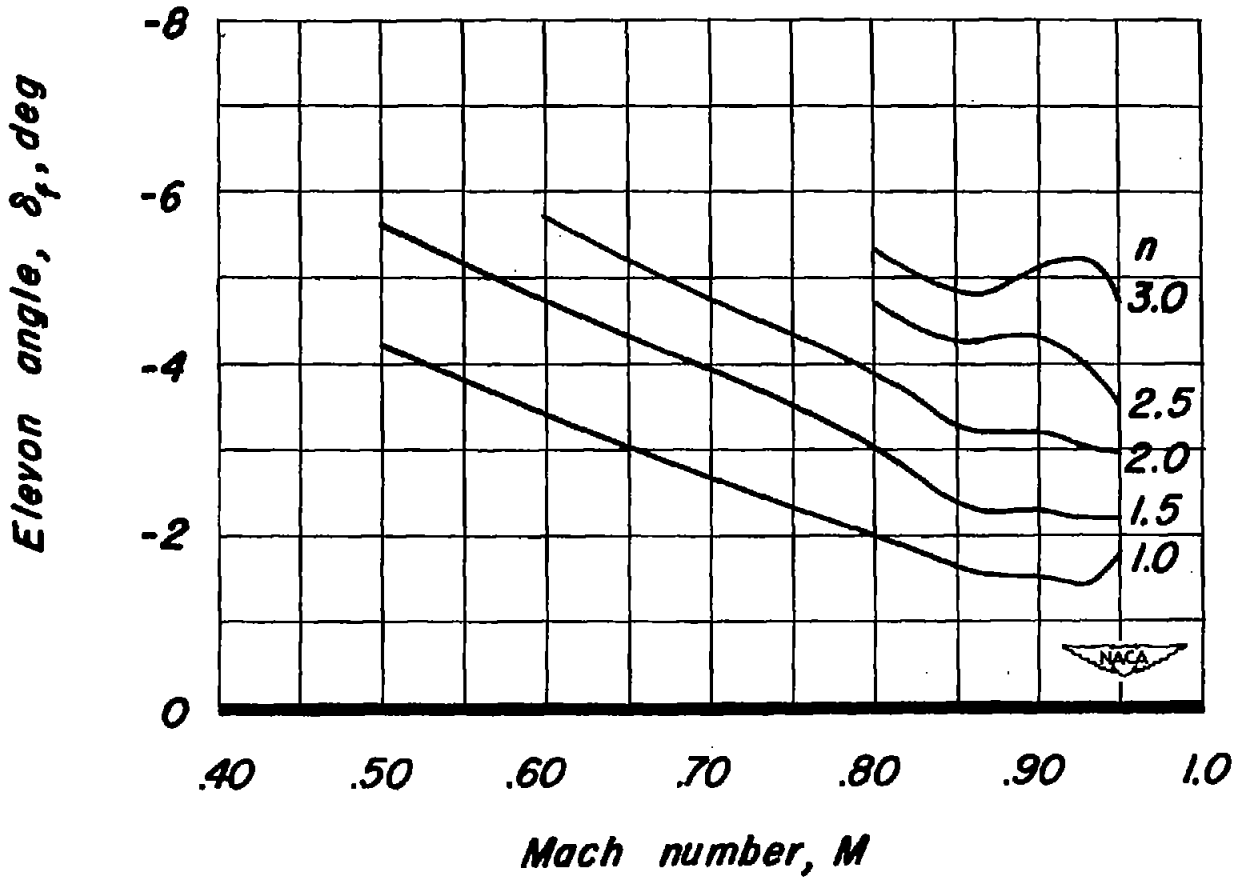

Figure 36.-The variation with Mach number of the elevon angle to balance a tailless airplane in level and accelerated flight. Wing loading, 50 lb per sq ft; c.g. at 0.32$\bar{c}$; altitude, 30,000 ft.

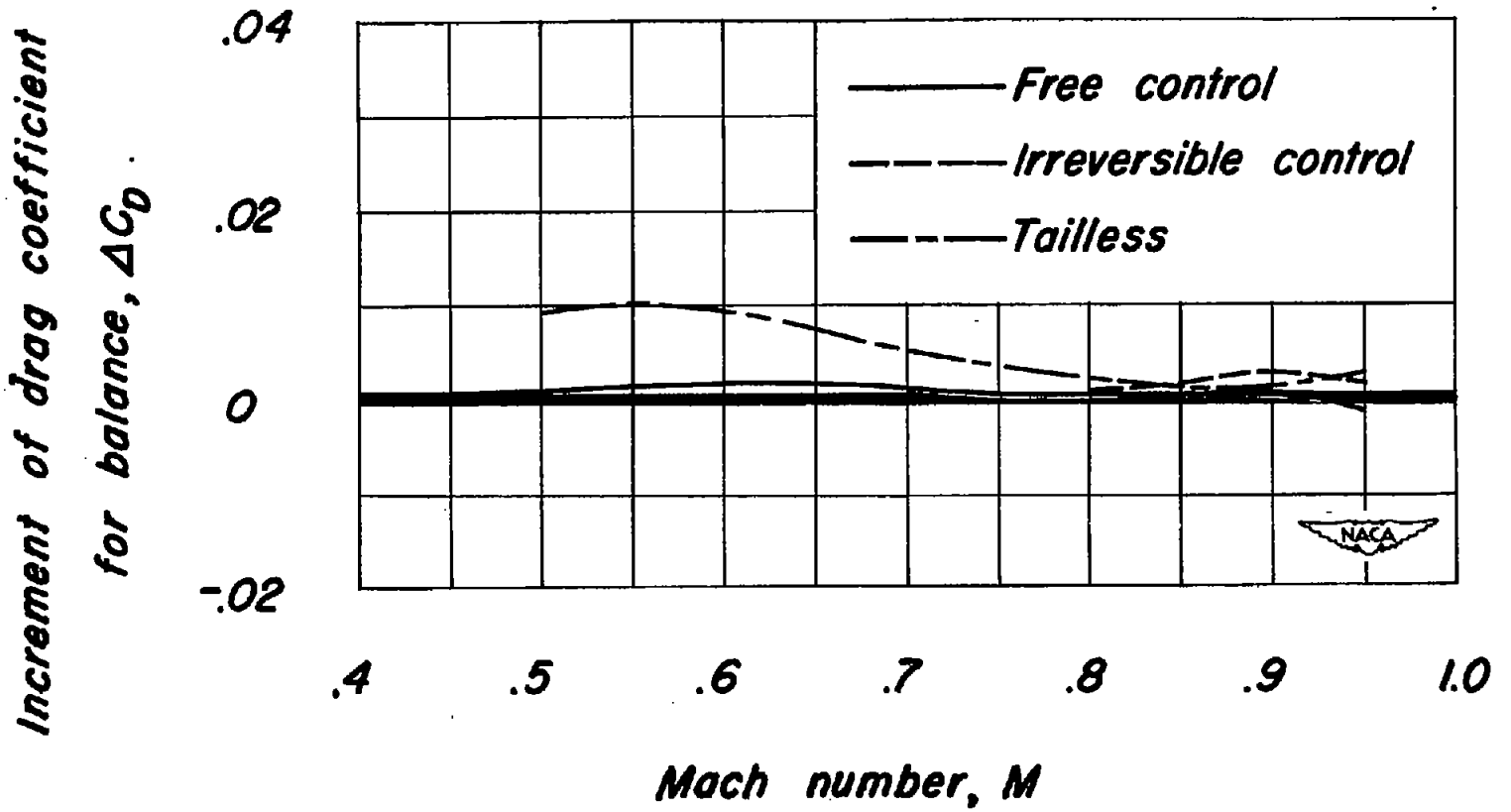

Figure 37.- The variation with Mach number of the increment in drag coefficient caused by deflection of the control surface for longitudinal balance. Wing loading, 50 lb per sq ft; altitude, 30,000 ft.

NACA-Langley - 12-3-51 - 980